Roles of M-phase cell cycle regulatory paralogs in the urochordate Oikopleura dioica

Haiyang Feng

Thesis for the Degree of Philosophiae Doctor (PhD)
University of Bergen, Norway
2018

UNIVERSITY OF BERGEN

Roles of M-phase cell cycle regulatory paralogs in the urochordate Oikopleura dioica

Haiyang Feng

Thesis for the Degree of Philosophiae Doctor (PhD)
at the University of Bergen

2018

Date of defence: 16.11.2018

Year: 2018

Title: Roles of M-phase cell cycle regulatory paralogs in the urochordate Oikopleura dioica

Name: Haiyang Feng

Print: Skipnes Kommunikasjon / University of Bergen

Scientific environment

The work presented in this thesis was carried out in the Thompson Group at the Sars International Centre for Marine Molecular Biology. It is part of the PhD programme of the Department of Biological Sciences at the Faculty of Mathematics and Natural Sciences of the University of Bergen.

Acknowledgements

This project was carried out and funded by Department of Biological Sciences and the Sars Centre at University of Bergen.

Foremost my sincere thanks go to my supervisor Professor Eric M. Thompson for giving me this invaluable opportunity to undertake my PhD study in his group and for his sincere guidance, encouragement and support through my project. I am truly grateful for inheriting his spiritual attitude towards science.

I would like to express my gratitude to my co-supervisor Christofer Troedsson for his encouragement and suggestions to my PhD study.

My thanks also go to former and present members of S3 group at the Sars Centre for creating such an enjoyable working environment. Martina Raasholm and Heloisa Galbiati for maintaining the orders and routines in the lab. Xiaofei Ma for collaboration and discussions regarding my experiments. Pavla Navratilova and Gemma Danks for being great coworkers.

Thanks to former and present "Appypark" staff, Jean-Marie Bouquet, Magnus Reeve, Anne Aasjord, Anders Olsen, Kjerstin Nilsen Nøkling, for maintaining the appendicularia culture and providing me animals to work with.

Thanks to the MDB group at Department of Biological Sciences for the generous support in my former office. Special thanks to Katrine Sandnes Skaar, Jon Vidar Helvik, Ståle Ellingsen and Geir Kåre Totland.

Especially, to my parents and my brother, words can hardly express my gratitude.

Table of Contents

Abstract

Cell cycle progression is controlled by a series of regulators with complex spatial-temporal dynamics, ensuring faithful transitions of different phases. The urochordate *Oikopleura* has systemically employed diverse cell cycle variants, including proliferative mitotic cycles, numerous endocycle variants and reproductive meiotic cycles, to support its rapid growth and reproduction in an extraordinarily short chordate life span. It also possesses an expanded complement of some mitotic regulators that are variably expressed during development. This study focuses on M-phase events and investigates functional diversification and specialization of CDK1-Cyclin B complements during female meiosis and of duplicated chromosomal passenger complex (CPC) components in embryonic mitosis. The molecular mechanisms involved in meiosis resumption during oogenesis echo those in G2/M transition of mitosis, whereas coenocystic oogenesis in the semelparous *Oikopleura* is characterized by the unique feature that vitellogenesis precedes the timing of oocyte selection. We revealed dynamic deployment of two specialized CDK1 paralogs during oogenesis. Both CDK1a and CDK1d are localized at Organizing Centres (OCs) before oocyte selection. CDK1a relocates to selected meiotic nuclei at the beginning of phase 4 of oogenesis, and CDK1d then relocates to selected meiotic nuclei, concomitant with its binding partner Cyclin Ba. Targeted RNAi knockdowns revealed that CDK1a is required for coenocystic vitellogenesis, whereas CDK1d-Cyclin Ba is required for meiosis resumption and meiotic spindle assembly during prometaphase I. Additionally, Cyclin B3a plays a minor, dispensable role in promoting CDK1d activity, implying Cyclin B3 has undergone divergent evolution in the urochordate subphylum. *Oikopleura* embryonic divisions are fast and synchronized. Within the CPC, two INCENP paralogs always co-exist, with significant expression levels during mitosis, and display distinct localizations and subfunctionalizations. INCENP paralog switching on centromeres modulates Aurora B kinase activity and localization, thus regulating CPC functional transitions during fast embryonic divisions. The INCENPa paralog regulates early mitotic events whereas the INCENPb paralog is required for abscission during mitotic exit.

Abbreviations

1-MeAde	1-Methyladenine
APC/C	Anaphase promoting complex/cyclosome
ATM	Ataxia telangiectasia mutated kinase
ATR	Ataxia telangiectasia and Rad3-related protein
CAK	CDK activating kinase
cAMP	Cyclic adenosine monophosphate
CDK	Cyclin dependent kinase
Chk1/2	Checkpoint kinase 1/2
CKI	CDK inhibitor proteins
CLS	Centrosomal localization signal
cmRNA	Capped messenger RNA
COs	Crossovers
CPC	Chromosomal passenger complex
CPE	Cytoplasmic polyadenylation elements
CPEB	CPE-binding protein
CPSF	Cleavage and polyadenylation specificity factor
CREB	cAMP response element binding protein
CRS	Cytoplasmic retention sequence
CSF	Cytostatic factor
DDR	DNA damage response
DSBs	Double-strand breaks
dsRNA	Double stranded RNA
EC	Error correction
EGF	Epidermal growth factor

FoxM1	Forkhead box protein M1
GVBD	Germinal vesicle breakdown
INCENP	Inner centromere protein
LH	Luteinizing hormone
MAPK	Mitogen-activated protein kinase
MCC	Mitotic checkpoint complex
MPF	Maturation promotion factor
MT-KT attachment	Microtubule-kinetochore attachment
MTOC	Microtubule organizing center
NEBD	Nuclear envelope breakdown
NES	Nuclear export sequence
NLS	Nuclear localization signal
NPC	Nuclear pore complex
NRE	Nanos response element
OC	Organizing center
PABP	Poly(A) binding protein
PAP	Poly(A) polymerase
Pg	Progesterone
PGCs	Primordial germ cells
Plk1	Polo-like kinase 1
RINGO	Rapid inducer of G_2/M progression in oocytes
SAC	Spindle assembly checkpoint
SAF	Spindle assembly factor
SAH	Single α-helix domain
SC	Synaptonemal complex

SCF	Skp1-Cul1/Cdc53-F-box

1 Introduction

1.1 Definition of the cell cycle and its various forms in three domains of life

The cell cycle is a sequence of events that leads to the reproduction of the cell (Morgan, 2007). All cells in a living organism are descendants of a single cell. It is thought that every living cell today is derived from an ancestral cell dating back 3 or 4 billion years ago. Cell reproduction is a fundamental process that passes genetic information from one generation to the next. Among the three domains of life, unicellular prokaryotes including archaea and bacteria lack a nucleus, and must adapt their growth rate to nutrient fluctuations and metabolic status. As a result, the cell division cycle is coordinated with mass doubling, chromosome replication and segregation (Wang and Levin, 2009). Eukaryotes have a nucleus, are more complex and employ a series of independent control systems to regulate discrete steps of the cell cycle. In unicellular organisms, cell division is the only way to generate new organisms. In multicellular organisms, countless cell divisions provide cell resources to make up the tissues and organs, and also replace dead or damaged cells from natural apoptosis or environmental damage. Violations of cell cycle regulation can lead to unscheduled cell proliferation, genomic instability and chromosomal instability, which are common defects in cancer cells.

1.2 The eukaryotic cell cycle

A typical eukaryotic cell cycle consists of interphase (G1, S, and G2 phase) and mitotic (M) phase (Fig. 1). During S (synthesis) phase, when DNA replication and chromosome duplication occur, increased histone translation supports packaging of newly synthesized DNA into chromosomes, which are linked by cohesion establishment between sister chromatids. Centriole biogenesis also occurs at the beginning of S phase. M phase includes nuclear division (mitosis) and cell division (cytokinesis), with distribution of the duplicated chromosomes into daughter nuclei. Mitosis is divided into five sub-phases: prophase, prometaphase, metaphase, anaphase, and telophase, and each sub-phase is defined by a series of cell cycle events. During prophase, chromosomes condense, nucleoli disappear and

centrosomes migrate towards opposite poles. Prometaphase is marked by nuclear envelop breakdown (NEBD), spindle formation and attachment of sister chromatids by microtubules from opposite poles. By metaphase, sister chromatids are aligned on an equatorial plane under the tension of spindle microtubules. When anaphase starts, cohesins joining sister chromatids are cleaved by the protease separase, and sister chromatids are pulled to opposite poles by spindle microtubules. During telophase, the nuclear envelope reforms around each set of separate chromosomes, chromosomes decondense and nucleoli reappear. Mitosis is completed by cytokinesis to pinch the cell into two, though the time scale of cytokinesis varies greatly in different species, and is even not complete until after the next S phase during early embryogenesis of sea urchins.

Gap phase (G1 before S phase and G2 before M phase) is generally much longer than S and M phases, since during gap phase the cell grows and synthesizes mRNA and protein for the following DNA replication and cell division. G1 is a key regulatory phase where critical decisions are made as to whether to commit to continuous mitosis, pause for an extended period under unfavorable conditions, or enter a quiescent stage called G0. It is worth noting that gap phase barely exists during rapid embryogenesis of *Xenopus* or syncytial embryonic divisions of *Drosophila*.

The endocycle, also called endoreduplication, is a common cell cycle variant in which the cell undergoes many rounds of S phase without cell division, giving rise to polyploidy (Edgar et al., 2014). Polyploidy can arise from a truncated mitosis when certain mitotic phases are bypassed. It is widely used for post-mitotic cell growth in diverse invertebrates. *Drosophila* polytene salivary glands augment cell size by increasing the ploidy up to 2048 C. *Oikopleura* epithelial cells help to support 10-fold body growth from metamorphosis to maturity by employing extensive endocycles to achieve polyploidy ranging from 34 to >1300 C in a bilaterally symmetric pattern of defined cellular fields (Ganot and Thompson, 2002). By increasing DNA content, endocycles increase the number of individual loci for maximizing mRNA and protein production, which can be used as resources for particular developmental purposes.

For instance, the *Drosophila* germline derived ovarian nurse nuclei are highly polyploid (up to 2048 C) (Hammond and Laird, 1985), and support oogenesis by synthesizing and transporting mRNA and protein to growing oocytes residing in the syncytial ovariole (Bastock and St Johnston, 2008). It is believed that polyploidy can have advantages over diploidy under conditions that damage DNA, since multiple copies of alleles can overcome mutations in individual alleles (Van de Peer et al., 2009).

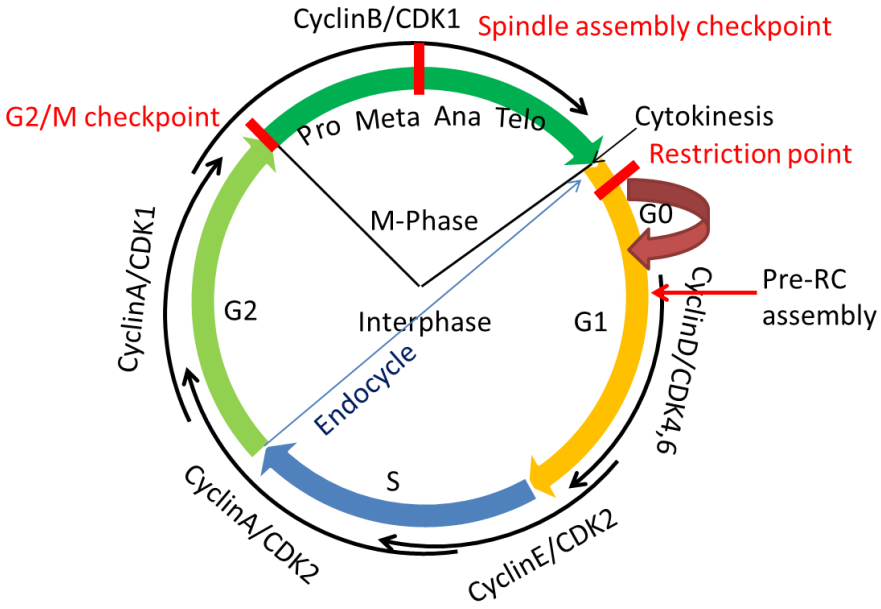

Figure 1. Mitotic cell cycle and cell cycle variants. A prototypical eukaryotic cell cycle contains interphase and the mitotic phase. Three major checkpoints are labelled in red. Each cell cycle phase is driven by Cyclin-CDK complexes: Cyclin D-CDK4/6 initiates the new round of cell cycle in early G1 phase, Cyclin E-CDK2 triggers S phase, Cyclin A-CDK2 completes S phase, and Cyclin A/B-CDK1 drives M phase. One common cell cycle variant is the endocycle, in which M phase is truncated or skipped and the G-S cycle is repeated, giving rise to polyploidy.

1.3 Regulations at checkpoints

The progression of the cell cycle is regulated by checkpoints, which usually lie at the boundary of cell cycle phases and survey the fidelity of the previous phase. When detrimental events occur, the cell cycle will be arrested at checkpoints and trigger machinery to rectify errors. Three checkpoints are generally found among different species, and the core molecular machineries controlling each checkpoint are highly conserved, although the strength of checkpoint control may vary in different developmental contexts.

1.3.1 G1 checkpoint

The G1 checkpoint also known as the restriction (R) point determines whether the cell commits to proliferation based on internal and external inputs. When conditions are suitable and in the presence of mitogens such as growth factors, Cyclin D bound CDK4/6 can drive the cell past the R point. Some studies suggest that there is a cell growth checkpoint at late G1 phase (also known as START in yeast) distinguishable from the R point, which senses nutritional sufficiency and is governed by mTOR (the mammalian target of rapamycin) pathway. This suppresses TGF-β signaling and activates Cyclin E-CDK2, generating a positive feedback loop to aid progression through late G1 and entry into S phase (Foster et al., 2010).

The G1 checkpoint exhibits various developmental requirements among eukaryotes. The G1 checkpoint is absent in early *Drosophila* embryogenesis due to absence of external nutritional input, and it starts to control cell proliferation only after hatching into larva, whereas the G1 checkpoint is under strict control in budding yeast (Vidwans and Su, 2001). In mammals, G1 checkpoint control is not essential for the proliferation of most cell lineages demonstrated by the fact that D-type cyclins and CDK4/6 knockout mice can survive until E16.5, but its deregulation often causes cancer (Satyanarayana and Kaldis, 2009).

1.3.2 G2/M DNA damage checkpoint

The G2/M DNA damage checkpoint is used to prevent entry into M phase when DNA damage occurs or chromatin is under-replicated during S phase (Shaltiel et al., 2015). The main target is the activity of CDK1, which is controlled by the balance

between inhibitory kinases Wee1/Myt1 and counteracting Cdc25 phosphatases. ATM/ATR-Chk1/Chk2 signaling cascades initiate CDK1 inhibition during early DNA damage response (DDR) by mediating the inhibition of Cdc25A and the stabilization of Wee1 (Beck et al., 2010). Downstream p53-p21 signaling cascades amplify CDK1 inhibition in late DDR by inhibiting CAK or activating APC/C^{Cdh1} to promote degradation of Cyclin A and Cyclin B for a persistent G2 arrest (Wiebusch and Hagemeier, 2010).

1.3.3 The spindle assembly checkpoint

The Spindle Assembly Checkpoint (SAC) acts during the metaphase to anaphase transition and delays sister chromatids separation in mitosis until amphitelic attachment of all sister chromatids by microtubule at kinetochores is established (Lara-Gonzalez et al., 2012). Essentially, the SAC monitors the status of kinetochore-microtubule attachment. When kinetochores lack microtubule attachment, the SAC is activated and prevents anaphase by inhibiting anaphase-promoting complex or cyclosome (APC/C), an E3 ubiquitin ligase that ubiquitylates Securin and Cyclin B1 for proteasomal degradation and drives anaphase onset and mitotic exit (Sivakumar and Gorbsky, 2015). Unattached kinetochores are sensed by Bub1, which links the SAC module to the outer kinetochore and assembles the mitotic checkpoint complex (MCC) including Mad2, BubR1, Bub3 and Cdc20 (Sudakin et al., 2001). MCC inhibits the APC in two ways. First, Mad2 can sequester the APC co-activator Cdc20 and prevent APC activation (Fang et al., 1998). Second, BubR1 blocks substrate binding by either inducing a conformational change of bipartite substrate receptor between APC subunit Apc10 and co-activator (Herzog et al., 2009), or occupying the receptor as a pseudosubstrate (Burton and Solomon, 2007). Once correct kinetochore microtubule attachment is established, the SAC is satisfied and is extinguished. The Mad1-Mad2 core complex is removed by the minus-end directed motor protein, dynein, along kinetochore microtubules towards the spindle poles, known as stripping (Howell et al., 2001). In addition, the Mad2 dimerization interface is blocked by its antagonist $p31^{comet}$, which further prevents Mad2-Cdc20 production and liberates Cdc20 (Fig. 2).

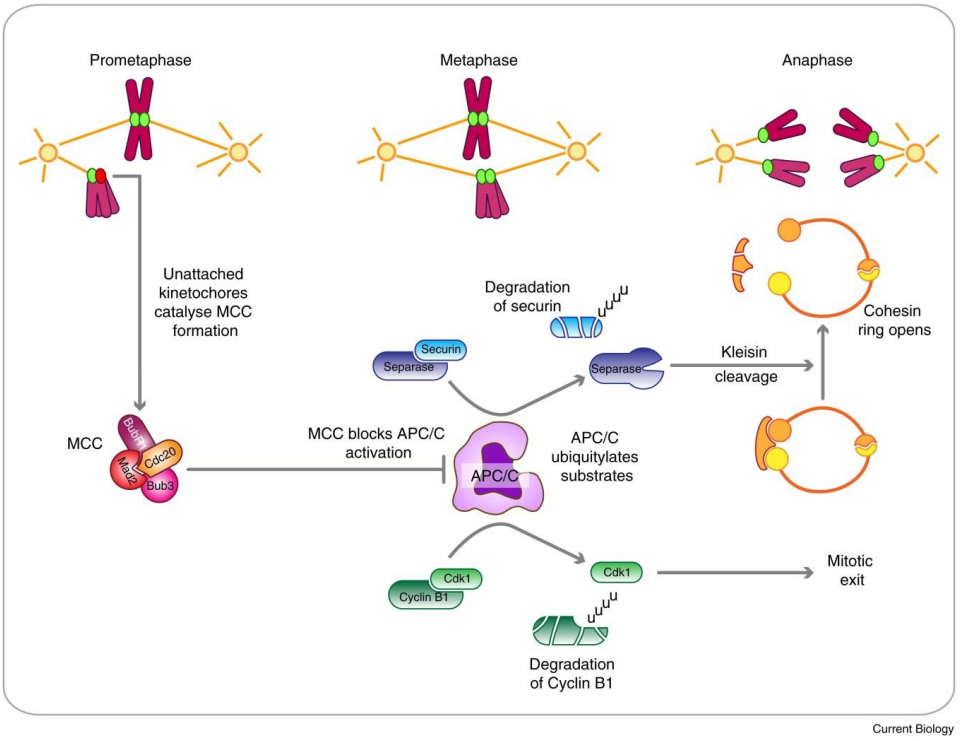

Figure 2. The principle of the Spindle Assembly Checkpoint (SAC). Unattached kinetochores during prometaphase trigger the formation of the mitotic checkpoint complex (MCC), consisting of BubR1, Bub3, Mad2 and Cdc20, which inhibits the APC/C and blocks mitotic progress. The SAC is not satisfied until amphitelic attachment of sister chromatids is established during metaphase, leading to MCC disassembly and APC/C alleviation. Active APC/C targets Securin and Cyclin B1 for ubiquitylation and degradation. Separase then is activated and cleaves the kleisin subunit Scc1 of the cohesin complex to allow sister-chromatid separation at anaphase onset. Cyclin B1 degradation results in CDK1 inactivation and mitotic exit. Adapted from Lara-Gonzalez et al (2012).

Even when the SAC is not satisfied, many animal cells can escape mitotic arrest through a process termed mitotic checkpoint slippage. This slippage is caused by continuous degradation of Cyclin B in vertebrates (Brito and Rieder, 2006), or downregulation of CDK1 activity through CKI in yeast and *Drosophila* (Rieder and Maiato, 2004). Different organisms show different strengths of SAC response in terms of cell type and developmental stage. Many embryonic cells lack a persistent

SAC during rapid cleavage stages, such as *Xenopus*, zebrafish, sea urchin and *Drosophila*, and the SAC is only acquired during the mid-blastula transition (MBT). This is proposed to be regulated by a maternally programmed developmental timer (Zhang et al., 2015a). The first division of *C. elegans* embryos shows moderate delay under nocodazole treatment (2.5-fold increased duration from NEBD to NER) (Encalada et al., 2005), and gradually increases SAC strength after each round of cell division due to the decrease of cell size and increase in the kinetochore-to-cytoplasm ratio (Galli and Morgan, 2016). Mouse embryos show a strong SAC response after fertilization. It is generally thought that the SAC functions as a rheostat by adjusting the amount of Mad2 on unattached kinetochores (Collin et al., 2013), and cell size is a factor that modulates SAC signaling and tunes APC inhibition.

1.4 Mitotic CDK and cyclins

The central cell cycle regulators are cyclin-dependent kinases (CDKs) and their regulatory subunit cyclins. Sequential activation of these complexes drives transition through different cell cycle phases (Fig. 1). CDK1 and A- or B-type cyclins are responsible for driving entry into M phase and continuation of mitosis. The concentration of CDK1 is constant through mitosis, and its activity is mainly regulated through its phosphorylation, the oscillation of partner cyclin levels, and CDK inhibitor proteins (CKIs).

1.4.1 Structure of the CDK1-Cyclin B complex

CDK1 is a 34-40 kDa Serine/Threonine protein kinase with a classical bi-lobed structure consisting of a small amino-terminal (N-) lobe and a large carboxyl-terminal (C-) lobe. The cleft between the two lobes accommodates the substrate and ATP. In the inactive form of CDK1, the α1-helix (PSTAIRE motif) in the N-lobe is displaced out of the cleft, such that the γ-phosphate of ATP is not ideally oriented for reaction, and the unphosphorylated activation segment (T-loop) projects from the C-lobe and blocks substrate entry into the cleft.

Cyclin B is a key determinant of CDK1 activity in all eukaryotes. It consists of two cyclin boxes: a well conserved N-terminal 5 α-helix bundle (CBOX1) and a divergent C-terminal 5 α-helix bundle (CBOX2). The destruction box (D-box) that

targets Cyclin B for proteolysis during mitotic exit and the cytoplasmic retention sequence (CRS) that regulates shuttling between the nucleus and cytoplasm are located near the N-terminal. The "MRAIL" motif in the CBOX1 mainly contributes to the hydrophobic groove for recognition of substrates containing the "RXL" sequence, and the "RRASK" motif in CBOX2 is important for Myt1 and Cdc25c recognition (Petri et al., 2007).

The interface of CDK1-Cyclin B spans two lobes of CDK1 (mostly around the α1-helix and less so at the activation segment), and the two cyclin-box folds of Cyclin B (CBOX1 and the first helix of CBOX2) (Fig. 3). Cyclin B-binding remodels the

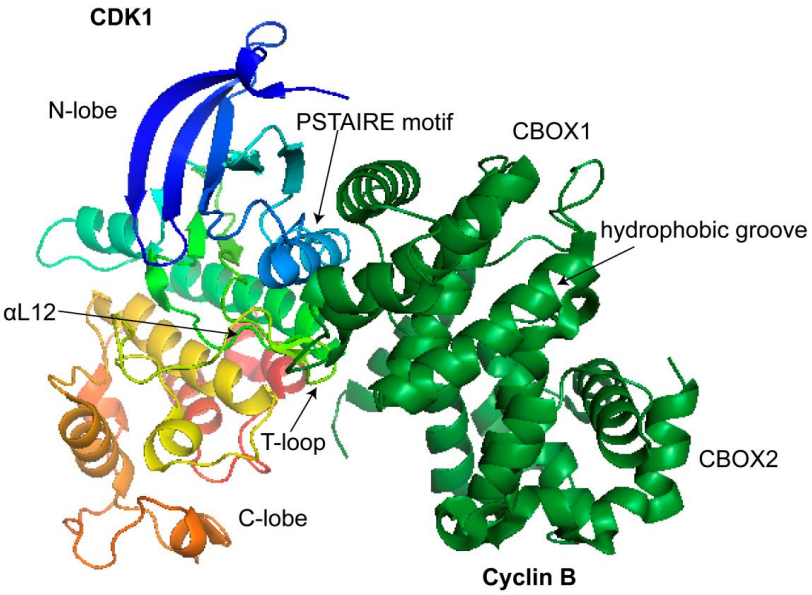

Figure 3. Structure of CDK1-Cyclin B (PDB code 4Y72). CDK1 (rainbow color) is on the left, Cyclin B (green) is on the right. Crucial motifs involved in their interaction and substrate binding are indicated. Adapted from Brown et al (2015).

conformation of CDK1, causing the α1-helix to move inward and the DFG motif (β-hairpin) at the start of activation segment to move further out and deeper into the active site cleft. The phosphorylation of Thr161 in the activation segment and further re-arrangement of CDK1 upon substrate binding position the γ-phosphate of ATP

towards the hydroxyl oxygen of Ser/Thr on the substrate for catalysis. Compared to CDK2-Cyclin A, the overall interface of CDK1-Cyclin B is 30% smaller, and Cyclin B has less interaction with CDK1 at the activation segment, such that the activation segment retains local flexibility after Thr161 phosphorylation and has relaxed substrate specificity (Brown et al., 2015).

1.4.2 Regulation of CDK1 by phosphorylation

Metazoan CDK1 requires phosphorylation by CDK Activating Kinase (CAK) at Thr161 for full activation after cyclin binding (Lolli and Johnson, 2005). CAK consists of CDK7, Cyclin H and Mat1, and it is also part of the transcription factor TFIIH that phosphorylates the RNA polymerase II large subunit C-terminal domain (CTD) to regulate progress of transcription (Palancade and Bensaude, 2003). At mitosis, CAK dissociates from TFIIH and phosphorylates CDKs. CDK1-Cyclin B can phosphorylate Ser164 and Thr170 of CDK7, boost CAK kinase activity, and form a positive feedback loop (Garrett et al., 2001). In the metazoan monomer CDK1, or after CKI binding to CDK1-Cyclin B, the activation segment is not accessible for CAK (Aprelikova et al., 1995). The level of CAK is invariant during the cell cycle, so CAK regulation is not a rate-limiting step for CDK1 activation.

In addition to phosphorylation of the T-loop by CAK, CDK1 is regulated by the opposite effects of Wee1/Myt1 kinases and Cdc25 phosphatases near the N-terminal. Wee1 is a soluble nuclear protein, and phosphorylates Tyr15. Another Wee1-type kinase in vertebrates, membrane-associated cytoplasmic Myt1 kinase, phosphorylates both Thr14 and Tyr15. The inhibitory phosphorylation of Tyr15 at the roof of the ATP binding site doesn't change the overall conformation of CDK but creates an environment which favors non-productive orientation of the γ-phosphate of ATP that is not compatible with an in-line phospho-transfer mechanism (Welburn et al., 2007). This inhibitory phosphorylation is removed by Cdc25 phosphatase to initiate CDK1 activation to drive the G2/M transition. Then active CDK1 can phosphorylate Wee1/Myt1 to inhibit its inhibitors and phosphorylate Cdc25 to further activate its activator, forming double-negative and positive feedback loops, making CDK1 activation switch-like and mitotic entry robust and irreversible.

1.4.3 The trigger of mitotic entry

The trigger of mitotic entry is still an ill-defined event although the central players of G2/M transition have been known for more than 30 years. The focus is first concentrated on Cdc25, a highly conserved dual specificity phosphatase often overexpressed in cancer cells. One Cdc25 is found in lower eukaryotes (fission yeast Cdc25, budding yeast Mih1, *C. elegans* Cdc25, and *Drosophila* String), and three Cdc25 (Cdc25A, B and C) are present in mammals (Boutros et al., 2007). In mammals, Cdc25A is present in the nucleus in late G1, where it activates CDK2-Cyclin E/A during the G1/S transition, and possibly also activates CDK1-Cyclin B during the G2/M transition (Molinari et al., 2000). Cdc25B is present during S phase and is found mainly in the nucleus. A pool of Cdc25B is present on centrosomes in early prophase and first initiates activation of CDK1-Cyclin B on centrosomes (Lindqvist et al., 2005). Cdc25C is activated abruptly during prophase, translocates from the cytoplasm to nucleus concomitant with CDK1-Cyclin B, and is involved in auto-amplification of CDK1 activity (Gabrielli et al., 1997). It is thought that the three Cdc25 isoforms cooperate spatially and temporally to activate their CDK substrates (Boutros et al., 2007).

Multiple kinases have been shown to phosphorylate Cdc25 and regulate its activity, localization, stability and interaction with partners. In species with a single Cdc25 such as fission yeast, CDK1 ultra-sensitively activates Cdc25 through a distributive and disordered multiple site phosphorylation mechanism to refine mitotic entry (Lu et al., 2012). In vertebrates, besides Chk1/Chk2 phosphorylating Cdc25 in response to DNA damage, Aurora A phosphorylates Cdc25B on Ser353 at the centrosome during early prophase at the onset of mitosis (Dutertre et al., 2004). CDK1 phosphorylates Ser214 of Cdc25C, which inhibits 14-3-3 binding on its neighbor residue Ser216 and is required for properly ordering events in mitotic entry (Bulavin et al., 2003). MAPK cascade components are involved in Cdc25 activation for mitotic induction. RSK phosphorylates Cdc25A at Ser293/Ser295 and Cdc25B at Ser353/Thr355 (Wu et al., 2014), and ERK1/2 interacts with Cdc25C during interphase and phosphorylates Cdc25C at Thr48 during mitosis (Wang et al., 2007). This has been proposed as a key initiation step of Cdc25 activation and is also

involved in an amplification loop consisting of Cdc25-CDK1-Mos-MEK-MAPK. The polo-box domain (PBD) of *Xenopus* Polo-like kinase (Plx1) recognizes pT130 of Cdc25C, and Plx1 further phosphorylates and activates Cdc25C (Qian et al., 2001; Elia et al., 2003). In addition, Plk1 and CDK1 phosphorylate human Wee1A at Ser53 and Ser123, respectively, which can serve as an unconventional phospho-degron for recognition by $SCF^{\beta\text{-}TrCP}$ and proteasomal degradation (Watanabe et al., 2004). In *Xenopus* mitosis, Plx1 can dock with CDK1-phosphorylated Thr478 of Myt1, further hyperphosphorylate Myt1 and inhibit it (Inoue and Sagata, 2005). Thus, Plk1 is likely involved in feedback loop of CDK1 activation.

Transcriptional regulation of G2/M genes also contributes to proper mitotic entry. The best known transcription factor involved in G2/M transition is FoxM1, belonging to the evolutionarily conserved Forkhead Box family. FoxM1 binds the promoter region of target genes and enhances transcription. The target G2/M genes include Plk1, Cdc25A/B, cyclin A2, cyclin B1/B2, Nek2, Aurora B, and CENP-F, which regulate essential events such as mitotic initiation and the spindle assembly checkpoint (Laoukili et al., 2005). FoxM1 is the major, but not the only, factor regulating the transcription of G2/M genes, and it collaborates with other transcription factors such as NF-Y and B-Myb to achieve maximal expression of genes essential for mitotic progression. FoxM1 is in the Plk1-Cdc25-CDK1 positive feedback loop. First, FoxM1 transcriptional activity relies on CDK-Cyclins. S/M-phase CDK-Cyclin binds the LXL motif of FoxM1 and phosphorylates Thr596 (human FoxM1B sequence), which recruits the histone acetyltransferase CREB binding protein (CBP) as a coactivator to the FoxM1 transcriptional activation domain, such that several essential G2/M genes are transcribed (Major et al., 2004). Second, active Cdc25A and Plk1 can interact with CDK1-phosphorylated FoxM1, and both associations increase the transcriptional regulatory activity of FoxM1. Cdc25A has been proposed to relieve the inhibitory effect of the N-terminal repressor domain of FoxM1 (Sullivan et al., 2012), whereas Plk1 has been shown to hyperphosphorylate FoxM1 to maximize its activity for the G2/M transition (Fu et al., 2008). Many signaling pathways are integrated at the entry into mitosis (Fig. 4), when

stimulation from positive signaling cascades triggers entry decision with negative regulatory inputs being down regulated.

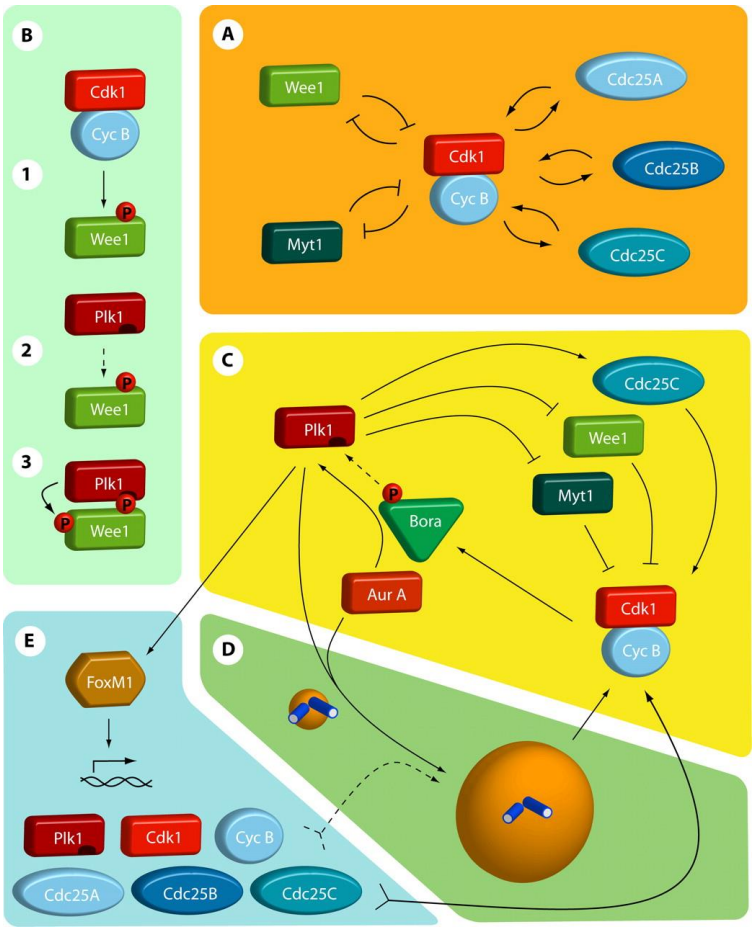

Figure 4. Feedback loops in the mitotic entry network. (A) Activated CDK1-Cyclin B inhibits its inhibitor Wee1/Myt1 kinases, and activates its activator Cdc25 phosphatases, forming a stimulatory feedback loop. (B) Wee1 phosphorylation by CDK1-Cyclin B primes Plk1 binding, such that Plk1 adds further inhibitory phosphorylation on Wee1. (C) CDK1-Cyclin B phosphorylated Bora can bind Plk1 and facilitate Aurora A phosphorylation and activation of Plk1. Subsequently, Plk1 participates in a feedback loop of CDK1 activation, centrosome maturation and local Cyclin B accumulation at centrosomes during late G2 (D), and transcriptional regulation of mitotic genes through activation of FoxM1 (E). Adapted from Lindqvist et al (2009).

1.4.4 Temporal and spatial control of mitotic cyclins

The rise and fall of two novel proteins with the rhythm of sea urchin embryo cell division caught the attention of Tim Hunt during his physiology courses at the Marine Biology Laboratory at Woods Hole in 1982, and later were named as cyclin A and cyclin B (Evans et al., 1983). These were then linked to CDK1 activity and work as an engine to drive mitotic entry and exit in all eukaryotes. In mammalian cells, synthesis of Cyclin A2 initiates in early S phase and is subsequently degraded during prometaphase. Cyclin A2 associates with CDK2 to drive DNA replication in late S phase, before switching to partner CDK1 at the S/G2 boundary to drive early mitotic events, such as chromosome condensation. Cyclin B1 appears during G2 phase and reaches its peak during metaphase just before its degradation. Cyclin B1 associates with CDK1 and collaborates with Cyclin A2-CDK1 to bring about early mitotic events such as chromosome condensation and nuclear envelope breakdown. Cyclin B1 and Cyclin B2 act synergistically at late mitotic events including SAC maintenance (Gong and Ferrell Jr., 2010).

The levels of mitotic cyclins are regulated at both transcriptional (see regulation of G2/M genes above) and translational levels. Temporal control of cyclin B translation is determined by the interplay between cis-acting elements and trans-acting factors. For example, CPE-binding protein (CPEB) binds cytoplasmic polyadenylation elements (CPEs, consensus sequence of $UUUUA_{1\text{-}2}U$) in the 3'UTR of cyclin B, mediating its polyadenylation and translation (Jong and Richter, 2007). Pumilio1 binds Pumilio-binding element (PBE) in the 3'UTR of cyclin B mRNA, forming granules that are asymmetrically distributed in cytoplasm of vertebrate immature oocytes. Granule formation represses translation, and their disassembly temporally controls cyclin B mRNA translation and MPF activation during oocyte maturation (Kotani et al., 2013). In primordial germ cells (PGCs) of *Drosophila* embryos, Nanos spatially restricts cyclin B translation and retains quiescence in PGCs through binding to Nanos Response Elements (NREs) in the cyclin B 3'UTR (Asaoka-Taguchi et al., 1999; Kadyrova et al., 2007).

In addition to the above transcriptional and translational controls, subcellular localization of cyclins is also important. Cyclin A actively shuttles between the nucleus and cytoplasm via the RanGTP pathway and CDK binding, though Cyclin A is mostly present in the nucleus (Jackman et al., 2002). In the cytoplasm, Cyclin A localizes to the centrosome by virtue of the centrosomal localization signal (CLS) near the hydrophobic patch (Pascreau et al., 2010) and interacts with several centrosomal proteins like Nde1, Ckap5, Ofd1, Cep97, Cep131 and Pcm1 (Pagliuca et al., 2011). CDK2-Cyclin A coordinates DNA replication in the nucleus and timely centrosome duplication during S phase in somatic cells (Meraldi et al., 1999). Cyclin A interacts with Cdc6 through the CLS domain and recruits Cdc6 to the centrosome to prevent untimely centrosome duplication when cells progress into S phase. Cdc6 localizes to the proximal side of the centrioles, binds Sas-6 and competitively inhibits the assembly of PLK4-STIL-Sas-6 module that is initial step for daughter centriole formation (Xu et al., 2017). Cyclin A also recruits DNA replication licensing factors MCM5 and Orc1 in a CLS-dependent and CDK-independent manner to centrosome during late S and G2 to prevent centrosome reduplication (Ferguson et al., 2010). In the nucleus, CDK2-Cyclin A drives the progression of DNA replication and has been found specifically at DNA replication foci (Cardoso et al., 1993), where the substrates of CDK2-Cyclin A include the origin recognition complex (ORC), Cdc6, Cdt1 and Sld3 (Pagliuca et al., 2011).

Cyclin B1 localizes to the cytoplasm during G2, and translocates into the nucleus during prophase. It has been proposed that export mediator CRM1 associates with the nuclear export sequence (NES) of Cyclin B1 and actively transports it out of nucleus during interphase (Hagting et al., 1998). During mitosis, phosphorylation of the cytoplasmic retention sequence (CRS) of Cyclin B1 blocks CRM1 interaction, reduces its nuclear export and promotes nuclear accumulation (Yang et al., 1998). It was proposed that Plk1 is required to phosphorylate S147 in the NES of Cyclin B1 to trigger its nuclear import during prophase (Toyoshima-Morimoto et al., 2001). However, further study showed that S133 is the main phosphorylation site catalyzed by Plk1, and phosphorylation by Plk1 didn't cause the translocation of Cyclin B1 into the nucleus (Jackman et al., 2003). Phosphorylated Cyclin B1 prefers to bind active

CDK1 and first localizes at the centrosome during prophase in mammalian cells, suggesting that the centrosome functions as the coordination center for triggering mitosis (Jackman et al., 2003). By using biosensors to monitor CDK1-Cyclin B1 activity in living cells, an elegant study showed that phosphorylation in the NES or Plk1 activity significantly contribute to nuclear import of Cyclin B1 in interphase, but not in prophase. Subsequently, it is the activity of CDK1-Cyclin B1 that triggers rapid translocation of Cyclin B1 into nucleus at late prophase by synchronizing changes in cellular architecture with the nuclear transport machinery (Gavet and Pines, 2010). A spatial positive feedback loop has been proposed recently with Cyclin B phosphorylation promoting nuclear translocation of CDK1-Cyclin B, and conversely, nuclear translocation promoting Cyclin B phosphorylation, thus ensuring rapid and irreversible G2/M phase transition (Santos et al., 2012). A subsequent study indicated that temporal and spatial positive feedback loops are a recurrent cellular strategy that helps to insulate M phase from interphase (Araujo et al., 2016).

1.4.5 Quantitative threshold versus qualitative substrate specificity models

Fission yeast geneticists formulated the CDK1 activity threshold model to explain cell cycle control with a single CDK (Fig. 5 A). In G1, CDK activity is low to allow resetting of replication origins, then increases to a moderate level to initiate S phase and maintains this level to prevent re-initiation of DNA replication. A further increase to the highest level triggers mitosis with a return to low levels during mitotic exit (Stern and Nurse, 1996). This model is supported by quantitative phosphoproteomic analyses of CDK substrates in *S. pombe*, in two aspects (Swaffer et al., 2016). First, CDK substrate phosphorylation is temporally controlled by rising CDK activity from Cdc13-Cdc2. Second, the differential sensitivity of substrates to CDK activity and cyclin-substrate specificity from G1/S cyclins (Cig1, Cig2 and Puc1) work alongside the generic CDK activity threshold to fine-tune the precise timing of substrate phosphorylation at the G1/S transition. However, biochemical evidence from budding yeast and mammals favors a qualitative model (Fig. 5 B). Different cyclin-CDK complexes possess distinct specificity toward substrates because of different substrate binding affinities or different subcellular localizations. In budding yeast, intrinsic CDK1 activity increases in the order Cln2-Clb5-Clb3-Clb2

(G1/S-S-G2/M-M cyclin), and substrate specificity changes with the different cyclin partners. Cln2 uses a hydrophobic LP docking site and different CDK1 consensus motif (PXT/SPK/RX) to recognize G1-specific targets. Clb5 and Clb3 rely on a R/KXL-hydrophobic patch interaction for affinity toward S phase targets in addition to the optimal consensus motif (PXT/SPXK/R). Clb2 doesn't depend on the hydrophobic patch and has a broad range of mitotic targets with both optimal and suboptimal consensus motifs (S/TP) (Kõivomägi et al., 2011). In mammals, multiple CDK-Cyclin complexes temporally interact with overlapping but distinct sets of substrates to coordinate cell cycle control. Quantitative proteomics revealed that Cyclin E1 binds 73 targets, Cyclin A2 binds 227 and Cyclin B1 binds 192, among which only 11% of the targets were shared, 34% were Cyclin A2-specific, and almost one third were Cyclin B1-specific (Pagliuca et al., 2011).

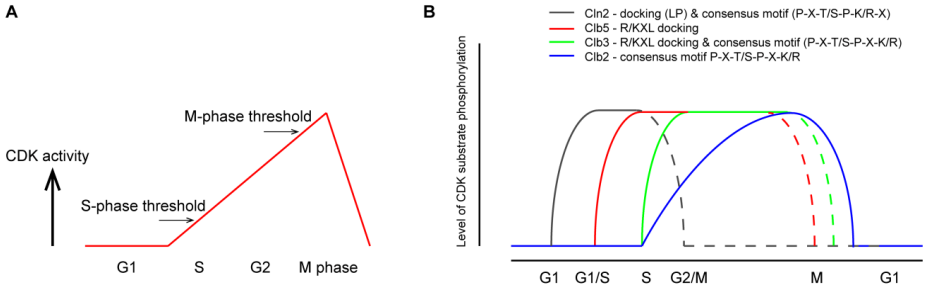

Figure 5. (A) CDK activity threshold model. (B) Substrate specificity model. Adapted from Hochegger et al (2008) and Kõivomägi et al (2011).

1.5 Conservation and divergence of the CDK1-Cyclin B complement

CDK-type kinases have experienced functional diversification during eukaryote evolution. There is one CDK1 ortholog in yeast ($p34^{cdc2}$ in fission yeast and $p34^{cdc28}$ in budding yeast) and its associated cyclins drive the entire cell cycle. In contrast to the single multi-functional CDK expressed in yeast, metazoans express interphase CDKs (CDK4/6 at G1 and CDK2 at S) and a mitotic CDK (CDK1), each associating with diverse cyclins to regulate different cell cycle phases (Harashima et al., 2013). However, mice lacking all the interphase CDKs can develop to mid-gestation indicating that vertebrate CDK1 retains the competence of interacting with interphase

cyclins and driving the entire cell cycle (Malumbres and Barbacid, 2009). The divergence of CDK1 in plant alters the classical view of core cell cycle regulators. *Arabidopsis thaliana* contains multiple CDK1 paralogs. The only PSTAIRE-containing CDK, CDKA;1, binds to D-type cyclins and S-phase-specific Cyclin A3, and primarily regulates cell cycle entry and the G1/S transition, whereas the plant-specific B-type CDKs, CDKB1s and CDKB2s, form complexes with mitotic Cyclin A2 and all B-type cyclins and predominantly regulate entry into and progression through M phase (Van Leene et al., 2010).

Multiple B-type cyclins have been found in eukaryotes, and yeast genetic analyses uncovered a high degree of functional redundancy. A single fission yeast mitotic cyclin $p56^{cdc13}$ is sufficient to drive both S phase and mitosis in the absence of G1 cyclins, although two other B-type cyclins (Cig1 and Cig2) play minor but non-essential roles during G1 and S phase (Connolly and Beach, 1994). Budding yeast has 6 B-type cyclins: Clb1-6, which all associate with Cdc28. They are expressed at different times and control different cell cycle events: clb5 and 6 transcripts increase during G1-S, and control DNA replication; clb3 and 4 increase in mid-S phase as spindle pole bodies separate; clb1 and 2 increase thereafter as the spindle assembles. Clb1-4 are involved in mitotic spindle formation, but Clb2 alone can drive the G2/M transition with some delay (Bloom and Cross, 2007).

Gene knockout/knockdown analyses in a few multicellular model organisms disclose widespread functional compensation among mitotic cyclins, and the importance of each B-type cyclin varies among species. *Drosophila* possesses Cyclins A, B and B3 (Sigrist et al., 1995). Unlike Cyclin B, Cyclin B3 is exclusively located in the nucleus and binds CDK1 (Jacobs et al., 1998). The same study from Jacobs showed that neither Cyclin B nor B3 is essential for mitosis, but Cyclin B seems more critical than Cyclin B3 in mitotic spindle assembly. Both are required for female meiosis, and Cyclin B is also required for male meiosis. Cyclin A is critical for mitosis and is probably involved in chromosome condensation (Knoblich and Lehner, 1993). Triple mutants of Cyclins A, B and B3 arrest at mitosis 15 of the rapid embryonic syncytial cycles with less condensed chromatin, showing that Cyclins B

and B3 collaborate with Cyclin A in mitotic regulation (Jacobs et al., 1998). Real-time analysis of cyclin RNAi in syncytial embryos showed that mitotic events are coupled to the appearance and destruction of Cyclins: Cyclin A degrades before metaphase, Cyclin B degrades at the metaphase-anaphase transition, and Cyclin B3 degrades during anaphase (McCleland et al., 2009). Cyclins A and B restrain the APC/C, whereas Cyclin B3 promotes the metaphase-anaphase transition by activating the APC/C (Yuan and O'Farrell, 2015). In *Drosophila* female meiosis, Cyclin A seems to play a major role in promoting NEBD and bi-orientation of homologs in meiosis I, Cyclin B is required for metaphase maintenance and meiotic spindle organization, and Cyclin B3 is required for anaphase progression (Bourouh et al., 2016).

C. elegans expresses CYB-1, CYB-2.1, CYB-2.2 and CYB-3, that exhibit distinct as well as overlapping functions. CYB-1 is required for full condensation and proper congression of chromosomes at the metaphase plate (van der Voet et al., 2009). CYB-3 is mostly nuclear and interacts with CDK1. The role of CYB-3 is debated. Genetic studies showed that CYB-3 is required for anaphase chromosome segregation by promoting mitotic dynein function to strip SAC components away from kinetochores (Deyter et al., 2010). However, double or triple dosage of CYB-3 combined with loss of dynein can rescue MDF-1 (Mad1 homolog) mutants, supporting the positive influence of CYB-3 on the SAC (Tarailo-Graovac et al., 2014). The most recent study showed that CYB-3 also supports S-phase progression and is a major contributor to promoting NEBD in mitotic entry (Michael, 2016). In meiosis, CYB-1, CYB-2 and CYB-3 show more redundancy than in mitosis. Depletion of all the B-type cyclins causes diakinesis arrest, similar to the CDK1 knockdown phenotype (van der Voet et al., 2009).

Xenopus has 5 B-type Cyclins, B1 to B5, with B4 and B5 expressed as maternal mRNAs until the mid-blastula transition (MBT). This extent of Cyclin B diversity is only known in frogs and is believed to be an adaptation to the large size of the oocyte (Hochegger et al., 2001). Due to pseudo-tetraploidy of *Xenopus laevis*, cyclin B1 has two variants: α and β, and both contribute to CDK1 activity during the

first 5 embryonic divisions (Tsai et al., 2014). Though most subtypes of Cyclin B are present during female meiosis, maternal stockpiles of Cyclin B2 and B5 can drive meiosis I without new cyclin synthesis, while newly synthesized cyclin B1 and B4 are required for meiosis II. Cyclin B2 localizes in and around the germinal vesicle, and is involved in the first meiotic spindle formation, possibly by stimulating phosphorylation of bipolar kinesin Eg5 in the perinuclear region (Yoshitome et al., 2012).

In mammals, three B-type Cyclins have been identified: B1, B2 and B3. Cyclin B1 associates with microtubules and centrosomes in the cytoplasm during interphase, and is also present in free form in cytoplasm. It translocates to the nucleus at prophase, then localizes to chromatin, unattached kinetochores and the spindle (Bentley and King, 2006). Cyclin B2 associates with intracellular membranes, the Golgi apparatus and centriolar satellites during interphase (Spalluto et al., 2013). A small amount of Cyclin B2 has been observed in the nucleus before NEBD and co-localizes with centrosomes and the spindle. Most Cyclin B2 disperses throughout the cell after NEBD (Jackman et al., 1995). The subcellular localization of Cyclin B1 and B2 is determined by their NH_2 termini. NH_2 termini swapping experiments demonstrated that replacing the NH_2 terminus of Cyclin B1 with a corresponding B2 fragment (1-130 aa) can guide Cyclin B1 to the Golgi apparatus. Conversely, replacing NH_2 terminus of Cyclin B2 with the corresponding B1 fragment (1-144 aa) distributes Cyclin B2 throughout the cytoplasm, but not to the nucleus (Draviam et al., 2001). Vertebrate Cyclin B3 shares the properties of both Cyclins A and B1 and localizes in the nucleus throughout the cell cycle. Chicken Cyclin B3 interacts with both CDK1 and CDK2 and exhibits histone H1 kinase activity (Gallant and Nigg, 1994), whereas mouse Cyclin B3 only interacts with CDK2 and doesn't have histone H1 kinase activity (Nguyen et al., 2002).

In terms of the temporal expression of mammalian B-type cyclins, Cyclin B1 and B2 are co-expressed from G2 to M phase and then degraded after metaphase in proliferating cells, though B2 is expressed at a considerably lower level (Brandeis and Hunt, 1996). Cyclin B3 is degraded over the metaphase to anaphase transition

after Cyclin B1 degradation (Nguyen et al., 2002). At the tissue level, Cyclin B1 and B2 co-exist in the intestine, spleen, thymus, ovary and testis (Brandeis et al., 1998), whereas Cyclin B3 is restricted to the ovary and testis. During spermatogenesis, Cyclin B1 is mostly expressed in early zygotene, Cyclin B2 shows higher expression in late pachytene and diplotene stages, and Cyclin B3 is expressed in leptotene and zygotene stages (Nguyen et al., 2002). Gene knockout mice showed that *cyclin B1-null* mice die at about E10.5 in *utero* whereas *cyclin B2-null* mice are viable and fertile, though with reduced body size (Brandeis et al., 1998) and *cyclin B3-null* males are fully fertile, though females are sterile (Mehmet Erman Karasu, personal communication). These genetic manipulations demonstrate that Cyclin B1 is essential, Cyclin B2 is dispensable, and Cyclin B3 is dispensable in mitosis and male meiosis, but required in female meiosis. The division of functions between mammalian B-type cyclins is as follows: Cyclin B1-CDK1 reorganizes the cytoskeleton in G2 phase and is involved in chromosome condensation and NEBD when it translocates to the nucleus. It also promotes spindle assembly, spindle checkpoint induction on unattached kinetochores (Chen et al., 2008) and mitosis maintenance during metaphase. It further coordinates abrupt separation of sister chromatids by promoting CDK1 inhibitory activity on separase through direct interaction with separase prior to the onset of anaphase (Shindo et al., 2012). Cyclin B2-CDK1 has limited functions in Golgi fragmentation, which can be substituted by Cyclin B1 with similar efficiency. It also has a critical function in centrosome separation through triggering the activation of Aurora A and Plk1 during G2 (Nam and van Deursen, 2014). Cyclin B2 compensates some functions of Cyclin B1 when a residual level of Cyclin B1 is present in knockdown assays on mammalian cells (Huang et al., 2013). Cyclin B3 bound CDK1 or CDK2 promote the metaphase to anaphase transition during meiosis I in female mice by activating APC/C^{cdc20} independently of SAC activity (Zhang et al., 2015b). Such diverse functions among the same subfamily of B-type cyclins in metazoans are intriguing, given that the main core cell cycle regulatory machineries are conserved through evolution. Apparently, gene duplications and subcellular targeting have allowed some cell cycle regulators to exert distinct regulatory modes.

1.6 Amplification of *Oikopleura dioica* cell cycle regulatory genes and their evolutionary implications

Many cell cycle related genes in *Oikopleura dioica* are amplified, and many of these isoforms are in addition, alternatively spliced or use alternative promoters (Campsteijn et al., 2012). Some of the amplified core cell cycle regulatory genes relevant to this thesis work are presented in Table 1.

Table 1. Cell cycle regulatory gene complements in metazoan models.

	Od	Hs	Ci	Dm
CDK1	5	1	1	1
CDK2	1	1	1	1
CDK4/6	1	2	1	1
Cyclin D	4	3	1	1
Cyclin E	1	2	1	1
Cyclin A	1	2	2	1
Cyclin B	3	2	1	1
Cyclin B3	2	1	1	1
Cdc25	5	3	1	2
Wee1	2	1	1	1
Myt1	1	1	1	1
Plk1	2	1	-	1
Ringo	2	3	1	ND
Cks	2	2	ND	ND
CKI	3	7	2	2
Aurora A	1	1	1	1
Aurora B/C	1	2	-	1
INCENP	2	1	1	1
Survivin	2	2	1	1
Borealin	ND	1	1	2

Note: Od, *Oikopleura dioica*; Hs, *Homo sapiens*; Ci, *Ciona intestinalis*; Dm, *Drosophila melanogaster*. ND, not determined.

Gene duplication leads to four possible outcomes: pseudogenization, conservation of gene function, subfunctionalization and neofunctionalization (Zhang, 2003). Purifying selection can prevent duplicate genes from diverging and sustain similar sequence and function. In subfunctionalization, some functions of the ancestral gene are inherited by nearly neutral duplicate genes, which are fixed by positive selection. Subfunctionalization can operate on gene expression levels through division of expression patterns or reduced expression of duplicate genes to maintain functional redundancy, with such traits applying to recent duplication (Qian et al., 2010). Subfunctionalization can also operate at the protein function level, where each duplicate gene becomes better at carrying out certain functions of the progenitor gene. Neofunctionalization means that the duplicated gene obtains novel functions, which requires a number of genetic changes. Gene duplication is believed to be a driving force of evolution by providing new genetic material for selection, altering genome plasticity, establishing complex gene networks and species-specific functions.

This thesis examines roles of CDK1 and Cyclin B duplications in female meiosis of *O. dioica* and on duplications of key components of the chromosomal passenger complex (CPC) during embryonic mitoses. The core CDK1 kinase, restricted to a single gene locus in all other studied metazoans, has been dramatically expanded to five paralogs in *O. dioica*. The CDK1 PSTAIRE motif, invariant among metazoans, has been diversified into P(S/P/A)TS(I/V/L)RE variants, implying that individual CDK1 paralogs may have distinct cyclin binding partners and have evolved specialized functions during endocycling, mitosis and meiosis (Campsteijn et al., 2012). The S_2 to P_2 substitution in CDK1b/d mimics plant CDKB, which is known to interact with A and B type Cyclins and function in M phase (Van Leene et al., 2010). The A_4 to S_4 substitution in all CDK1 paralogs mimics the T_4 residue in CDK4/6, raising the possibility of interactions between CDK1 paralogs and D-type Cyclins. CDK1d/e and Cyclins Ba/b, B3a exhibit overlapping expression patterns in the ovary during oogenesis, contrasting the ubiquitous expression of CDK1a/b/c throughout *O. dioica* development. The expression profiles of B-type cyclins show a general fit to their known roles in mitosis and meiosis. The current study explores

possible specializations in these putative roles during meiosis resumption and oocyte maturation. The process of meiosis resumption is driven by maturation promoting factor (MPF) and recapitulates biochemical mechanisms regulating the G2/M transition of mitosis, which will be described in detail later.

Within the CPC complex, there are unusual duplications of both INCENP (INCENPa and b), the scaffolding component of the CPC, and the centromeric targeting module Survivin (SurvivinA and B). INCENP duplication is very rare in metazoans, and thus far the only other known species with INCENP paralogs is chicken, where one of the paralogs is only expressed at very low levels and cannot sustain CPC function (Xu et al., 2009). The interplay between the CPC, CDK1-Cyclin B and Plk1 controls mitotic entry and exit. Under the circumstances of CPC duplication, how such interplay spatiotemporally modulates different kinase activities to adapt to rapid cell divisions is a fascinating question.

Do the amplifications of core cell cycle regulators belong to any aforementioned categories of gene duplication? Given the sometimes inconsistent functional evidence of these regulators in vertebrate and invertebrate model organisms, we set out to investigate the functional diversification and potential redundancies of amplified CDK1, B-type Cyclins and INCENPs during *O. dioica* development.

1.7 The life cycle of *Oikopleura dioica*

Oikopleura dioica is an urochordate appendicularian (also sometimes referred to as larvaceans). Together with ascidians and thaliaceans, they are the closest living relatives to vertebrates (Delsuc et al., 2008). Appendicularians are distributed globally, and are among the most abundant zooplankton in marine ecosystems (Troedsson et al., 2002). Appendicularians reside inside an extracellular, gelatinous house, which is secreted from the oikoplastic epithelium and used for filter-feeding. Water flow through the house is controlled by stereotypical movements of the tail, which is retained after metamorphosis in this lineage. The animals continuously renew their houses every four hours (15℃), and discarded houses are a main source of marine snow, providing food for benthic animals and contributing to vertical

carbon flux in the ocean (Troedsson et al., 2009). In addition to its ecological significance, *O. dioica* possesses a highly compact genome of 70 MB with 18,020 predicted genes and is an emerging model in phylogenomic studies (Denoeud et al., 2010).

O. dioica is the only dioecious appendicularian and has a short life span of 6 days at 15℃. Mature females lay naked eggs (about 80 μm diameter) without accessory follicle cells surrounding the chorion. The oocytes arrest at metaphase I prior to fertilization. Post-fertilization, the egg extrudes the first polar body and completes MI in 5 min, and then extrudes the second polar body and completes MII in 15 min. Maternal and paternal nuclei migrate towards the egg center, duplicate their chromosomes, and enter the first mitosis at about 30 min post fertilization. The first and second divisions are symmetric and meridional, after that, asymmetric divisions are found in different cell lineages (Stach et al., 2008). Gastrulation starts at 2 h at the 32-cell stage, with the ingression of vegetal cells. Neurulation commences at the 64-cell stage. The tailbud stage is visible at 4 h, and the larvae hatch at 6 h to become free-swimming. Metamorphosis occurs at 12 h, during which the tail undergoes a 90° counterclockwise rotation relative to the trunk, known as the tail shift (Nishida, 2008). Most somatic cells enter endocycles to support the rapid body growth, and the trunk size increases from 200 μm at day 1 to 1000 μm at day 6. The epithelial cells are grouped into bilaterally symmetric territories according to nuclear size, and are highly polyploid, ranging from 34 C to 1300 C at maturity (Ganot and Thompson, 2002). In Day 3 animals, germline nuclei undergo endomitosis, and many of the intestinal cells continue to undergo mitotic proliferation. Meiosis in females starts from Day 3.5, and gonads increase rapidly in size from this point onwards. In males, the testes also expand rapidly in size from Day 3.5 onwards but meiotic entry occurs later at Day 6. When animals are sexually mature, the ovarian wall ruptures at an anlagen referred to as the “moustache” (Ganot et al., 2006) to release oocytes into the surrounding seawater. Males release sperm through the spermiduct. The animals are semelparous, dying after spawning, and fertilization occurs in seawater (Fig. 6).

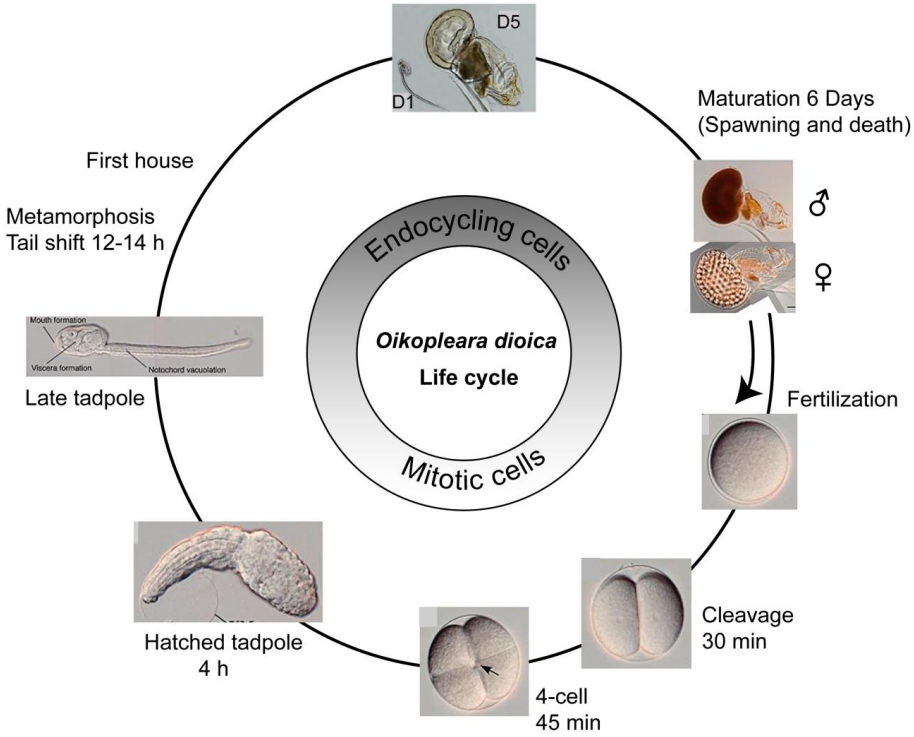

Figure 6. The life cycle of *O. dioica*. See text for details. Modified from Thompson and Moosmann.

1.8 Oogenesis

1.8.1 Meiosis

Meiosis is the specialized cell division, in which DNA duplicates once but chromosomes segregate twice, producing haploid gametes from diploid parents. Here, we focus on female meiosis I, where homologous recombination and subsequent segregation generate genetic diversity. During this process, chromosome segregation errors are the major contributing factor to aneuploidies, such as Down's syndrome, while meiosis II is very much like mitosis. After meiotic S phase, sister chromatids are tightly linked by cohesins. In the canonical meiotic program, programmed double-strand breaks (DSBs) occur during G2/leptotene and result in linkage between homologous chromosomes, leading to homolog pairing (Morgan, 2007). Leptotene

chromosomes are thin, thread-like structures, and co-oriented sister linear loops radiate from a central axis, which comprises a meshwork of protein/DNA, associated with the recombination complex (Spo11 and Dmc1). Presynaptic alignment is visible as a series of bridges between axes with an inter-axis distance of ~400 nm. In zygotene, synapsis brings homolog axes closer to ~100 nm and synaptonemal complexes (SC) are established all along the homolog axes. The SC is an evolutionary conserved ladder-like structure, consisting of lateral elements (LEs) that are connected by transverse filaments (TFs) and a central element (CE). The SC may stabilize chromosome structure around mature crossovers (CO) and have a positive role in homologous recombination. The SC is complete in pachytene and disassembles after COs mature at the end of pachytene. Then chromosomes condense again in diplotene and chiasmata appear. Cohesins are almost completely lost between sister chromatid arms except at COs between homologous chromosomes, which provide the physical links for congression of bivalents at the metaphase plate of meiosis I. Diakinesis is the last stage in prophase I before entering the first meiotic division.

In some organisms, DSB-independent homologous pairing has been reported. In *Drosophila* male meiosis, during which chiasmata do not form, major autosome pairing relies on multiple interstitial sites in euchromatin, and sex chromosome pairing relies on homology of tandem arrays of rDNA in heterochromatin (McKee, 2004). In *Drosophila* female meiosis, three large homologous chromosomes pair before DSB formation and chiasmata form afterward, whereas the small fourth homologous chromosome pair lacks chiasmata (Zickler and Kleckner, 2015). In *C. elegans*, each chromosome contains a pairing center (PC) at the end of chromosome, which recruits PC protein in order to anchor chromosomes to the nuclear envelop and the microtubule cytoskeleton to permit homolog sorting through cytoplasmic forces and to initiate synapsis (Tsai and McKee, 2011). In female silkworms, homologous chromosomes form a modified SC through heavy deposition of the lateral components as a substitute for chiasmata such that homolog segregation is ensured (Rasmussen et al., 1977).

1.8.2 Comparison of oogenesis models

Oogenesis originates as a germline cyst in many metazoans, in which a group of inter-connected cells are produced from a single founder cell by synchronous divisions but with incomplete cytokinesis, leaving intercellular bridges (Pepling et al., 1999). The cyst organization is thought to ensure developmental synchrony of the germline and to facilitate reorganization and transport of organelles between the cells inside the cyst. The cyst stage only exists in the pre-adult stage of most vertebrate females. Female mice enter meiosis I at E13.5 and cyst breakdown occurs around the time of birth, coincident with massive apoptosis of germ cells (known as attrition), and formation of the primordial follicle pool that consists of a single small oocyte in pachytene, surrounded by a monolayer of somatic pre-granulosa cells (follicle cells) (Motta et al., 1997). Oocyte determination occurs during pachytene, followed by vitellogenesis (Lei and Spradling, 2013). Granulosa cells rapidly proliferate to several layers, and communicate with the oocyte via gap junctions, enabling oocyte growth (Grive and Freiman, 2015). In contrast to such vertebrates, the germline cyst is a long-lived structure in some insects, and cellularisation happens at the very end of oogenesis (Matova and Cooley, 2001). In the *Drosophila* 16-cell egg chamber, two cells with four intercellular bridge connections enter meiosis. One of these differentiates as the future oocyte during pachytene while the other loses meiotic features and joins the other 14 cyst cells as polyploid nurse cells (Bastock and St Johnston, 2008). The egg chamber is surrounded by a single follicular layer originating from somatic stem cells. Nurse cells synthesize nutrients, RNA, and protein for transport to the growing oocyte by cytoplasmic streaming. During stage 11, nurse cells contract and dump their cytoplasm into the oocyte within 30 minutes. They then undergo apoptosis, leaving behind the full-sized oocyte (Bastock and St Johnston, 2008). How the hermaphrodite *C. elegans* syncytial gonad is formed is not fully understood yet. Germline nuclei are arranged around the cytoplasmic core (rachis) and are connected through cytoplasmic bridges, with somatic sheath cells comprising the outer layer of gonad. Germ cells either differentiate as oocytes or undergo apoptosis when reaching the pachytene zone. At the bend of the gonad arm,

actomyosin-dependent cytoplasmic streaming drives oocyte growth, which also requires the presence of major sperm protein (MSP) (Kim et al., 2013).

O. dioica oogenesis occurs in a single-cell coenocyst, which contains thousands of inter connected germline nuclei and is surrounded by a monolayer of follicle cells on both the inner and outer surfaces (Ganot et al., 2006). The follicle cells have gap junction contacts with the coenocyst and actin bundles project into the coenocyst. The animal is semelparous and the germline progresses synchronously through an oogenesis that is divided into 5 phases (P1-P5) based on distinct cellular and meiotic events (Ganot et al., 2008). Post-metamorphic proliferation of germline nuclei in a syncytium occurs until Day 3, when at P1, equal proportions of germline nuclei either enter meiosis or asynchronous endocycles to become polypoid nurse nuclei. P2 (Day 3-3.5) corresponds to leptotene and zygotene stages, during which meiotic nuclei undergo telomere bouquet clustering. P3 (Day 3.5-5.5) corresponds to pachytene and diplotene, during which synaptonemal complexes have formed and the pro-oocytes become obvious, connected to the common coenocystic cytoplasm through ring canals. Meiotic nuclei locate to the pro-oocyte cortex (future animal pole) opposite ring canals (Ganot et al., 2007). In this region, clustered nuclear pore complexes (NPC) localize adjacent to the telomere bouquet. During P3, nurse nuclei increase in size to support global growth of the coenocyst. Oocyte selection occurs during P4 (Day 5.5-6), with a subset of meiotic nuclei continuing meiosis. Chromosomes are condensed and show a stereotypic π-configuration, which represents three pairs of homologous chromosomes (bivalents). The NPC cluster is fragmented and an MTOC-like organizing center (OC) contacts selected meiotic nuclei at NPC cluster fragments. Pro-oocytes harboring selected meiotic nuclei, begin growing synchronously via cytoplasmic transfer through ring canals. In concert, the common cytoplasm experiences general rearrangement of its actin network, and non-selected meiotic nuclei lose meiotic features and associate with invagination pockets of nurse nuclear envelopes. During P5 (Day 6-6.5), pro-oocytes achieve their maximal volume, close the ring canals and undergo the final maturation stage. Non-selected meiotic nuclei and nurse nuclei undergo apoptosis. At spawning, mature oocytes are arrested at metaphase I.

Oocyte selection usually occurs when immature oocytes or pro-oocytes exit pachytene but prior to vitellogenesis (Fig. 7). Animals may restrain the number of developing oocytes prior to vitellogenesis in order to achieve successful oocyte production, especially in semelparous species. *O. dioica* adapts reproductive output to fluctuating nutrient conditions by the selection of the number of oocytes to grow. The accumulated resources of cytoplasm in the coenocyst dictate the spawned oocyte number. *O. dioica* experiencing food limitation or high culture density exhibit significantly reduced fecundity (Subramaniam et al., 2014). On the contrary, under favorable conditions such as algal blooms, oocyte production increases over two orders of magnitude, supporting rapid rates of population increase (Troedsson et al., 2002).

Another salient feature of *O. dioica* oogenesis is that meiotic nuclei are essentially transcriptionally quiescent (Ganot et al., 2008). Only two small meiotic nuclear transcription loci are present. The three bivalents are tightly enclosed by the nuclear envelope, and do not form a germinal vesicle, similar to the transcription mode of syncytial oogenesis in higher insects and nematodes, but different from vertebrates, whose germline cysts break down shortly after entry into meiosis. Thereafter the nucleus in vertebrate oocytes forms a large germinal vesicle that is transcriptionally active. It has been reported that in the solitary ascidian *Ciona* (Silvestre et al., 2011) and thaliacean salps (Boldrin et al., 2009), the two sister classes to appendicularians, individual oocytes cellularize during early oogenesis, and contain a readily identifiable germinal vesicle, that is surrounded by follicle cells during vitellogenesis and after spawning. Representatives of cephalochordates (*Branchiostom*), echinoderms (sea urchin), and hemichordates (*Saccoglossus*) all possess germinal vesicles during oogenesis (Frick et al., 1997). To our knowledge, *Oikopleura* is the only exception among deuterostomes in that a germinal vesicle is not formed during oogenesis.

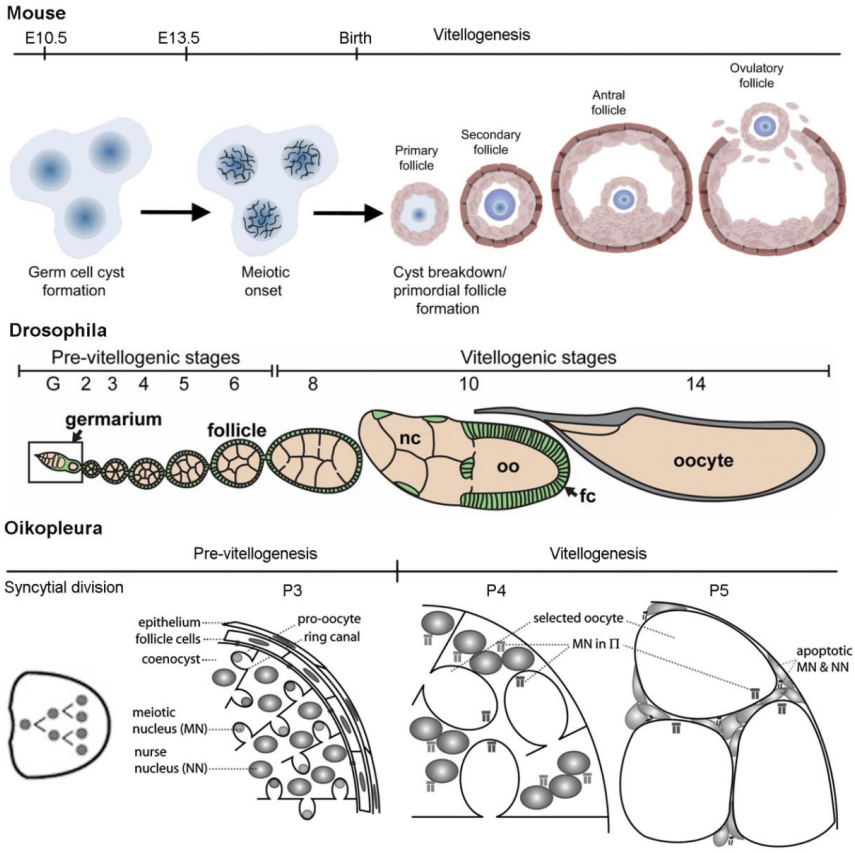

Figure 7. Comparison of oogenesis between mouse, *Drosophila* and *O. dioica*. Mouse primordial germ cells (PGC) colonize the somatic gonad at E10.5, undergo incomplete division and form a cyst, before entering meiosis I at E13.5. The cyst breaks down around the time of birth and forms a primordial follicle pool. During vitellogenesis, primordial follicles develop into the primary, secondary and antral follicles. During puberty, oocytes mature before ovulation. In *Drosophila*, one descendant cell of a germline stem cell undergoes 4 incomplete divisions and forms a 16-cell egg chamber, which is covered by a layer of follicle cells. One cell is selected as the future oocyte as the cyst travels through the germarium. Vitellogenesis starts from stage 8 and oocytes mature at stage 14. In *O. dioica*, germline cells undergo syncytial division and form a coenocyst, which is surrounded by a monolayer of follicle cells. After cell fate commitment of meiotic nuclei and nurse nuclei (1:1 ratio), meiotic nuclei are enclosed in pro-oocytes during P3, oocyte selection and vitellogenesis occur at P4, and oocyte cellularization occurs at P5 before final maturation. Modified from Grive and Freiman (2015) and Ganot et al (2008).

1.9 Developmental control of oocyte maturation

1.9.1 Meiosis arrest and resumption

In most animals, oogenesis arrests at two points (Von Stetina and Orr-Weaver, 2011). The primary arrest point is at prolonged diplotene of prophase I (called dictyate in mammals), permitting oocyte growth, differentiation and the stockpile of maternal mRNAs and proteins for future embryonic development. The duration of prophase I arrest varies depending on the species. It may last for an extraordinary long period - several months in mouse or decades in women, while it only lasts about 2 days in *Drosophila* and *O. dioica*, and about 23 minutes in hermaphrodite *C. elegans* when sperm is present (Greenstein, 2005). The primary arrest is released in response to appropriate hormonal stimuli, and this process is called meiosis resumption or oocyte maturation, which enables oocytes to continue meiotic division. After primary arrest, most species, except nematodes, will experience a secondary arrest at metaphase I (*Drosophila*, some mollusks, tunicates), metaphase II (most vertebrates) or the pronuclear stage (sea urchins and starfish) (Von Stetina and Orr-Weaver, 2011). The secondary arrest serves to coordinate the completion of meiosis with fertilization and is maintained by elevated MPF activity and cytostatic factor (CSF). The cMOS/MEK/MAPK pathway and early mitotic inhibitor 2 (Emi2) are responsible for APC/C inhibition during metaphase II arrest (Kubiak et al., 2008).

Maturation inducing hormones have been identified, such as luteinizing hormone (LH) in mammals, MSP in *C. elegans*, 1-Methyladenine (1-MeAde) in starfish, and progesterone (Pg) in *Xenopus* (Von Stetina and Orr-Weaver, 2011). LH binds G protein-coupled receptors in the mural granulosa cells, reduces cGMP in the somatic follicular cell layer and blocks its diffusion through gap junctions between follicular cells and the oocyte. PDE3A (phosphodiesterase) is activated and hydrolyzes cAMP (high level of cAMP inhibit meiotic maturation), and prophase I arrested oocytes resume meiosis (Norris et al., 2009).

Maturation promotion factor (MPF) promotes meiosis resumption in a wide variety of species including *Xenopus*, clam, starfish, several fish species, mouse, etc (Nagahama and Yamashita, 2008). MPF shows generally conserved and species-

specific regulatory mechanisms in terms of its formation, activation and upstream and downstream molecular pathways during oocyte maturation. However, the modes of synthesis of its cyclin B component vary from species to species. Cyclin B protein exists in immature oocytes (germinal vesical stage) of marine invertebrates and most higher vertebrates, forming pre-MPF with a small pool of CDK1 (Gautier and Maller, 1991). The level of pre-MPF is enough to drive meiotic maturation in mouse and starfish, although the rate of cyclin B1 synthesis can control the length of the first meiotic M phase (Polanski et al., 1998). In *Xenopus*, the pre-MPF stockpile is completely inhibited by Myt1 during prophase I arrest and newly formed Cyclin B-CDK1 is required to phosphorylate and inhibit Myt1, triggering an MPF auto-amplification loop along with newly synthesized Mos-MAPK (Gaffré et al., 2011). In striking contrast, pre-MPF doesn't exist in immature oocytes of some fish species, such as goldfish (Yamashita et al., 1995). Cyclin B protein is synthesized just before GVBD, and Cyclin B synthesis and CDK1 activation by Thr161 phosphorylation are critical for meiotic maturation (Yamashita, 1998). CDK1-Cyclin B is first activated in the cytoplasm, and then translocates to the nucleus. GVBD follows in 30 minutes in mouse (Marangos and Carroll, 2004) and 5 minutes in starfish (Ookata et al., 1992). These observations indicate that meiosis-specific modulations of CDK1-Cyclin B share some common pattern among species, as well as distinct features as to when Cyclin B protein is synthesized and how it is distributed during oogenesis and oocyte maturation.

1.9.2 The relationship between Cyclin B-CDK1, the MAPK pathway, Plk1 and Greatwall kinase during meiosis resumption

Some general and specific signaling pathways have been clarified in *Xenopus* and starfish (Fig. 8). In *Xenopus*, upon progesterone stimuli, PKA (cAMP-dependent protein kinase A) is inhibited, partially relieving the S109 phosphorylation of ARPP19 (cAMP-regulated phosphoprotein-19) (Dupre et al., 2014). This weakly antagonizes PP2A-B55δ and promotes protein synthesis of MOS or Cyclin B, leading to inhibition of Myt1 and initial activation of CDK1. Thereafter, Gwl (Greatwall kinase) phosphorylates ARPP19 at S67, which strongly inhibits PP2A. MOS-MAPK and Plk1 are involved in an MPF auto-amplification loop by phosphorylating Cdc25,

shifting the balance of Cdc25/Myt1 and irreversibly driving meiosis resumption (Dupre et al., 2014). In starfish, the MAPK pathway, Plk1 and Gwl are all downstream of CDK1 activation. MAPK and Plk1 activate Cdc25 and inhibit Myt1 to ensure the meiosis I to II transition (Kishimoto, 2011). Gwl is also regarded as a critical component of MPF by suppressing PP2A-B55 (Hara et al., 2012). In *C. elegans*, MAPK is necessary for the progression of pachytene and is inactivated after pachytene exit. Sperm reactivate MAPK in proximal oocytes to promote M phase

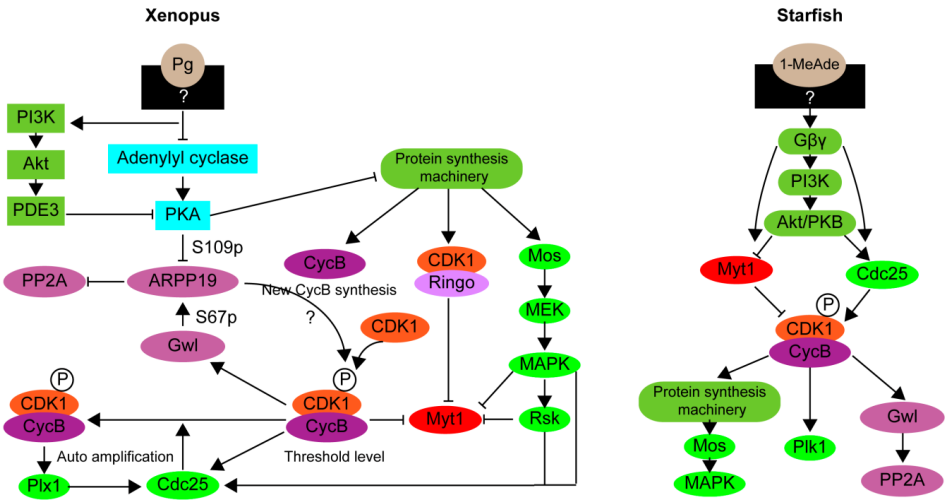

Figure 8. Meiosis resumption in *Xenopus* and starfish. In *Xenopus*, progesterone (Pg) triggers inactivation of PKA, and partially relieves S109 phosphorylation of ARPP19, which is required for initial activation of CDK1, possibly by controlling protein synthesis or facilitating S67 phosphorylation of ARPP19 by Gwl. On the other hand, newly synthesized Cyclin B binds CDK1 and inhibits Myt1, and Ringo/CDK1 also phosphorylates and inhibits Myt1 during early stages of meiosis resumption. Once initiating amounts of CDK1 are activated, an MPF auto-amplification loop is triggered. The MOS-MAPK-Rsk pathway, Plx1, Gwl and ARPP19, are all involved in this auto-amplification loop. In starfish, 1-MeAde triggers release of Gβγ and activates the PI3K-Akt/PKB pathway, which directly inhibits Myt1 and activates Cdc25 together with the atypical Gβγ pathway, leading to MPF activation. Protein synthesis, the MOS-MAPK pathway, Plk1 and Gwl all function downstream of this activation. Modified from Kishimoto (2003).

entry, but the exact function of MAPK in oocyte maturation is not fully understood (Hajnal and Berset, 2002). In *Drosophila*, although MAPK is active during oocyte maturation, MOS is not essential for meiosis, indicating the MOS-MAPK pathway might be dispensable (Ivanovska et al., 2004).

1.9.3 Meiotic spindle assembly

Canonical centrosomes are lost during early stages of oogenesis in most metazoans except starfish, and the meiotic spindle is assembled independently of centrosomes (Dumont and Desai, 2012). Two chromatin-induced spindle assembly pathways have been shown to replace centrosomes for microtubule nucleation and meiotic spindle assembly in oocytes, though their relative contributions and interactions in this process are less known. In one pathway, a RanGTP gradient is established near chromosomes and unloads spindle assembly factor (SAF) cargos from importins with the collaboration of RCC1 on chromosomes (Kalab and Heald, 2008). This allows the SAF to associate with the spindle, or specific sites within the spindle apparatus, and facilitates microtubule nucleation. This RanGTP gradient is present during mouse and *Xenopus* meiotic maturation, but it is not essential for meiosis I. A longer spindle, or a delay in establishing spindle bipolarity are found when the RanGTP pathway is inhibited. This pathway is essential for meiosis II (Dumont et al., 2007).

In a second pathway, Aurora B kinase, a component of the chromosomal passenger complex (CPC), phosphorylates and inhibits mitotic centromere-associated kinesin (MCAK), a negative regulator of microtubule polymerization in the centromeric region (Andrews et al., 2004). This creates a local favorable environment for microtubule polymerization. Phosphorylated MCAK is recruited to the inner centromere and stable kinetochore-microtubule attachments are promoted. Aurora B also phosphorylates and inhibits Op18/stathmin, a microtubule destabilizing protein that can sequester tubulin heterodimers and cause microtubule catastrophe (Houghtaling et al., 2009). The CPC localization pattern at metaphase I is not as consistent as during mitosis, and is species-dependent (Dumont and Desai, 2012). In mouse, Aurora B localizes at kinetochores, and Aurora C localizes along the chromosome arms that hold bivalents together (Shuda et al., 2009). In *Drosophila*,

CPC localizes on the equatorial region of spindle (Colombié et al., 2008). In *C. elegans*, Aurora B localizes to the chromosome arms distal to chiasmata (Rogers et al., 2002).

Taking advantage of high-resolution live imaging, a model of meiotic spindle assembly has been proposed in mouse oocytes (Schuh and Ellenberg, 2007; Clift and Schuh, 2015). Mouse immature oocytes form more than 80 acentriolar microtubule organizing centers (aMTOC) *de novo* from the cytoplasmic microtubule network. These aMTOCs move centripetally and congress around the nucleus. Plk1 triggers the decondensation of aMTOCs, and then BicD2-anchored dynein stretches aMTOCs into ribbons along the nuclear envelope. Subsequently, GVBD occurs, KIF11 further fragments aMTOCs, and microtubules massively nucleate around aMTOCs and contact individual bivalents. A gradual clustering of aMTOCs to opposite poles occurs and the spindle elongates under the sliding force created by plus-end-directed motor kinesin-5. Finally, chromosomes oscillate around the metaphase plate and achieve biorientation. The whole process from GVBD to biorientation takes 5 hours. In *Drosophila*, Nonclaret disjunctional (Ncd) motor and microtubules first form asters in close proximity to the meiotic nucleus, and asters migrate to the endobody at NEBD to nucleate microtubules (Skold et al., 2005). Bivalents associate with microtubules first and later associate with each other through motor-mediated microtubule crosslinking. Multiple transient poles tend to form during very early stages, but shortly thereafter, one axis quickly becomes dominant and establishes bipolarity. The entire process takes about 40 minutes (Skold et al., 2005).

Although mouse oocytes use aMTOCs to nucleate microtubules, aMTOCs don't increase the efficiency of acentriolar spindle assembly in somatic fly cells (Baumbach et al., 2015). Indeed, many species assemble meiotic spindles without any obvious aMTOCs, and the formation of spindle poles relies on microtubule motors and microtubule-associated proteins. Kinesin-14 Ncd can crosslink kinetochore fibers and focus spindle poles without centrosomes. Dynein-Dynactin-nuclear mitotic apparatus (NuMA) can crosslink parallel microtubules and tether minus ends of microtubules together, and NuMA accumulates at the meiotic poles in *Xenopus*, mice,

and humans (Bennabi et al., 2016). Without a typical MTOC, the shape of the poles is broader except in *Drosophila*. A typical vertebrate meiotic spindle shows a barrel shape, and is composed of 95% non-kinetochore microtubules and 5% kinetochore microtubules (Houghtaling et al., 2009). The non-kinetochore microtubules interact with chromosome arms and intersect antiparallel at the spindle equator.

1.10 The chromosomal passenger complex (CPC) is an essential regulator of mitosis

Successful mitosis requires the faithful coordination of chromosome segregation and cytokinesis, which are spatiotemporally controlled by a subset of proteins. Among these proteins, the chromosomal passenger complex (CPC) is a central actor in a remarkably complex network and displays striking dynamics during mitosis. The term "chromosomal passenger" is derived from the dynamic localizations of the CPC during mitosis (Fig. 9). The CPC associates with chromosome arms from late S phase and progressively becomes concentrated at the centromeres by metaphase. Subsequently, the CPC leaves the inner centromeres and relocates to the central spindle and equatorial cortex at the onset of anaphase. Ultimately, the CPC is enriched at the midbody during telophase and cytokinesis (Ruchaud et al., 2007).

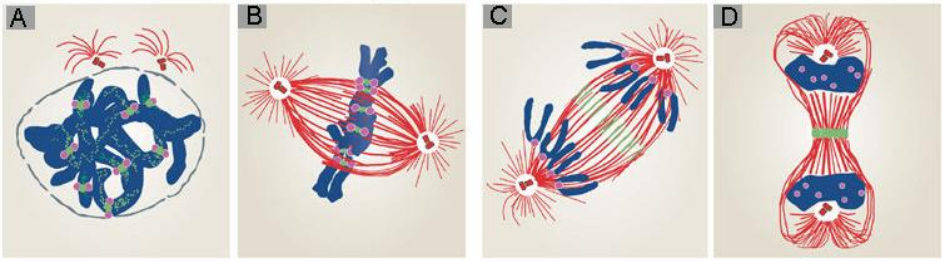

Figure 9. Schematic representation of the CPC localization during mitosis. The CPC is shown in green, chromosomes in blue, kinetochores in pink and the spindle in red. The CPC is localized on chromosome arms in prophase (A), at the inner centromeres in metaphase (B), at the central spindle in anaphase (C) and at the midbody in telophase (D). Adapted from Ruchaud et al (2007).

The CPC is composed of the catalytic, Aurora B kinase, and the regulatory components Borealin, Survivin and the inner centromere protein (INCENP) (Fig. 10)

(Carmena et al., 2012). The C-terminus of INCENP interacts with Aurora B and activates it (Honda et al., 2003). The N-terminus of INCENP, the C-terminal helical domain of Survivin, and Borealin form a tight three-helical bundle and modulate CPC localization to the centromeres and central spindle (Jeyaprakash et al., 2007).

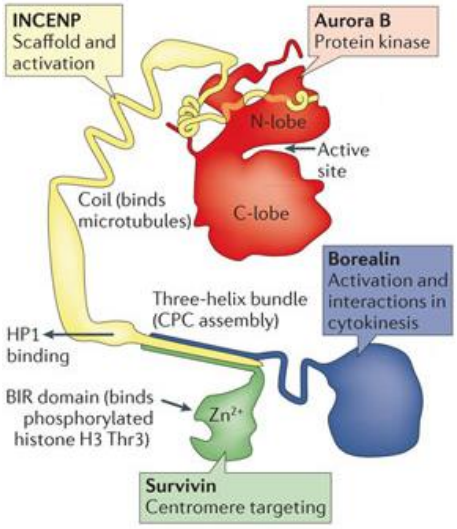

Figure 10. Schematic representation of CPC components. The domains and functions for each CPC component are indicated. Adapted from Carmena et al (2012).

1.10.1 INCENP

INCENP was first identified in chicken cells by an anti-mitotic chromosome scaffold fraction antibody screening (Cooke et al., 1987). The initial study revealed two INCENP isoforms of 155 and 135 KD, which were co-expressed throughout mitosis and were generated by alternative splicing of a single transcript (Mackay et al., 1993). Thereafter INCENP homologs have been identified in a wide variety of species from yeast to human and show conserved functional domain organization (Ruchaud et al., 2007).

The N-terminal CEN module targets the CPC to the inner centromeres via the BIR (baculovirus inhibitor of apoptosis repeat) domain of Survivin, which recognizes Haspin-mediated phosphorylation of histone H3 at T3 (Wang et al., 2010). The HP1 (heterochromatin protein 1) binding domain (human INCENP residues 124-248) mainly interacts with the C-terminal chromo shadow domain (CSD) and to a less extent hinge region of HP1, targeting HP1 to centromeres (Kang et al., 2011). The

SAH (single α-helix) domain in the central region (chicken INCENP residues 503-715) acts as a flexible spring and can stretch up to 80 nm. The N-terminal half of the SAH domain can bind to microtubules, such that Aurora B is directed to substrates near microtubules and can phosphorylate substrates at outer kinetochores (Samejima et al., 2015). The SAH domain is flanked by phosphor-regulatory domains (PRD), which are phosphorylated by CDK1 to attenuate the microtubule binding affinity of SAH (Wheelock et al., 2017). The C-terminal IN box is highly conserved, where the TSS motif is phosphorylated by Aurora B *in trans* to fully activate Aurora B (Sessa et al., 2005) (Fig. 11).

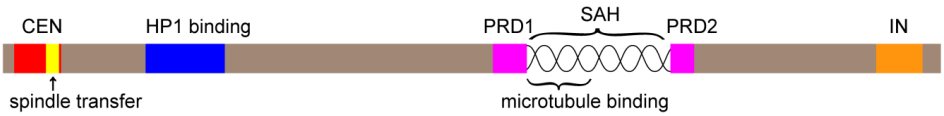

Figure 11. Schematic representation of the main domains of INCENP. The CEN module is the minimum region for centromere targeting. The HP1 binding domain is the region for interacting with HP1. The SAH domain with the N-terminal half required for microtubule binding is represented as a spring. Two PRD motifs flanking the SAH domain are shown. The C-terminal IN box is the region for Aurora B activation.

INCENP knockout in mice results in embryonic lethality, with severe defects in chromosome segregation and cytokinesis (Kaitna et al., 2000). INCENP knockdown in *Drosophila* shows that INCENP is required for Aurora B kinase activity for H3S10 phosphorylation and sister kinetochore disjunction, but it is not critical for the initiation of the contractile ring and the formation of central spindle during syncytial division (Adams et al., 2001). *C. elegans* INCENP is also required for the assembly of the central spindle (Kaitna et al., 2000).

The iconic relocation of the CPC from centromeres to the central spindle at anaphase onset requires high Aurora B activity in chicken DT40 cells (Xu et al., 2009). In contrast, Aurora B-dependent phosphorylation of Sli15/INCENP prevents CPC binding to the central spindle until late anaphase in budding yeast, facilitating anaphase spindle elongation (Nakajima et al., 2011). The relocation of the CPC is an evolutionarily conserved mechanism to prevent SAC reactivation when tension

between sister centromeres is lost at anaphase onset (Vázquez-Novelle and Petronczki, 2010). This process is subject to combinatorial regulation between CDK1 and phosphatases. CDK1 mediated phosphorylation at T59 of INCENP is removed during anaphase, such that the CPC is directed to the central spindle via Mklp2 (mitotic kinesin-like protein2) in human cultured cells (Hümmer and Mayer, 2009). In budding yeast, Cdc14 phosphatase is activated by separase from FEAR (Cdc14 Early Anaphase Release) (Queralt and Uhlmann, 2008), and dephosphorylates multiple CDK1-phosphorylated sites of Sli15/INCENP, directing the CPC to spindle and incapacitating the SAC (Pereira and Schiebel, 2003; Mirchenko and Uhlmann, 2010).

1.10.2 Aurora B

Aurora B belongs to the Aurora family of Ser/Thr kinases and was first discovered as a gene essential for the centrosome cycle in *Drosophila* (Glover et al., 1995). It consists of a variable N-terminal domain, a conserved catalytic domain and a short C-terminal extension. Active Aurora B is phosphorylated at Thr232 in the T-loop. Thr232 fits the consensus Aurora target sequence [R/K]X[T/S][I/L/V], and is auto-phosphorylated, generating positive feedback (Yasui et al., 2004).

Aurora B activation is a complex process. In addition to the two-step activation via the IN box of INCENP, microtubules can activate Aurora B-INCENP subcomplexes through local concentration mechanisms (Tseng et al., 2010). On centromeres, TD-60 (telophase disc-60kD) can allosterically activate Aurora B (Rosasco-Nitcher et al., 2008) and Plk1-mediated Survivin phosphorylation at Ser20 promotes Aurora B activity (Chu et al., 2011). Chk1 phosphorylates Aurora B at Ser331 at kinetochores during prometaphase, which is required for full activation of Aurora B (Petsalaki et al., 2011).

Other post-translational modifications also influence the activity and localization of Aurora B. Cul3/KLHL9/KLHL13 E3 ligase ubiquitylates Aurora B on chromosomes, which triggers the removal of the CPC components from chromosomes and their accumulation on the central spindle during anaphase (Sumara et al., 2007). Ubiquitylated Aurora B is removed by AAA-ATPase p97 (Dobrynin et

al., 2011), which also extracts chromatin associated-Aurora B to allow chromatin decondensation and nuclear envelope reformation during mitotic exit (Ramadan et al., 2007). In addition, SUMOylation of Aurora B promotes its centromeric concentration and function (Fernández-Miranda et al., 2010). Aurora B is degraded by the APC/$C^{Cdc20\ or\ Cdh1}$-proteasome pathway via KEN, A and D-boxes in late mitosis and G1 (Stewart and Fang, 2005; Nguyen et al., 2005).

1.10.3 Survivin and Borealin

Survivin, the smallest member of the mammalian inhibitors of apoptosis proteins (IAPs), is composed of an N-terminal zinc-finger fold called baculovirus IAP repeat (BIR) domain, and a C-terminal helical extension. Survivin is extensively expressed in various human cancers and is a target for cancer therapy (Altieri, 2003). In addition to its involvement in cell death regulation, Survivin has been identified as part of the CPC regulating cell cycle progression. Survivin possesses an evolutionary conserved leucine-rich Crm1-dependent nuclear export signal (NES), which determines its intracellular localization (Knauer et al., 2006). Survivin predominantly localizes in the cytoplasm in tumor cells and has cytoprotective activity. Nuclear Survivin localizes to the mitotic machinery and regulates mitosis (Connell et al., 2008). Human Survivin can be phosphorylated on Thr34 by CDK1-Cyclin B1, which enhances its stability and regulates its levels in tumor cells (Wall et al., 2003). On the contrary, this phosphorylation site is dispensable for Survivin function in chicken DT40 cells (Yue et al., 2008).

Borealin/Dasra B was identified as the fourth member of the CPC in humans and Xenopus (Gassmann et al., 2004; Sampath et al., 2004). Borealin-like proteins have been identified from fungi to animals. Despite low protein sequence identity, they all possess a structurally conserved N-terminal three-helix bundle forming domain, implying that the fundamental structural organization of the CPC is conserved (Nakajima et al., 2009). Yeast Nbl1 (novel Borealin-like 1) has independently lost the C-terminal, but retains the second helical stretch following the N-terminal helix (Bohnert et al., 2009). In the crystal structure of human Borealin, the equivalent region to this helical stretch packs against the homodimerization interface

of Survivin, such that Survivin cannot dimerize when bound to Borealin (Bourhis et al., 2007). The human Borealin C-terminal contains 4 Threonine residues, which are phosphorylated by Mps1 (Jelluma et al., 2008). These phosphorylations enhance Aurora B activity at centromeres, coordinating attachment error correction and the SAC.

1.10.4 CPC paralogs

Paralogs of some CPC components exist in some organisms, and they are thought to function in certain developmental contexts. Only mammals have Aurora B and Aurora C paralogs, which evolved from duplication of an ancestral Aurora B/C gene found in cold-blooded vertebrates (Brown et al., 2004). Aurora B and C share high sequence similarity, particularly in their ATP-binding domain. Aurora C is highly expressed in the germ line and pre-implantation embryos. Aurora C mutation results in large-headed multiflagellar polyploid spermatozoa and male sterility (Dieterich et al., 2007). Aurora C knockout female mice are sub-fertile and ectopic expression of Aurora B can rescue loss of Aurora C (Schindler et al., 2012). Aurora B knockout mice can develop normally until implantation due to the compensation effect of Aurora C during early embryonic cell divisions (Fernández-Miranda et al., 2011). The reciprocal compensation effects indicate the two kinases have some functional equivalence. However, they do have non-overlapping functions. *Aurora C* is maternally transcribed and its translation efficiency increases more during oocyte maturation than does that of *Aurora B* (Schindler et al., 2012). Aurora C is the dominant CPC kinase during female meiosis and locates on the interchromatid axis, centromeres and spindle poles, whereas Aurora B locates on the spindle (Nguyen and Schindler, 2017).

Nonmammalian vertebrates have two Survivin paralogs: class A similar to mammalian counterparts, and class B. One crucial residue in the phosphobinding pocket of BIR domain interacts with H3T3 phosphorylation and determines the binding affinity towards H3 tail on centromeres. His80 in Survivin A has higher binding affinity than Arg89 in Survivin B (Niedzialkowska et al., 2012). Xenopus, zebrafish and chicken have two Borealin paralogs (Dasra A and B), whereas

mammals have a single Borealin closely related to Dasra B. The additional Borealin paralog is thought to aid in rapid spindle formation during early embryonic cell cycles. In *Drosophila* male meiosis, Borealin (Borr) is replaced by Australin (Aust) (Gao et al., 2008). Aust is functionally equivalent to Borr and can substitute Borr in *Drosophila* S2 cells. Thus far, an INCENP paralog (INCENP-like) has only been found in chicken, but it is expressed at very low levels, and cannot sustain a functional CPC (Xu et al., 2009).

1.11 Roles of the CPC in error correction and the SAC

One proposal as to how Aurora B phosphorylates its substrates is the spatial separation model (Lampson and Cheeseman, 2011). The proximity of the substrates to Aurora B determines their phosphorylation potential, which is best exemplified by the mechanism of attachment error correction (EC). In the absence of tension across sister kinetochores, such as syntelic or monotelic attachments, KMN network components in the outer kinetochores are positioned within a phosphorylation gradient of centromeric Aurora B and can be phosphorylated to destabilize erroneous MT-KT attachment. When amphitelic attachment is established, mechanical tension stretches the outer kinetochores further away from the kinase, exposing these substrates to phosphatases such that they are dephosphorylated in order to sustain stable attachment.

Aurora B contributes to the SAC through two models (Krenn and Musacchio, 2015). In the "microtubule occupancy" model, Aurora B is indirectly involved in the SAC by generating unattached kinetochores, which is sensed by SAC components. In the "intra-kinetochore tension" model, intra-kinetochore stretch behaves like a "mechanical switch" to control SAC activity, where short distances switch on the SAC and longer distances switch it off (Maresca and Salmon, 2009). In this model, independent of destabilizing KT-MT attachment, Aurora B is an intrinsic component of the SAC. It could either function downstream of Mad1-Mad2 recruitment to maintain the SAC (Maldonado and Kapoor, 2011), or concomitantly function with Mps1 at unattached kinetochores (Santaguida et al., 2011).

1.12 Roles of the CPC in cytokinesis

Sustained Aurora B activity on the central spindle and equatorial cortex is required for the initiation and ingression of the cleavage furrow until stable midbody formation (Kitagawa and Lee, 2015). CPC relocation to the central spindle at anaphase onset requires timely association between INCENP and Mklp2 (mitotic kinesin-like protein 2), which is facilitated by a decrease of CDK1 activity and an increase of phosphatase activity (Hümmer and Mayer, 2009; Kitagawa et al., 2014). INCENP also binds actin directly to enrich CPC at the equatorial cortex (Landino et al., 2017), probably acting in concert with Mklp2 to ensure successful cleavage furrow ingression (Kitagawa et al., 2013). Aurora B enables clustering and accumulation of centralspindlin at the spindle midzone through phosphorylating Mklp1 (Douglas et al., 2010). As a spindle midzone anchor, centralspindlin binds and activates the guanine nucleotide exchange factor Ect2, creating a concentration gradient of Ect2 around the spindle midzone and allowing Ect2 association with the equatorial membrane (Su et al., 2011). Ect2 acts as the cytokinetic signal and activates the small GTPase RhoA, initiating assembly and constriction of the contractile ring (Yüce et al., 2005).

The CPC also controls abscission timing. Aurora B phosphorylates Mklp1 at S911 to stabilize the midbody and intercellular bridge, preventing cleavage furrow regression (Steigemann et al., 2009). Aurora B phosphorylates Mklp2 at S878 in the lipid association motif (LAM) during mitotic exit, impeding the interaction between the plasma membrane and microtubules at the intercellular bridge, thus controlling abscission timing (Fung et al., 2017). The final membrane scission is driven by ESCRT machinery (the endosomal sorting complex required for transport). Borealin interacts with the ESCRTIII subunit CHMP4C, and Aurora B subsequently phosphorylates CHMP4C at S210, activating the abscission checkpoint to protect against genetic damage (Carlton et al., 2012). The most downstream component of ESCRTIII machinery, the ATPase VPS4 (vacuolar protein sorting 4), is retained on the midbody ring by ANCHR (Abscission/NoCut Checkpoint Regulator) and CHMP4C in an Aurora B-dependent manner before relocalizing to the abscission

zone to allow abscission (Thoresen et al., 2014). These mechanisms for abscission all function downstream of Aurora B activity during cytokinesis.

2 Aims of the study

Oikopleura dioica possesses diverse cell cycle variants to support rapid development in a very short chordate life span. Previous work on regulatory mechanisms underlying endo-, mitotic and meiotic cycles in *O. dioica* have opened interesting new questions. In particular, we wished to better understand the functional roles of gene duplications in core M-phase cell cycle regulator components, CDK1-Cyclin B and the chromosomal passenger complex (CPC). We have focused on CDK1-Cyclin B duplications during meiosis in an intriguing form of coenocystic oogenesis and INCENP duplications in the CPC during embryonic mitoses.

Oogenesis in *O. dioica* occurs in one giant coenocyst where thousands of asynchronously endocycling nurse nuclei share a common cytoplasm with meiotic nuclei in a 1:1 ratio. Meanwhile, the expressions of several CDK1 and Cyclin B paralogs are enriched in the ovary. A primary requirement for transition to and progression through endocycles is suppression of CDK1 activity, whereas meiosis progression depends on sustainable CDK1 activity. How the constraints on the spatiotemporal dynamics of CDK1 activity are imposed in such a coenocystic mode is an open question. Our first aim was to explore the spatiotemporal expression profiles of principal CDK1 and Cyclin B paralogs, focusing on the timing of their cytoplasmic and nuclear accumulation as oogenesis progresses. Targeting the most abundant CDK1 and Cyclin B paralogs, we wanted to investigate their functions in oogenesis and oocyte maturation through RNAi knockdown approaches, especially with respect to their respective contributions to total kinase activity of CDK1 and major cellular events such as NEBD and meiotic spindle assembly. We also attempted to determine the partnerships between CDK1 and Cyclin B paralogs based on phenotypic evidence from loss-of-function analyses. Cyclin B paralogs show different degrees of functional diversification and redundancy across taxonomic groups. Due to the evolutionary position of the urochordate as a sister group to vertebrates, additional data from our work would shed light on the evolutionary trajectory of the functions of metazoan Cyclin B paralogs during oogenic meiosis.

The CPC coordinates faithful chromosome segregation with cytokinesis through its dynamic subcellular localizations at different phases of mitosis and meiosis. The Inner Centromere protein (INCENP) in the CPC modulates Aurora B kinase activity directed towards critical substrates on centromeres, kinetochores and microtubules. Our initial genome-wide search identified two INCENP paralogs in *O. dioica*. Given the potential roles of CPC in regulating kinetochore components, our first aim was to determine the *O. dioica* kinetochore network complement by performing in-depth homolog searches. We also wished to establish a centromeric epigenetic landscape, focusing on histone H3 phosphorylation and methylation modifications. Reasoning that INCENP paralogs could impose differential localization and activity on Aurora B, we investigated the localization of INCENP paralogs throughout mitosis. As tight orchestration between mitotic kinases and their opposing phosphatases is crucial for mitotic progression, we aimed to test the effects on centromeric localization of the CPC using specific inhibitors of Aurora B and Plk1 kinases, and PP1 phosphatases. After compiling this information, we wished to investigate INCENP paralog functions by RNAi, to understand how the localization and activity of Aurora B is affected under respective loss-of-function conditions. Our final overall objective was to address fundamental mechanisms through which duplicated CPCs were redundant, or coordinated, to regulate faithful chromosome segregation during very rapid cell divisions.

3 List of papers

Paper I

Haiyang Feng and Eric M. Thompson

Specialization of CDK1 and Cyclin B paralog functions in a coenocystic mode of oogenic meiosis

Cell Cycle, 2018 (In press). DOI: 10.1080/15384101.2018.1486167

Paper II

Haiyang Feng, Martina Raasholm, Coen Campsteijn and Eric M. Thompson

Chronological switching of INCENP paralogs controls transitions in mitotic chromosomal passenger complex functions in the urochordate *Oikopleura*

Manuscript

4 Summary of results

4.1 Specialization of CDK1 and Cyclin B paralog functions in a coenocystic mode of oogenic meiosis (Paper I)

This work dissects functional redundancy and specialization of CDK1 and cyclin B paralogs during oogenesis. Oogenesis in the urochordate *O. dioica* occurs in a large coenocyst in which vitellogenesis precedes definitive oocyte selection in order to rapidly adapt oocyte production to nutrient conditions over a short life cycle. Two essential CDK1 paralogs, CDK1a and CDK1d, and two B-type Cyclins, Cyclin Ba and B3a, are enriched at transcriptional levels during oogenesis. CDK1a, CDK1d and Cyclin Ba were first found on the Organizing Centers (OCs) during P3, reminiscent of the first appearance of CDK1-Cyclin B on MTOCs before GVBD in other models. CDK1a translocated from OCs to selected meiotic nuclei at the beginning of P4, and regulated coenocystic vitellogenesis by participating in rapid nurse nuclei dumping and cytoplasmic flow during the pro-oocyte growth period. CDK1d-Cyclin Ba translocated from OCs to selected meiotic nuclei during late P4, and Cyclin Ba protein dramatically increased during late stages of oogenesis, implying Cyclin Ba may act as the regulatory subunit of MPF. Knockdown of Cyclin Ba resulted in infertile oocytes with intact nuclear envelopes, indicating that CDK1d-Cyclin Ba drives meiosis resumption and promotes NEBD. We demonstrated that the CDK1d-Cyclin Ba complex is involved in H3S28 phosphorylation on centromeres, as well as meiotic spindle assembly through regulation of the localization of Aurora B to centromeres during prometaphase I. In addition, we found Cyclin B3a also contributed to meiotic spindle assembly and CDK1 kinase activity but its loss could be compensated by Cyclin Ba, suggesting Cyclin B3a is dispensable in this chordate species. Taken together, this study demonstrates sub-functionalization of CDK1 paralogs in coenocystic oogenesis, and reveals overlapping functions between Cyclin Ba and B3a in promoting CDK1 activity and meiotic spindle assembly, with Cylin Ba being essential for these processes.

4.2 Chronological switching of INCENP paralogs controls transitions in mitotic chromosomal passenger complex functions in the urochordate *Oikopleura* (Paper II)

This work investigates how two INCENP paralogs modulate CPC activity and localization during rapid embryonic mitoses in *O. dioica*. *O. dioica* is distinct in appendicularians in that most components of constitutive centromere-associated network (CCAN) at the inner kinetochore, a central mitotic regulatory platform, are secondarily lost. We identified *O. dioica* mitotic centromeres by determining the deposition of GFP fusion CenH3/CENP-A on chromosomes, demonstrating that *O. dioica* chromosomes are monocentric. Furthermore, *O. dioica* mitotic centromeres were enriched with the H3 phosphorylation marks H3pT3, H3pT11 and H3pS28, but lacked the H3 methylation marks H3K4me2 and H3K9me3 characteristic of centromeres in other species. We then demonstrated that Aurora B is the sole kinase responsible for H3-S10 and S28 phosphorylation in mitosis, consistent with its roles reported in other models. The two INCENP paralogs exhibited intriguing localization patterns during the mitotic cycle, with INCENPa and Aurora B (CPCa) colocalizing on the chromosome arms and centromeres by (pro)metaphase, and INCENPb and Aurora B (CPCb) colocalizing on the centromeres from metaphase onwards and relocalizing to the central spindle after anaphase onset. We showed that Polo-like kinase (Plk1) recruitment to CDK1 phosphorylated INCENPa was crucial for INCENPa-Aurora B enrichment on centromeres, whereas Plk1 activity indirectly influenced centromeric INCENPb-Aurora B. By RNAi of the two INCENP paralogs individually, we found that INCENPa is required for spindle assembly and phosphorylation of H3-S10 and H3-S28, whereas INCENPb is critical for the localization and activity of Aurora B at the central spindle and midbody during mitotic exit. In the absence of INCENPb, cleavage furrows initiated, and ingressed but then regressed before abscission was completed. Based on these data, we propose an INCENP paralog switching model that regulates CPC activity and localization, to control different chronologically ordered events through M-phase.

5 General discussion

Numerous CDK-cyclin complexes in metazoans likely originate from a common ancestor. The hypothesized two rounds of whole genome duplication in the vertebrate lineage considerably expanded the families of core cell cycle regulators, in concert with increases in morphological and biochemical complexity (Van de Peer et al., 2009). Studies from a few model organisms have disclosed conserved as well as lineage-specific functions of cell cycle regulation as an adaptation to different lifestyles. We explored the specialized functions of core cell cycle regulators in both meiosis and mitosis of the urochordate *O. dioica* and bring new insights into evolution of cell cycle regulation in the chordate lineage. *O. dioica* represents the first metazoan possessing 5 CDK1 paralogs with variable PSTAIRE motifs, compared with a single CDK1 with an invariant PSTAIRE motif found thus far in all other metazoans. An interesting question that remains to be addressed is to what extent the structures, functions and interactions of each CDK1 paralog have become adapted to specific and/or diversified functional roles.

5.1 The role of CDK1a in coenocystic vitellogenesis

The specific functions of CDK1 in meiosis are less known due to early embryonic lethality of CDK1 knockout mice, and most knowledge about CDK1 comes from knockdown assays in several invertebrate model organisms (Satyanarayana and Kaldis, 2009). Our previous work demonstrated that CDK1a knockdown affected vitellogenesis, resulting in small infertile oocytes. Based on new evidence in this thesis, we propose that CDK1a may regulate the actin-myosin network to drive nurse nuclei contraction during nurse dumping. During mitotic prophase, CDK1 can phosphorylate the nuclear RhoGEF Ect2 at T341 (Hara et al., 2006), which releases the auto-inhibition of Ect2, or at T412 (Niiya et al., 2006), which recruits Plk1 for additional phosphorylation and hyper-activation of Ect2. Subsequently, Ect2 is exported to the cytoplasm and activates cortical RhoA (Matthews et al., 2012). RhoA activates Rho-kinase. Rho-kinase stimulates cortical Myosin II activity, which promotes mitotic cortex tension and intracellular pressure (Fig. 12) (Ramanathan et al., 2015). This pathway could be applied in a one-cell coenocyst, where

vitellogenesis occurs during diplotene of prophase I when CDK1 is present, though expressed at low levels. CDK1a might have positive roles in myosin II recruitment and activity, to regulate nurse nuclei contraction and cytoplasmic transport during pro-oocyte growth.

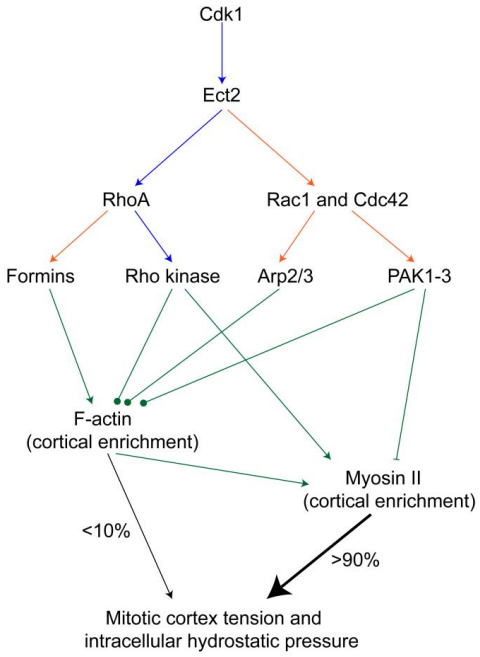

Figure 12. CDK1-dependent actin-myosin regulatory pathways. Stimulation is represented by arrowheads, inhibition by bars and no discernible effect by dots. Adapted from Ramanathan et al (2015).

What could be the advantages of using an additional CDK1 paralog for vitellogenesis? The coenocyst consists of different cytoplasmic domains characterized by differential allocations of kinase activities between growing pro-oocytes and nurse nuclei compartments (Ganot et al., 2008). *O. dioica* probably employs CDK1a specifically on the OCs in the common cytoplasm, possibly helping to regulate the actin-myosin network for oocyte growth. CDK1d is particularly evolved to promote meiosis resumption after oocyte growth and regulate pre-metaphase I. Sequential employment of two CDK1 paralogs could prevent precocious meiotic resumption during vitellogenesis, and promote timely oocyte maturation when full-size oocytes have acquired competence. CDK1a is found in selected meiotic nuclei at early P4, which indicates CDK1a does not promote meiosis resumption even though it is present in meiotic nuclei. Only shortly after CDK1d

translocates to selected meiotic nuclei at late P4, does meiosis resumption occur. Thus CDK1a and CDK1d exhibit functional specialization during meiosis in *O. dioica*. The intrinsic differences between CDK1a and CDK1d might involve differences in substrate specificities. For example, CDK1a might be better at phosphorylating Ect2, and CDK1d better at phosphorylating Lamin and Haspin.

5.2 Molecular mechanisms of oocyte maturation in *O. dioica*

Long-range hormonal signals and surrounding somatic cells stimulate release from primary arrest and trigger meiosis resumption in most vertebrates. Whether maturation inducing hormone is present is not known in *O. dioica*. It should be noted that *O. dioica*, pro-oocytes do not all have direct contacts with somatic follicle cells, and mature oocytes are naked after spawning. In other oikopleurid species, such as *O. longicanda*, type III follicle cells surround the oocytes during late stages of oocyte growth, and mature oocytes are covered with a monolayer of follicle cells (Ganot et al., 2006). Interestingly, *O. longicanda* has three CDK1 paralogs (CDK1a, b and c, unpublished data). Could the more recent duplicate in *O. dioica*, CDK1d, be related to the absence of type III follicle cells surrounding growing oocytes? Although there is no answer at the moment, studies from other model organisms might provide some hints. In mammals, fully grown oocytes are surrounded by two layers of follicle cells: mural and cumulus granulosa cells (Grive and Freiman, 2015). In *C. elegans*, oocytes contact directly with gonadal sheath cells (Kim et al., 2013). In *Drosophila*, the surrounding follicle cells ensure correct oocyte maturation (Bastock and St Johnston, 2008). In *Ciona*, there are inner follicle cells and test cells surrounding oocytes during vitellogenesis (Sugino et al., 1987). Gap junctions between follicle cells and oocytes act as a switch to control meiosis resumption (Von Stetina and Orr-Weaver, 2011). The inhibitory signals diffuse through gap junctions into oocytes and sustain CDK1 inactivation. Conversely, the closure of gap junctions promotes CDK1 activation. This circuit is probably missing in *O. dioica*. In addition, high cAMP levels inactivate CDK1-Cyclin B through PKA-mediated activation of Wee1 and inhibition of Cdc25. The cAMP signaling cascade has not been investigated during oogenesis in *O. dioica*. We suggest that the recent duplicate, CDK1d, might be an adaption to the potential absence of the canonical pathway for driving oocyte

maturation. More fundamental knowledge on the ultrastructure of the ovary and hormonal regulation is needed to further explore this idea.

Although the initial signaling for CDK1d activation remains unknown, the downstream signaling cascades can be inferred. The MAPK cascade probably lies downstream of CDK1d, since pERK was absent after CDK1d depletion (Fig. A1-A). pERK was present at OCs from P3 and in nurse nuclei from P4. pERK inhibition by U0126 did not affect meiosis resumption but caused multiple nurse nuclei and meiotic nuclei to pass through ring canals and reside in growing oocytes, indicating that the MAPK cascade is not essential for meiosis resumption (Ganot et al., 2008). In mice, MAPK-dependent gap junction closure in ovarian follicle cells is one pathway to induce meiosis resumption (Norris et al., 2008). In *C. elegans*, MAPK is activated by MSP in the most proximal five oocytes, and is required for timely oocyte maturation (Lee et al., 2007). In ascidians, MOS/MAPK acts as CSF in meiosis I arrest and limits the number of meiotic divisions, and maintaining MAPK activity in fertilized eggs leads to several rounds of meiotic-like asymmetric divisions, but its activity is not necessary for MPF reactivation (Dumollard et al., 2011). *O. dioica* mature oocytes arrest at metaphase I when MAPK reaches its highest activity (Fig. A1-B), similar to ascidians. Further studies are needed to identify CSF in *O. dioica* oocytes. Potential candidates include high activities of CDK1d and MOS/MAPK, as well as the early mitotic inhibitor 2 (Emi2).

5.3 CDK1d-Cyclin Ba is crucial for Plk1 docking on chromosomes during meiosis resumption

Phosphorylated Plk1-T210 was absent on chromosomes and MPM2 foci were absent on centromeres after Cyclin Ba depletion. MPM2 foci normally indicate phosphorylated substrates of CDK1 and Plk1. It is tempting to suggest that Plk1 is first activated at OCs during P3 independent of CDK1. CDK1d-Cyclin Ba would then phosphorylate centromeric substrates when translocating to meiotic nuclei during P4. Subsequently, Plk1 would be recruited to these substrates, and then phosphorylate its own targets on centromeres, kinetochores and chromosomes, to generate its own docking sites.

O. dioica has two Plk1 paralogs: Plk1a and Plk1b. Plk1b is specifically present in Day 3 animals and oocytes (Fig. A2-C), whereas Plk1a is mainly present during embryonic divisions. Mammalian Plk1 is phosphorylated at Ser137 and Thr210 at different times in mitosis, and the two phosphorylations may alter substrate specificities (van de Weerdt et al., 2005). odPlk1-pS137 was present in meiotic nuclei in P5 ovaries (Fig. A2-A). In addition to meiotic nuclei, odPlk1-pT210 was also found in nurse nuclei shortly before they underwent apoptosis (Fig. A2-B). Whether Plk1 is involved in massive apoptosis of polyploid nurse nuclei has not yet been investigated. The overlapping pattern of the two phosphorylated forms of Plk1 is different from what is found in mouse oocytes. During prometaphase I, Plk1-pS137 is consistently present at the MTOCs and centromeres and dynamically localizes between chromosome arms from prometaphase I to MI, and is involved in meiotic spindle assembly, SAC activation and REC8 cleavage, respectively. Plk1-pT210 is present across the whole body of chromosomes during meiosis resumption (Du et al., 2015). The localization pattern of Plk1-pT210 on the chromosomes is similar to what has been found in *C. elegans* and *Drosophila* (Chase et al., 2000). Plk1 is the trigger kinase to drive meiosis resumption through phosphorylating Cdc25 and subsequently activating CDK1-Cyclin B in *Drosophila* (Xiang et al., 2007). However, Plk1 is neither necessary nor sufficient to drive meiosis resumption in *Xenopus* (Gaffré et al., 2011). It would be interesting to further investigate the role of Plk1 in the initial steps of CDK1d-Cyclin Ba activation at OCs in *O. dioica*.

5.4 Is reduced expression or tissue/stage specific expression a way to maintain duplicated CDK1-Cyclin B complexes?

Duplicate B-type Cyclins show tissue or sex specificity, which is a frequent outcome of gene duplication. Since Cyclin Ba knockdown caused female infertility, its function in embryonic mitoses could not be tested. We can only infer its roles beyond meiosis resumption. As a maternal stock, Cyclin Ba protein levels dropped during rapid embryonic divisions, and its mRNA was eventually restricted to several spots in the trunk when most cells were undergoing mitosis. Coincidentally, CDK1d mRNA levels also dropped during embryonic divisions. By reducing the expression of Cyclin Ba and CDK1d and restraining their distributions to specific tissues, this duplicate

CDK1-Cyclin B complex could be retained. Intriguingly, the expression levels of Cyclin Bc, CDK1b and CDK1c increased during embryonic divisions, and Cyclin Bc mRNA was ubiquitously present in the trunk. Yeast two hybrid assays showed that Cyclin Bc interacted with CDK1b and *in situ* hybridizations showed that CDK1c mRNA co-localized with Cyclin Bc in D3 gonads (Ma et al., unpublished data), suggesting that CDK1b/c-Cyclin Bc might be another duplicate CDK1-Cyclin B complex. We speculate that CDK1b/c-Cyclin Bc could be employed in embryonic mitosis and germline endomitosis.

Cyclin Bc knockdown didn't cause any defects during oogenesis, such that embryonic development could be followed. Cyclin Bc was successfully knocked down by dsRNA in the oocytes, with no significant off-target effects on other B-type Cyclins (Fig. A7-A). In WT, more than 90% of the embryos developed to the tadpole stage. In Cyclin Bc knockdown embryos, about 50% underwent abnormal cleavages and arrested before tadpole stage. About 35% developed to normal tadpole. The rest didn't divide (Fig. A7-B). The partial phenotype of abnormal division could have arisen from reduced efficiency of dsRNA during embryogenesis, since high levels of zygotic transcription might outcompete target degradation caused by dsRNA. Alternatively, Cyclin Ba might compensate the loss of Cyclin Bc to some extent, supporting functional redundancy between the two paralogs. To avoid technical limitations of RNAi in embryos, Cyclin Bc knockout transgenic lines are needed to further explore the roles of Cyclin Ba and Bc in mitosis.

We argue that Cyclin Bc is a canonical Cyclin B1 homolog, whereas Cyclin Ba is a specialized duplicate employed in meiosis resumption. First, the N-terminal of Cyclin Ba is much shorter than the corresponding region of human Cyclin B1, which controls its localization, as shown by the N-terminal swapping assay between Cyclin B1 and B2 in mammalian cells (Draviam et al., 2001). The NES of Cyclin Ba is divergent, with a putative Plk1 phosphorylation site downstream of the NES. Second, a basic nuclear localization sequence (NLS), which is absent in human Cyclin B1, is present in the C-terminal of Cyclin Ba (Fig. A8). NLS-containing proteins interact with importin-β via the adaptor subunit importin-α and are transported into the

nucleus through nuclear pores (Clarke and Zhang, 2008). Nuclear pore complex clusters lie at the interface between selected meiotic nuclei and OCs during P4. It is possible that Cyclin Ba translocates to meiotic nuclei via nuclear pores using importin-α/β. Third, Cyclin Ba/b is exclusively found in the nucleus at early prophase of mitotic cells in tadpoles, but disappears at late prophase (Campsteijn et al., 2012), indicating that CDK1d-Cyclin Ba is not the main M-phase regulator in tadpoles. Lastly, Cyclin Bc retains the potential of translocating to selected meiotic nuclei. Cyclin Bc transcripts are expressed at low levels during oogenesis, but when introduced artificially into the P3 ovary, Cyclin Bc protein is found in selected meiotic nuclei at P4 (Fig. A9). As a hypothetical ancestor of Cyclin Ba, it is not surprising that Cyclin Bc is still capable of translocating to selected meiotic nuclei, even though it does not sustain meiosis resumption due to low expression in WT ovaries.

5.5 *O. dioica* Cyclin Ba is essential for NEBD and spindle assembly in female meiosis I: Evo-devo implications.

In representative model protostomes, Cyclin B1 is not essential for NEBD, and it collaborates with other mitotic Cyclins (Cyclin B2 and B3 in *C. elegans*, Cyclin A and B3 in *Drosophila*) to promote NEBD (van der Voet et al., 2009; Bourouh et al., 2016). Spindle morphology analyses in these Cyclin knockdowns show that Cyclin B1 may be required for meiotic spindle organization in *Drosophila* but is not required in *C. elegans*. In early-branching deuterostomes such as the echinoderm, sea urchin, new Cyclin B synthesis is not required for GVBD, but is required for spindle assembly, and Cyclin A can't compensate for the loss of Cyclin B in meiosis (Voronina et al., 2003). In another echinoderm, the starfish, Cyclin B subtypes and Cyclin A are not present during meiosis I (Okano-Uchida et al., 1998), such that CDK1-Cyclin B is the sole MFP to drive meiosis resumption (Kishimoto, 2011). In non-mammalian vertebrates such as *Xenopus*, Cyclin B2 is the dominant subtype in meiosis I, and its neosynthesis is critical to promote GVBD and spindle assembly (Gaffré et al., 2011; Yoshitome et al., 2012). In mammals such as mice, Cyclin B2 is critical for GVBD and the initial stages of spindle assembly during early M phase (Gui and Homer, 2013), whereas the rate of Cyclin B1 synthesis after GVBD

determines the progression of spindle assembly and the length of meiosis I (Polanski et al., 1998). In *O. dioica*, Cyclin Ba, the Cyclin B1 and B2 homolog, is critical for both NEBD and spindle assembly. The evolutionary track seems to be that M-phase Cyclins collaboratively control the progression of meiosis I in the common ancestor of metazoans. There is a growing trend towards specialization of Cyclin B1 in promoting meiosis resumption and meiotic spindle assembly from protostomes to deuterostomes. Cyclin B1 takes over spindle assembly in *Drosophila*, and becomes critical for GVBD in starfish. Our data support that the chordate common ancestor has Cyclin B1 and Cyclin B3, and Cyclin B1 controls both GVBD and spindle assembly. This feature is retained in urochordates. In vertebrates two rounds of whole genome duplication generate Cyclin B2, which adopts slightly different roles of driving the progression of meiosis I in different vertebrate lineages. Cyclin B2 obtains specialized functions in promoting GVBD and early-stage spindle assembly in mammals, whereas Cyclin B1 is further specialized in promoting late-stage spindle assembly.

5.6 The minor role of Cyclin B3a in spindle assembly

We revealed that Cyclin B3a is dispensable in *O. dioica* female meiosis I and plays a minor role in spindle assembly. Cyclin B3 originates at the base of metazoans, and is distantly related to Cyclin A and Cyclin B1 (Lozano et al., 2012). Previous studies revealed that Cyclin B3 promotes anaphase progression. Its depletion causes metaphase I arrest in *Drosophila* and mice (Zhang et al., 2015b; Bourouh et al., 2016) and prevents segregation of sister chromatids in meiosis II of *C. elegans* (van der Voet et al., 2009). *O. dioica* Cyclin B3a has lost this anaphase-promoting function, but retains non-essential overlapping functions with Cyclin Ba in promoting oocyte maturation, which has also been shown in *C. elegans* and *Drosophila* (van der Voet et al., 2009; Bourouh et al., 2016). Another *O. dioica* Cyclin B3 homolog, Cyclin B3b, is highly expressed in the testis, possibly recalling the expression pattern of mouse Cyclin B3 at leptotene and zygotene stages of spermatocytes (Nguyen et al., 2002). Based on these data, we speculate that Cyclin B3 in the chordate common ancestor collaborates with Cyclin B1 to promote oocyte maturation, and also controls anaphase progression in meiosis I. It may be involved in early meiotic events of

spermatogenesis. In urochordate *O. dioica*, Cyclin B3 duplication occurs. Cyclin B3a retains non-essential functions in promoting meiotic maturation and loses other functions, whereas Cyclin B3b may retain spermatogenesis functions with its expression restricted to the testis.

5.7 Aurora evolution

Yeast has a single Aurora kinase. Some protostomes have two Auroras, such as Aurora and IAL in *Drosophila* and AIR-1 and AIR-2 in *C. elegans*, which were generated by independent duplications (Schumacher et al., 1998; Reich et al., 1999). Non-vertebrate deuterostomes, such as echinoderms sea urchin and starfish, the ascidian *Ciona* and the cephalochordate, *Branchiostoma*, have a single Aurora, which is thought to be the ancestor of vertebrate Auroras (Abe et al., 2010). Vertebrates have two Auroras, Aurora A and B, probably due to two rounds of whole genome duplication. Mammals have three Auroras, Aurora A, B and C, among which Aurora B and C arose by gene duplication from the ancestral Aurora B/C gene in cold-blooded vertebrates (Brown et al., 2004). Intriguingly, the appendicularian, *O. dioica* possesses Aurora A and B. OdAurora A weakly forms a clade with social amoeba Aurora and protostome Aurora A, whereas OdAurora B weakly forms a clade with protostome Aurora B (Fig. A10). Since Bayesian posterior probabilities in these two clades are low, we were not able to confidently infer evolutionary relationships of OdAuroras based on this analysis.

The residues lining the catalytic pocket of OdAuroras, which are involved in positioning ATP and substrates for phosphotransfer, show highly conserved patterns to their metazoan counterparts (Fig. A11-A), supporting their close relationship to the single Aurora in non-vertebrates and Aurora A/B/C in vertebrates. A single amino acid (Gly198 in Aurora A and Asn142 in Aurora B) determines the respective partners, subcellular localizations and functions of Aurora kinase paralogs (Fu et al., 2009). The equivalent residues in OdAuroras are both Gly (Fig. A11-B), which is the same as that in the single Aurora of ascidian, amphioxus, echinoderm, amoeba and yeast. A-type Aurora is thought to be closer to the single ancestral Aurora in the vertebrate stem (Abe et al., 2010). *O. dioica* Auroras show distinct subcellular

localizations. OdAurora A is localized on centrosomes during embryonic mitoses (Fig. A12), consistent with Aurora A in other model organisms being involved in centrosome dynamics (Hochegger et al., 2013). OdAurora B exhibits typical CPC localizations and functions. Since the cephalochordate and the urochordate ascidian have a single Aurora kinase possessing dual functions on centrosomes and the spindle midzone, OdAurora A and B might arise from duplication of the single Aurora after the divergence of Oikopleuridae in the urochordate lineage, with division of labor between OdAurora A and B for centrosome and centromere regulation respectively. Thus, *O. dioica* Aurora A and B should probably be regarded as functionally equivalent homologs, rather than orthologs, to their respective vertebrate counterparts.

5.8 INCENPb: functions beyond CPC interactions with Aurora B?

In addition to the work presented in **Paper II**, we were curious as to the localization of INCENPb during early embryonic mitoses. We found that during these stages, INCENPb was exclusively located on centrosomes during the entire mitotic cell cycle (Fig. A13), co-localizing with Aurora A. When INCENPb was knocked down, in addition to Aurora B defects on the central spindle, active Aurora A was abrogated on centrosomes from late anaphase. This raises the possibility that INCENPb might bind to and activate Aurora A on centrosomes during embryonic divisions. It is a bit surprising that a metazoan INCENP can localize to centrosomes. However, social amoeba INCENP is co-localized with the single ancestral Aurora on the spindle poles from the initiation of mitosis until the beginning of anaphase (Li et al., 2008), exemplifying a possibility that INCENP can interact with Aurora on centrosomes. Mammalian Aurora A can bind with INCENP and phosphorylates Ndc80 at Ser69 on kinetochores (DeLuca et al., 2018). In mammals, the key interactor of Aurora A on centrosomes is Cep192, which activates Aurora A and promotes centrosome maturation and bipolar spindle assembly (Joukov et al., 2014). Another interactor with Aurora A is TPX2, which targets Aurora A to the spindle and activates it through shielding the phosphorylated Thr288 residue from dephosphorylation by PP1 (Bayliss et al., 2003). Interestingly, we were unable to detect a TPX2 homolog in the *O. dioica* genome. It had been proposed that TPX2 was not present in invertebrates. However, since the identification of *C. elegans* TPXL-1, TPX2 orthologs have been

reported in several invertebrates, including *Drosophila*, starfish and *Ciona* (Hebras and McDougall, 2012). Although targeting and activating Aurora A on the spindle is an ancient function of TPX2, the *Drosophila* TPX2 ortholog Ssp1/Mei-38 lacks the Aurora A binding domain and plays a minor role in spindle assembly (Goshima, 2011). TPX2 is not essential to build a bipolar spindle, though disrupting the TPX2-Aurora A interaction generates a short spindle in human cells (Bird and Hyman, 2008). *O. dioica* may employ other pathways to assist in assembling the mitotic spindle. During rapid early embryonic divisions in *O. dioica*, centriole disengagement and duplication occur in anaphase, such that a pair of new centrosomes has been separated to some distance during cytokinesis and is already well-positioned for spindle assembly in the subsequent cell cycle. This phenomenon has been observed during embryogenesis in *C. elegans* and *Drosophila* (Cabral et al., 2017; Oliveira and Nasmyth, 2013), and may aid in rapid embryonic cleavages in oviparous species. INCENPb may act as a substitute of TPX2 and activate Aurora A on the spindle. Active Aurora A functions in centrosome maturation and spindle assembly probably through Plk1 activation (Asteriti et al., 2015). Several potential Plk1 phosphorylation sites are present at the N-terminal of INCENPb, which could serve as γ-TuRC-binding sites. Interestingly, INCENPb knockdown did not affect the localization and activity of Aurora A on the centrosome from prophase to early anaphase, active Plk1 was present on centrosome throughout mitosis, and centrosome duplication and spindle assembly occured normally. This implies that INCENPb might only be necessary to stimulate Aurora A activity during mitotic exit, and that it is not critical for Plk1 activation and centrosome maturation.

5.9 The localization of INCENP paralogs are developmentally regulated

In early embryonic mitoses, INCENPb was localized on centrosomes, and during this period, it may be that INCENPa acts as a canonical CPC component. In the mitoses of tadpoles, INCENPb was localized at the centromeres and central spindle, and INCENPa was restricted to chromosome arms and then centromeres by (pro)metaphase. Meanwhile, Aurora A could not be detected on centrosomes, whereas Plk1 was still prominently present on centrosomes. We suspect that INCENPb may lose this centrosomal localization to be incorporated into the CPC at a

certain developmental stage. This may be related to the changes in cell division speed as development proceeds. Aurora A-INCENPb complexes on centrosomes might accelerate centrosome maturation and spindle formation, facilitating rapid early embryonic mitoses. We noticed that in some INCENPb knockdown embryos, the first cell division was significantly delayed, starting at 1 hpf, whereas the first division normally occurs at 0.5 hpf in control WT embryos. As the embryo develops and interphase is introduced, the division speed slows down (Stach et al., 2008). The centrosomes would then no longer require high levels of Aurora A activity to promote rapid microtubule nucleation from one cell cyle leading into the next. Consequently, INCENPb might lose this Aurora A-related function. It would be interesting to determine if, and when, such a switch might occur, and to investigate the molecular mechanisms of INCENPb relocation.

5.10 Possible biological benefits of CPC switching on centromeres

During prometaphase in mammalian cells, two populations of CPC locating on centromeres and kinetochores, respectively, have been observed (DeLuca et al., 2011). Inhibition of the Haspin-H3pT3 pathway reduced most of the inner centromere CPC pool and clearly revealed the kinetochore-proximal CPC pool under conditions of tenseless attachment, which is proposed to be involved in the SAC response (Bekier et al., 2015). Could *O. dioica* CPCa and CPCb correspond to centromere and kinetochore populations as described in mammals? One possibility is that CPCa might rely on the combinatorial action of CDK1 and Plk1 on the Haspin-H3pT3 pathway to localize at the inner centromere, whereas CPCb could depend on the Bub1-H2ApT120-Shugoshin pathway to localize at kinetochores. One could envisage a potential advantage of CPC switching during prometaphase. *O. dioica* has a small chromosome number (2n=6), and chromosome congression at the equator during prometaphase should be much faster than for mammals. If Plk1 activity were to be focused on the Haspin-H3pT3-CPCa pathway, centromeric CPCa could be established quickly when Aurora B activity is still low during prophase, and be devoted to correction of erroneous attachments and spindle assembly. As Aurora B activity increased, CPCb could be recruited to kinetochores later via the Bub1-H2ApT120-Shugoshin pathway, and be more dedicated to the SAC response. Since

"anaphase waiting" time after the first bipolar KT-MT attachment is achieved may be relatively short with a small chromosome number, specialization of CPCb towards the SAC response would help to avoid SAC reactivation by CPCa upon bi-orientation of all chromosomes in a short time window. The CPCb would then translocate to the central spindle to terminate the SAC at anaphase onset, accompanied by CDK1 inactivation as previously reported (Vázquez-Novelle and Petronczki, 2010; Rattani et al., 2014). CPC switching could uncouple two surveillance processes, making the meta-anaphase transition fast and irreversible. The SAC response is quite strong under Nocodazole treatment during embryonic division (unpublished data), however, with our current tools, measurement of meta-anaphase transition timing is difficult during *Oikopleura* embryonic development, and SAC component antibodies are not yet available, thus complicating further exploration of these ideas at the moment.

5.11 *O. dioica* is an emerging model for uncoupling M-phase and cytokinesis

A major investigative barrier in isolating cytokinesis from M phase is that many cell cycle regulators have crucial functions throughout M-phase, and it is difficult to specifically inhibit them at one phase without also influencing their other functions. Pharmacological treatments such as microtubule damaging drugs can block cells at metaphase, but only partially synchronize cytokinesis after they are washed out since cells take a variable time to exit mitosis. INCENPb depletion specifically inhibits CPC functions at cytokinesis without affecting earlier CPC functions in M phase. As a result, the mutant cells reach cytokinesis with perfectly separated chromosomes and normal localization of other kinases such as Plk1 on the midbody and centrosome. Cytokinesis is the last step of mitosis, and the CPC is involved in many key biochemical reactions, among which we only know very few. *O. dioica* INCENPb mutants provide an excellent model to investigate CPC function during mitotic exit and how it coordinates central spindle formation, nuclear envelope reformation, cleavage furrow ingression and abscission.

Some unsolved issues can be addressed in INCENPb mutants in the future. For instance, as a GTPase, RhoA needs to be switched off at the end of cytokinesis, but the molecular mechanism is not clear. One study proposes that in human cells Aurora

B phosphorylates MgcRacGAP on the midbody at late stages of cytokinesis, and converts it to a RhoGAP for RhoA inactivation (Minoshima et al., 2003). Another study proposed that in *C. elegans* the GAP activity of CYK-4 (MgcRacGAP homolog) inactivates Rac in parallel with RhoA activation to drive contractile ring constriction (Canman et al., 2008). If we introduce a RhoA probe to detect its activity on the midbody in INENPb mutants, the change of RhoA activity should specifically reflect how the CPC influences the Rho-GTP cycle at the end of cytokinesis without influencing cortical RhoA where the contractile ring initiates. A proteomic analysis in human cells has identified several novel binding partners of Aurora B, including the microtubule bundling protein PRC1 and KIF4 during cytokinesis, but the biological functions remain unknown (Ozlü et al., 2010). A more recent screening based on known Aurora B substrates showed that during cytokinesis, phosphorylation of Aurora B by Protein kinase C (PKC), altered the substrate preferences of Aurora B (Pike et al., 2016). We could compare Aurora B binding partners on a global scale in INCENPb mutants, to determine which categories of proteins and their phosphorylation status are significantly changed. Aurora B controls the abscission checkpoint and delays abscission in response to chromosome bridges (Steigemann et al., 2009), but the exact mechanism is poorly understood. One study suggests that CHMP4C in the ESCRT-III machinery interacts with Borealin and is phosphorylated by Aurora B, which delays abscission (Carlton et al., 2012). Another study argues that CHMP4C has an active role in ESCRT-III driving abscission, and that Aurora B and centralspindlin fine-tune the temporal distribution and activation of CHMP4C on the midbody (Capalbo et al., 2016). To distinguish among these two possibilities, we could mutate Aurora B consensus phosphorylation sites in CHMP4C to a phosphomimic residue and introduce it into an INCENPb mutant. If phosphomimic CHMP4C can rescue the abscission defects to certain extent, this may indicate that the second possibility is correct and also generally conserved in chordates.

5.12 Conclusions

The urochordate *O. dioica* has systemically amplified cell cycle regulators in proliferative and reproductive cell cycles. We demonstrate the spatiotemporal dynamics and functional specialization of two CDK1 paralogs and two B-type

Cyclins during coenocystic oogenesis. CDK1a regulates vitellogenesis, and CDK1d promotes meiosis resumption and oocyte maturation. The observation that Cyclin Ba is crucial for NEBD provides some possible insight into the evolutionary track of Cyclin B1 homologs in the chordate lineage. Cyclin B1 plays major roles in both meiosis resumption and meiotic spindle assembly in the chordate stem. These functions are inherited by Cyclin Ba, a Cyclin B1 homolog in the urochordate *O. dioica*, whereas they are adopted by Cyclin B1 and B2 homologs to variable extents in vertebrates. The redundant role of Cyclin B3a in *O. dioica* female meiosis suggests that this Cyclin B3 homolog has lost one of its known functions in other species (*C. elegans*, *Drosophila* and mouse) in promoting metaphase-anaphase transition in this urochordate. We also demonstrate that INCENP paralog switching modulates Aurora B kinase activity and localization in mitosis. INCENPa-Aurora B targeting to chromosome arms and centromeres by prometaphase is involved in H3-S10/S28 phosphorylation, chromosome condensation, spindle assembly, and Aurora B transfer from centromeres to the central spindle. INCENPb-Aurora B appears on centromeres during prometaphase, then translocates to the central spindle at anaphase onset. INCENPb is required to sustain the localization and activity of Aurora B on the central spindle and midbody during late mitotic phases, which is involved in cytokinesis and crucial for completion of abscission. *O. dioica* embryos can be used as a new model to study CPC functions up to M phase versus those during cytokinesis and mitotic exit.

5.13 Future perspectives

5.13.1 Phylogenetic inference of *Oikopleura* CDK1 paralogs

Three CDK1 paralogs (CDK1a, 1b and 1c) have been identified in *Oikopleura albicans* (oa) and several other *Oikopleura* species (unpublished data), whereas only one CDK1 is identified in another appendicularian family, the *Fritillariidae*. Phylogenetic analysis suggests that CDK1 duplication post-dated the separation of *Oikopleuridae* from *Fritillariidae* (Fig. 13). *O. dioica* CDK1a, 1b and 1c are clustered with their orthologs in *O. albicans*, indicating their recent common ancestor already had three CDK1 paralogs.

The distance-based Bayesian inference indicated that CDK1a is ancestral and is duplicated to generate CDK1b with nearly 100% posterior probability support, and CDK1b was then duplicated to generate CDK1c. CDK1d and 1e are the most recent duplicates. *O. dioica* CDK1a and 1b locate on autosome LG2, CDK1c and 1e locate on autosome LG1, and CDK1d locates on the X chromosome. The sequences around the oaCDK1a locus show synteny with the odCDK1a locus. However, oaCDK1b and 1c are very close to each other (about 170 kb away), and the sequences around them show synteny with a chromosomal region where no odCDK1 paralogs are present (Fig. 14). It is possible that CDK1a retains canonical CDK1 mitotic functions. Whether CDK1b and 1c in the two genera have similar functions is currently unknown. The recent duplication giving rise to the CDK1d gene on the X chromosome is transcribed as a maternal message and appears to have evolved specialized functions in driving meiosis resumption. The recent CDK1e duplicate is not essential in female meiosis, even though it is also a maternal message. To track the evolutionary history of CDK1 duplication in *Oikopleuridae*, we need to scrutinize the genome of more closely or distantly related genera in this family to identify CDK1 paralogs and analyze phylogenetic relationships, to infer the possible evolutionary forces behind the functional divergence of duplicate CDK1 paralogs.

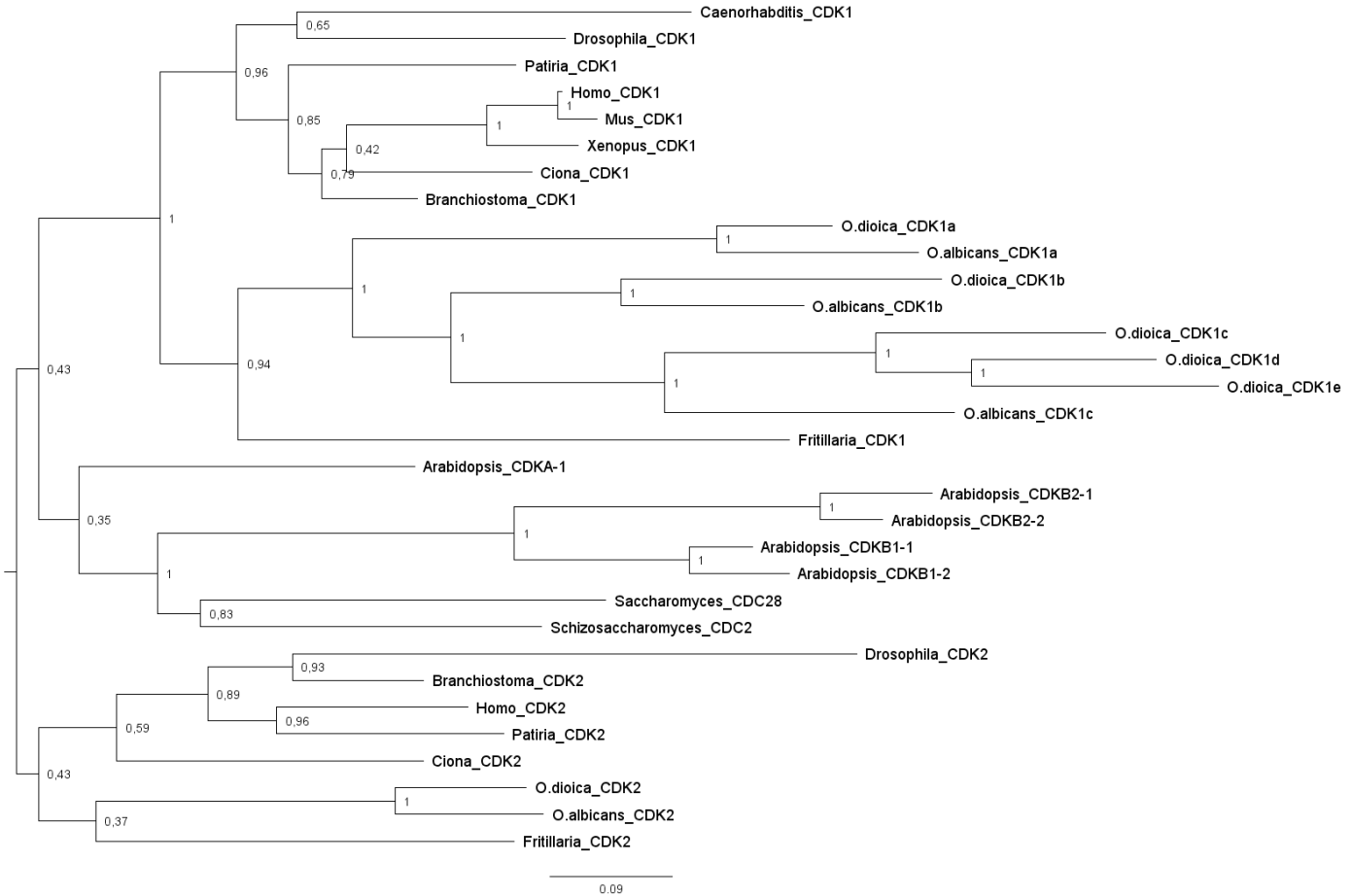

Figure 13. Bayesian inference analysis of CDK1 using the sequences of the kinase domain with posterior probabilities indicated at the nodes. A mixed amino acid model with 2,000,000 generations sampled every 100 generations was used. CDK2 was used as outgroup to root the tree.

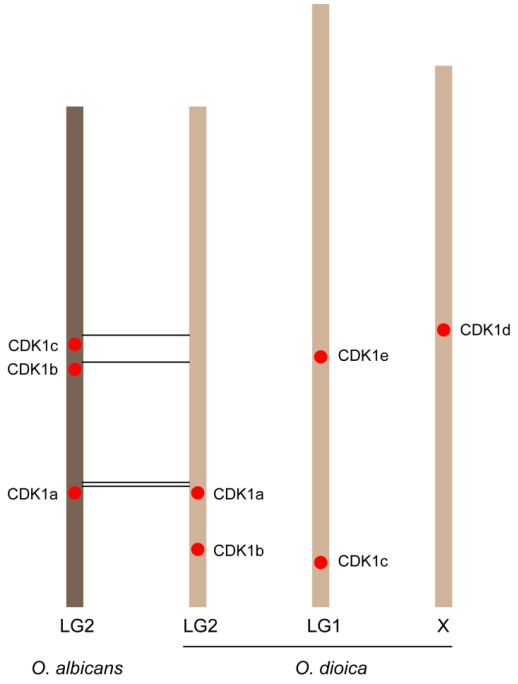

Figure 14. Schematic representation of chromosomal positions of CDK1 paralogs in *O. dioica* and *O. albicans*. The Y chromosome of *O. dioica* and other chromosomes of *O. albicans* are not shown for simplicity. Lines indicate 4 syntenic regions in autosome LG2 between *O. dioica* and *O. albicans*.

Does CDK1d also drive early embryonic divisions? As a maternal stock, CDK1d transcripts and Cyclin Ba protein are present during early embryogenesis, such that CDK1d-Cyclin Ba could drive early mitoses. What then would be the role of CDK1a during the same developmental period? Do CDK1a and d have overlapping functions or distinct functions in mitosis? The protein sequences of CDK1a and d share high similarity. Reduction in expression of duplicate genes can allow retention of functional similarities. If this model is applied to CDK1 duplication, individual knockouts of CDK1a or 1d in the embryo should have no defects, whereas simultaneous knockout is expected to cause mitotic arrest. Alternatively, does CDK1a take over M phase control from CDK1d at a certain developmental stage? If such CDK1 paralog switching is present, it would be of interest to define the time point of switching and with which alterations in the cell cycle this might correlate. Another possibility is that CDK1a and 1d have different kinase activities, and/or have different cyclin binding partners. These could determine their substrate specificities and spatiotemporal subcellular localizations. From an evolutionary view, such functional divergence requires long-term positive selection to

restrain CDK1 paralogs towards distinct targets. To assess this, *in vitro* kinase activity assays towards some representative CDK1 substrates are needed. Phospho-proteomic analysis of CDK1 substrates after inactivating individual CDK1 paralogs would also identify their substrate preferences, if any, *in vivo*.

5.13.2 The composition of two CPCs

Multiple CPCs have been isolated by immunoprecipitation and perform distinct mitotic functions. In human cells, the chromosomal passenger holocomplex contains Aurora B, INCENP, Survivin and Borealin, whereas the subcomplex contains Aurora B and INCENP. The subcomplex can phosphorylate H3S10 when the holocomplex is depleted, whereas the holocomplex is crucial to maintain spindle integrity (Gassmann et al., 2004). In budding yeast, three CPCs have been found: Sli15p (INCENP)-Ipl1p (Aurora), CBF3-Bir1p (Survivin)-Slip15p (INCENP)-Ipl1p (Aurora), and Bir1 (Survivin)-Sli15p (INCENP) (Thomas and Kaplan, 2007). We demonstrate CPCa and CPCb are present and carry out distinct functions in *O. dioica* mitosis, but their respective compositions were not investigated. Whether two Survivin paralogs or any additional components (Borealin and TD-60) are present in the two CPCs, and their potential contributions to the activation and localization of Aurora B should be addressed in the future.

It is thought that the four components are widely present in CPC from fungi to animal. However, we didn't identify Borealin in the *O. dioica* genome. Since the three-helical bundle of INCENP-Survivin-Borealin is a conserved feature of the CPC, the absence of Borealin opens the question as to how the localization module is defined in *O. dioica* CPCs. Interestingly, compared with vertebrate Survivin, *O. dioica* Survivin paralogs have a longer C-terminal extension after the C-helix, which also forms a helix. An intriguing model would be that the additional C-terminal helix of *O. dioica* Survivin turns back and replaces the helix of Borealin in the localization module of the CPC. To test this, the complex of the CEN domain of INCENP and Survivin could be crystalized and analyzed. Resolving the CPC regulatory core in *O. dioica* could bring new insights to centromere localization mechanisms.

Since two INCENP paralogs co-exist during mitosis, they may confer different levels of kinase activity on Aurora B as mitosis progresses and the CPC shifts location. INCENPa-AurB and INCENPb-AurB complexes could be produced in protein expression systems, and their intrinsic kinase activities assessed by *in vitro* kinase assays. To further test that odAurora A and B are the functional paralogs of their vertebrate counterparts, we could replace vertebrate Aurora A and B in mammalian cells with odAurora A and B respectively, and determine the extent to which they can restore defects of centrosome maturation, chromosome segregation and cytokinesis when mammalian Aurora A/B are depleted.

A subset of key motifs, including Lys-Glu salt bridge, αC-helix, Gly-rich loop, hydrophobic spine, HRD, DFG and GT motif, and activation segment, determine activation mechanisms of mitotic kinases (Bayliss et al., 2012). CDK1s and Aurora A/B kinases in *O. dioica* are functionally specialized to fulfill their regulatory roles in certain phases of meiosis and mitosis. From a structural view, it is still unclear to what extent the key motifs in these kinases are divergent between these paralogs, which could influence their activation mechanisms, binding partners and substrate specificities. Crystal structures of odCDK1-Cyclin B complexes and odAurora A/B-INCENPa/b complexes could be determined to address how evolutionarily driving forces bring about structural changes of crucial mitotic kinases with their binding partners.

O. dioica exhibits considerable evolutionary innovation in core cell cycle machineries. We have revealed functional innovations in CDK1-Cyclin B and CPC duplications. Through comparison of the pathways in which these M-phase regulators operate with the well studied models, we will ultimately provide insights into the molecular mechanisms as to which targets are conserved and which are adaptive to different evolutionary constraints. Such knowledge might open possibilities in the future for applications in cancer therapies by contributing to more thorough understanding of which target molecules, pathways and approaches are most likely to be fruitful in generating successful therapies with minimal side-effects and minimal opportunities for cancer cells to adopt alternative pathways to evade treatment.

6 Appendix

Substrates of metazoan CDK1

Hundreds of M-phase substrates phosphorylated by CDK1 have been identified based on large-scale screening approaches, high throughput mass-spectrometry and complementary computational approaches. Representative substrates identified by two proteomic approaches are listed in Table A1 (Errico et al., 2010; Pagliuca et al., 2011).

Table A1. List of CDK1 substrates

CDK1 substrate	Function
Actin/Cytoskeleton	
Actopaxin	Regulate actin cytoskeleton reorganization during cell division.
AML/RUNX1 transcription factor	AML1 (RUNX1) regulates hematopoiesis, angiogenesis, muscle function, and neurogenesis. AML1 phosphorylation may affect degradation mediated by APC^{Cdc20} to a greater degree.
ETS Variant gene 1	Novel Androgen receptor activated transcription factor
Nir2	Regulator of the small GTPase Rho in actin cytoskeleton reorganization and cell morphogenesis
Palmitoylated membrane protein 1	MAGUK family of cytoskeletal proteins
PDLIM7	Target of the ubiquitin ligase Nedd4-1 in skeletal muscle
PLEC1	Orchestrate dynamic changes in cytoarchitecture and cell shape.
SPTAN1	Interact with calmodulin and involve in the calcium-dependent movement of the cytoskeleton at the membrane.
α-actinin-4	Anchor actin to intracellular structures.
β-actin-like protein 2	Components of the cytoskeleton and mediators of internal cell motility
DNA replication and repair	
CCAAT/enhancer binding	Transcriptional regulator of key antioxidant and DNA repair genes

protein gamma	
MCM2	Component of origin recognition complex, phosphorylation prevents DNA re-replication in mitosis.
MSH2/6	MSH2-MSH6 heterodimer binds to DNA mismatches and initiates DNA repair.
Uracil-DNA glycosylase isoform	Prevent mutagenesis by removing uracil from DNA.
Rad9	DNA damage checkpoint component
Ribonucleotide Reductase R2	Coordinate the initiation of DNA synthesis.
RPA1	Single strand DNA binding protein complex
Srs2 DNA helicase	CDK1 phosphorylates Srs2 DNA helicase following DNA damage checkpoint activation.
Transcription and translation	
ATP-dependent RNA helicase A	Unwind double-stranded DNA and RNA in a 3' to 5' direction.
Diphthamide biosynthesis protein 2 isoform a	Modification of histidine residue on elongation factor EF2 to dipthamide.
Eukaryotic translation initiation factor 3 subunit A/E	Associate with the 40S ribosome.
Elongation factor 1	
FoxM1	Transcriptional factor regulating the expression of cell cycle genes essential for DNA replication and mitosis
FXR2	RNA binding protein, associate with polyribosomes.
Heterogeneous nuclear ribonucleoprotein Q/U	mRNA processing
HMG-1 (High mobility group-1)	Cell cycle-dependent phosphorylation significantly modulates their DNA binding affinity.
MyoD	Transcriptional activator that promotes transcription of muscle-specific target genes

NUCKS (Nuclear phosphoprotein)	Belong to HMG protein
Ras GTPase-activating protein-binding protein 1/2	Phosphorylation-dependent sequence-specific endoribonuclease

Centrosome and Golgi apparatus

GM130	cis-Golgi matrix protein, CDK1 phosphorylates N terminal of GM130, which triggers p115 dissociation from GM130 and further sequesters importin α. Then TPX2 is released, activates Aurora A and nucleates microtubules. GM130 captures microtubules and anchors Golgi to the spindle (Wei et al., 2015).
GRASP-65	Peripheral Golgi protein GRASP65, phosphorylation of Golgi components by mitotic kinases may regulate mechanisms of Golgi inheritance during cell division. CDK1 phosphorylates the C terminal of GRASP-65 and primes Plk1 to the Golgi, potentially sensing a Golgi checkpoint (Preisinger et al., 2005).
KIF11 (Eg5)	Required for establishing a bipolar spindle and centrosome separation.
Mps1	CDK1 phosphorylates Mps1 indirectly regulating Spc42 assembly in spindle pole body (SPB) and SPB duplication (Jaspersen et al., 2004).
Pericentriolar material 1 protein (PCM1)	Required to anchor microtubules to the centrosome, phosphorylation by CDK1 is supposed to prevent PCM1 self-aggregation and promote centriole satellite disassembly (Spalluto et al., 2013).
Rab1	Rab1Ap functions in ER-Golgi and intra-Golgi transport and maintenance of Golgi structure. Phosphorylated Rab1 recruits Plk1 to Golgi.
Rab4	ras-like GTP binding protein, Rab4p regulates endocytosis. Phosphorylation of Ser196 by CDK1 is responsible for its cytosol localization in mitosis.
Spc42	Spc42 complex forms a polymeric layer at the periphery of the SPB central plaque, CDK1 phosphorylates Spc42 and promotes its assembly in the SPB.

Mitosis

β-tubulin	Phosphorylation of tubulin may be involved in the regulation of microtubule dynamics during mitosis. Ser172 phosphorylation of β-tubulin in the T5 loop interferes with GTP/GDP turnover (Fourest-Lieuvin et al., 2006).
BubR1	CDK1 phosphorylation of BubR1 controls spindle checkpoint arrest and Plk1-mediated formation of the 3F3/2 epitope (Wong and Fang, 2007).

Cdc14	Dephosphorylates CDK1 substrates and anaphase entry
Cdc16	CDK1 negatively regulates itself by phosphorylating APC component Cdc16, Cdc20, Cdc27.
Cdc20	APC/C co-activator
Cdc25	Activates CDK1
Cdc27	CDK1 phosphorylation of Cdc27 is required for correct chromosomal localization and APC/C function.
CDK7	CAK subunit, phosphorylate and activate CDK1.
CK2 (Casein kinase 2)	Phosphorylated in arrest cell; in *Xenopus* oocyte maturation, phosphorylation occurs with GVBD and chromosome condensation.
Condensin I	Phosphorylation regulates condensin's supercoiling activity.
Condensin II CAP-D3	Phosphorylated CAP-D3 recruits Plk1 to hyperphosphorylate condensin II (Abe et al., 2011).
Connexin-43	Phosphorylation of Cx43 by CDK1-cyclin B may contribute to increased Cx43 phosphorylation and reduced gap junctional communication observed during mitosis.
Disabled 2 (Dab2) aka p96 or DOC-2	A signal transduction protein implicated in the control of cell growth.
Dynein light intermediate chain	Phosphorylation of DLIC by CDK1 leads directly to the loss of membrane-associated cytoplasmic dynein and an inhibition of organelle movement.
ECT2	The Rho activator ECT2 functions as a key regulator in cytokinesis. ECT2 is phosphorylated during G2/M phase.
Hcn1	An essential core component of the fission yeast APC/C, critical for maintaining complex integrity.
hHR6A (homolog of RAD6)	Ubiquitin-conjugating enzyme E2
Histone H1	non-specific CDK1 substrate
Inner centromere protein	Phosphorylated INCENP recruits Plk1 to centromeres.
Kar9	Phosphorylated microtubule-orientation protein Kar9 associates only with the old SPB, which is important for orientation of the mitotic spindle.

KID (chromokinesin)	Phosphorylated form binds chromosome and spindle, functions in chromosome alignment in metaphase.
Kinesin family member23/Zen-4	Phosphoregulation of the motor domain of MKLP1 kinesin ensures that central spindle assembly occurs at the appropriate time in the cell cycle and maintains genomic stability.
lamin A/B	Intermediate filament-type network underlying the inner nuclear membrane, phosphorylation of lamin causes its disassembly and NEBD.
MAP/microtubule affinity-regulating kinase 3	Inhibitory phosphorylation of CDC25C; Regulate activity of microtubules.
MAP4 (Microtubule associated protein 4)	Its phosphorylation affects microtubule properties and cell cycle progression, Cyclin B targets CDK1 to microtubule by binding to MAP4.
NBP-60/LaminB-receptor	Phosphorylation changes the interaction between the nuclear lamina and the inner nuclear membrane.
Nucleolin	Nucleolus protein, phosphorylated Nucleolin localizes on chromosomes during early prometaphase and on spindle poles from prometaphase to anaphase.
Nucleophosmin	CDK1 phosphorylated nucleophosmin associates with metastatic gene, ROCK2.
p21	p21 is phosphorylated by CDK1-Cyclin B1 during mitosis, which reduces p21's stability and binding affinity to CDK1-Cyclin B1.
P21-activated kinase	Phosphorylation by CDK1 alters its association with binding partners and/or substrates that are relevant to morphological changes associated with cell division.
PHF8	Histone H4K20me1 demethylase, CDK1 phosphorylates PHF8 in prophase to remove it from chromatin and accumulate H4K20me1 for condensin CAPD3 and CAPG2 binding (Liu et al., 2010).
Protein Phosphatase 1 Inhibitor 2	Regulator of pp1, only phosphorylated in prometaphase and metaphase.
RCC1	Phosphorylated RCC1 dynamically interacts with chromosomes during metaphase, which is important for localized generation of Ran-GTP on chromatin.
Separase	CDK1-Cyclin B1 phosphorylates and binds separase, inhibiting separase's proteolytic activity before anaphase.
Shugoshin1	CDK1 phosphorylates SGO1 to promote binding of SGO1 to centromeric cohesin.
Ski oncoprotein	Phosphorylation protects Ski from proteasomal degradation and Ski redistributes

	on centrosomes and the spindle during mitosis.
Survivin	Phosphorylated Survivin binds coiled-coil region of Shugoshin and targets it to the inner centromere.
TOPK (MAPKK in spermatogenesis)	Phosphorylation activates TOPK, possibly involved in chromosome segregation and cytokinesis.
WARTS tumor suppressor	Phosphorylated WARTS kinase localizes to the spindle poles at prometaphase and disappears at telophase.
Wee1	CDK1 inhibitor
Others	
Histone deacetylase 6	Inhibit acetylation of α-tubulin, regulating cell motility.
Net1	Nucleolar silencing Establishing factor and Telophase regulator
Stathmin	Phosphorylated Stathmin acts as a relay integrating various intracellular pathways regulating cell proliferation, differentiation and functions.
Serine protease inhibitor kunitz-type 2	Inhibit membrane associated serine protease.

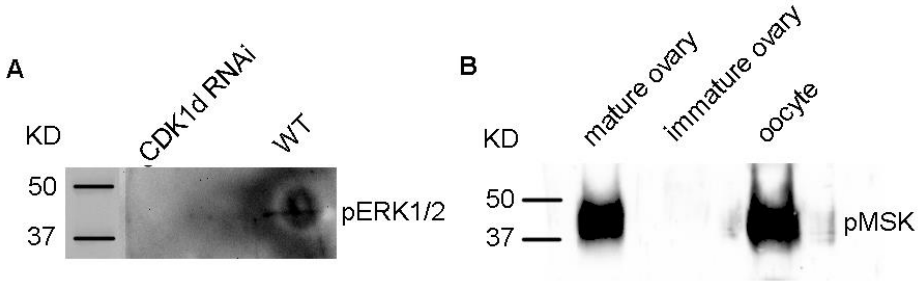

Figure A1. The MAPK signaling cascade lies downstream of CDK1d. (A) Western blot analysis using pERK1/2 antibody showed that pERK was absent in *CDK1d* RNAi oocytes. Equal numbers of oocytes were loaded. (B) Western blot analysis using pMSK antibody showed that MAPK activity was low in the immature ovary and increased dramatically in the mature ovary and oocytes. Equal amounts of total protein were loaded. Note: MSK is a downstream target of MAPK/ERK.

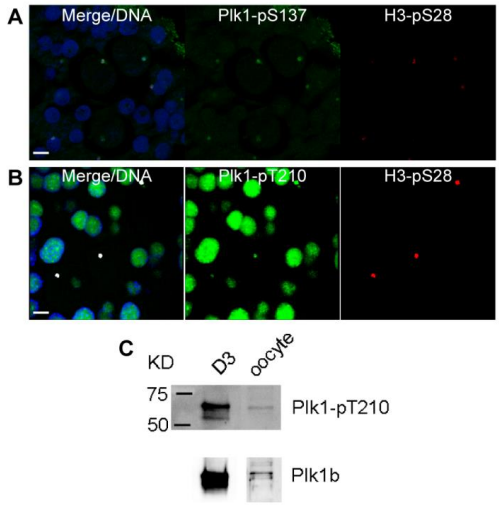

Figure A2. The subcellular distribution of Plk1-pS137 and Plk1-pT210 in P5 ovaries. (A) Plk1-pS137 (green) is localized in meiotic nuclei. (B) Plk1-pT210 (green) is localized in meiotic nuclei and nurse nuclei. H3-pS28 (red) marks meiotic nuclei. TO-PRO-3 staining (blue) marks DNA. Scale bars: 10 µm. (C) Western blot using Plk1-pT210 and custom made Plk1b antibodies shows Plk1b is highly expressed in D3 animals and oocytes.

O. dioica contains distinct subfamilies of B-type Cyclins

Five B-type Cyclins were identified in the *O. dioica* genome. Phylogenetic analysis showed that Cyclin Ba, Bb and Bc are closely related to each other and form a clade with Cyclin B1 and B2 orthologs of urochordates, cephalochordates, vertebrates, echinoderms, nematodes and insects. Cyclin B3a and B3b are closely related to other appendicularian Cyclin B3 orthologs, together forming a clade with other metazoan Cyclin B3 (Fig. A3). Intriguingly, *O. dioica* Cyclin Bc is clustered with *O. albicans* Cyclin Bc with nearly 100% probability support, indicating that the most recent common ancestor only possessed Cyclin Bc, and Cyclin Ba and Bb were generated by duplication post-dating the separation of *O. dioica* and *O. albicans*. Cyclin Ba and Bb display high gene structure similarity (Fig. A4-A) and share 97% similarity in protein sequence (Fig. A4-B). They showed an overlapping expression pattern during embryogenesis, though at certain stages one was expressed at higher levels than the other (Fig. A4-C). Cyclin Ba/b transcripts were symmetrically distributed at several spots in the trunk of tadpole. Cyclin Bc and Cyclin B3a were highly expressed during embryogenesis, and evenly distributed in the trunk. Cyclin B3b was not expressed during embryogenesis (Fig. A5). The ubiquitous expression patterns of Cyclins Bc and B3a support that they are the canonical Cyclin B1 and Cyclin B3 homologs functioning in embryonic mitoses, whereas the recent duplicate Cyclins Ba and Bb in *O. dioica* are specialized mitotic Cyclins driving early embryonic cleavages, and become tissue-specific during late developmental stages.

Comparison of expression levels of B-type Cyclins between males and females revealed sex-specific expression patterns. Cyclins Ba and B3aα were the dominant transcripts in the ovaries, whereas Cyclins Bc, B3aβ and B3b were specifically expressed in the testes (Fig. A6-A). In addition, Cyclin Bc protein was highly expressed in D3 gonads and is localized in mitotic proliferating germline nuclei, implying its potential roles to regulate mitosis (Fig. A6-B&C). In addition to the roles of Cyclins Ba and B3a in oocyte maturation, these observations support the other Cyclin B paralogs, Cyclins Bc and B3b, might play roles during spermatogenesis.

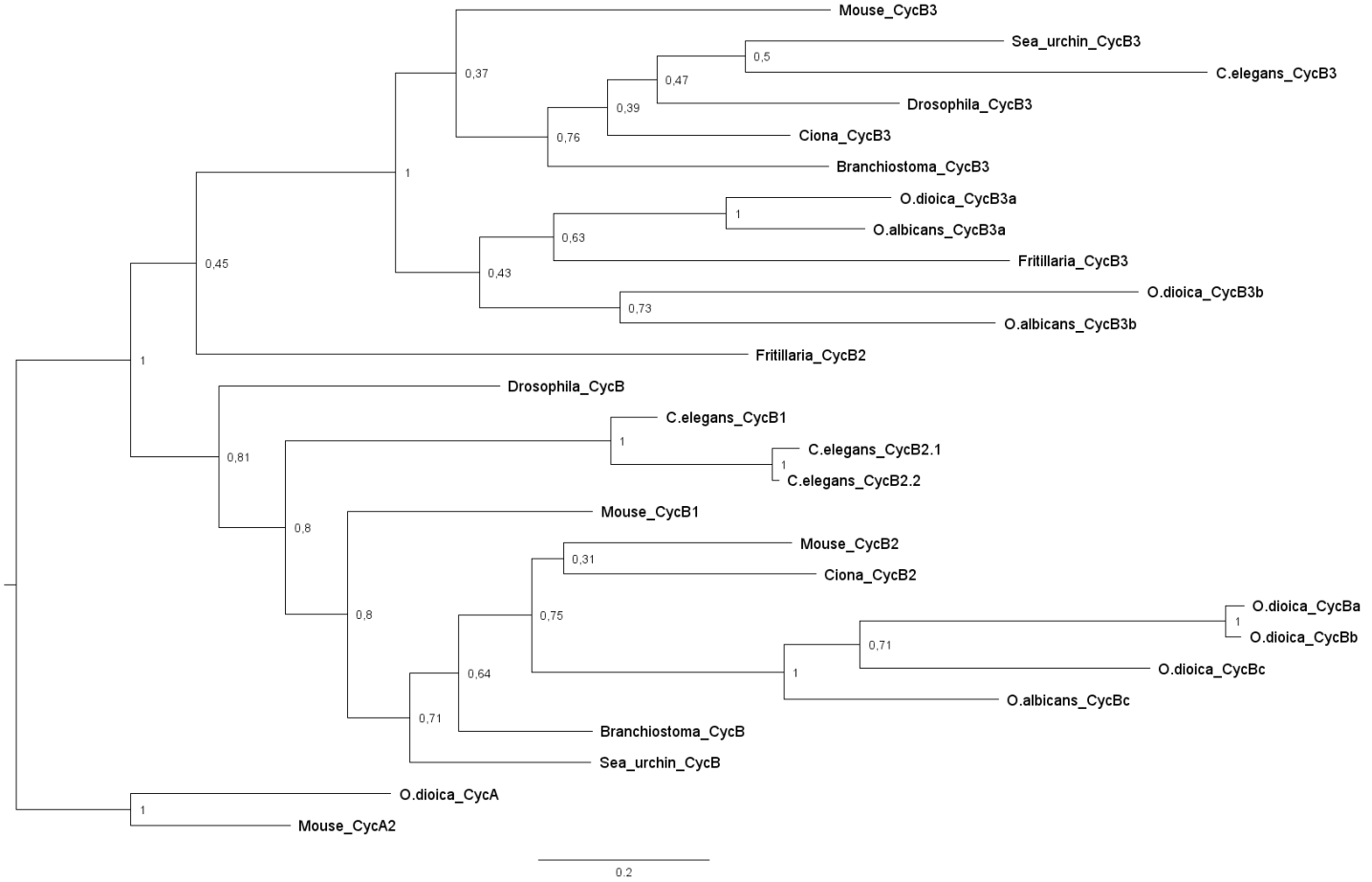

Figure A3. Phylogenetic tree of representative metazoan B-type Cyclins using N-terminal cyclin boxes constructed with Bayesian inference. Posterior probabilities are labeled at the nodes. A mixed amino acid model was used with 2,000,000 generations sampled every 100 generations. *O. dioica* Cyclin A and mouse Cyclin A2 were used as an outgroup.

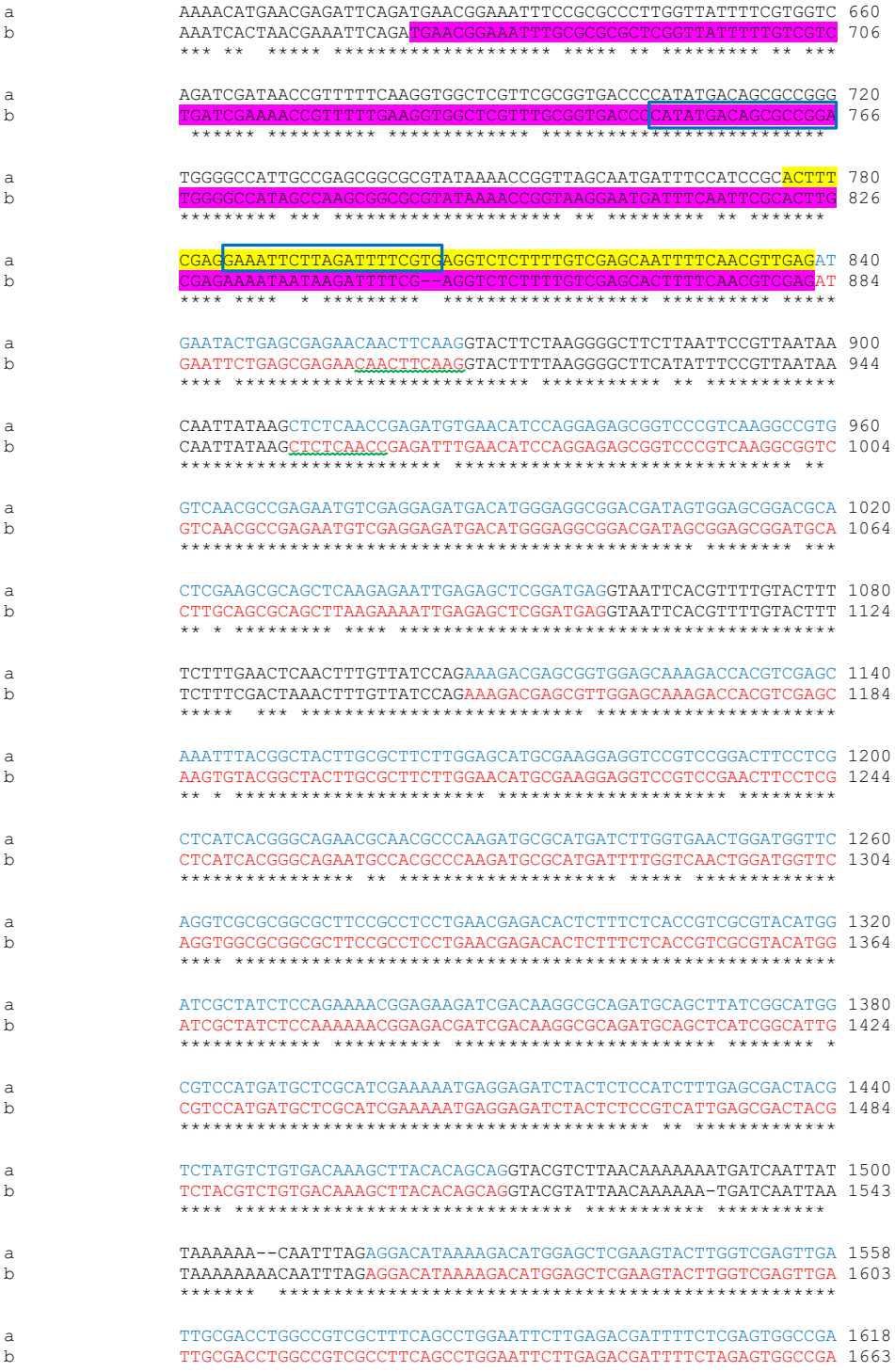
a AAAACATGAACGAGATTCAGATGAACGGAAATTTCCGCGCCCTTGGTTATTTTCGTGGTC 660
b AAATCACTAACGAAATTCAGATGAACGGAAATTTGCGCGCGCTCGGTTATTTTTGTCGTC 706
a AGATCGATAACCGTTTTTCAAGGTGGCTCGTTCGCGGTGACCCCATATGACAGCGCCGGG 720
b TGATCGAAAACCGTTTTTGAAGGTGGCTCGTTTGCGGTGACCCCATATGACAGCGCCGGA 766
a TGGGGCCATTGCCGAGCGGCGCGTATAAAACCGGTTAGCAATGATTTCCATCCGCACTTT 780
b TGGGGCCATAGCCAAGCGGCGCGTATAAAACCGGTAAGGAATGATTTCAATTCGCACTTG 826
a CGAGGAAATTCTTAGATTTTCGTGAGGTCTCTTTTGTCGAGCAATTTTCAACGTTGAGAT 840
b CGAGAAAATAATAAGATTTTCG--AGGTCTCTTTTGTCGAGCACTTTTCAACGTCGAGAT 884
a GAATACTGAGCGAGAACAACTTCAAGGTACTTCTAAGGGGCTTCTTAATTCCGTTAATAA 900
b GAATTCTGAGCGAGAACAACTTCAAGGTACTTTTAAGGGGCTTCATATTTCCGTTAATAA 944
a CAATTATAAGCTCTCAACCGAGATGTGAACATCCAGGAGAGCGGTCCCGTCAAGGCCGTG 960
b CAATTATAAGCTCTCAACCGAGATTTGAACATCCAGGAGAGCGGTCCCGTCAAGGCGGTC 1004
a GTCAACGCCGAGAATGTCGAGGAGATGACATGGGAGGCGGACGATAGTGGAGCGGACGCA 1020
b GTCAACGCCGAGAATGTCGAGGAGATGACATGGGAGGCGGACGATAGCGGAGCGGATGCA 1064
a CTCGAAGCGCAGCTCAAGAGAATTGAGAGCTCGGATGAGGTAATTCACGTTTTGTACTTT 1080
b CTTGCAGCGCAGCTTAAGAAAATTGAGAGCTCGGATGAGGTAATTCACGTTTTGTACTTT 1124
a TCTTTGAACTCAACTTTGTTATCCAGAAAGACGAGCGGTGGAGCAAAGACCACGTCGAGC 1140
b TCTTTCGACTAAACTTTGTTATCCAGAAAGACGAGCGTTGGAGCAAAGACCACGTCGAGC 1184
a AAATTTACGGCTACTTGCGCTTCTTGGAGCATGCGAAGGAGGTCCGTCCGGACTTCCTCG 1200
b AAGTGTACGGCTACTTGCGCTTCTTGGAACATGCGAAGGAGGTCCGTCCGAACTTCCTCG 1244
a CTCATCACGGGCAGAACGCAACGCCCAAGATGCGCATGATCTTGGTGAACTGGATGGTTC 1260
b CTCATCACGGGCAGAATGCCACGCCCAAGATGCGCATGATTTTGGTCAACTGGATGGTTC 1304
a AGGTCGCGCGGCGCTTCCGCCTCCTGAACGAGACACTCTTTCTCACCGTCGCGTACATGG 1320
b AGGTGGCGCGGCGCTTCCGCCTCCTGAACGAGACACTCTTTCTCACCGTCGCGTACATGG 1364
a ATCGCTATCTCCAGAAAACGGAGAAGATCGACAAGGCGCAGATGCAGCTTATCGGCATGG 1380
b ATCGCTATCTCCAAAAAACGGAGACGATCGACAAGGCGCAGATGCAGCTCATCGGCATTG 1424
a CGTCCATGATGCTCGCATCGAAAAATGAGGAGATCTACTCTCCATCTTTGAGCGACTACG 1440
b CGTCCATGATGCTCGCATCGAAAAATGAGGAGATCTACTCTCCGTCATTGAGCGACTACG 1484
a TCTATGTCTGTGACAAAGCTTACACAGCAGGTACGTCTTAACAAAAAAATGATCAATTAT 1500
b TCTACGTCTGTGACAAAGCTTACACAGCAGGTACGTATTAACAAAAAA-TGATCAATTAA 1543
a TAAAAAA--CAATTTAGAGGACATAAAAGACATGGAGCTCGAAGTACTTGGTCGAGTTGA 1558
b TAAAAAAAACAATTTAGAGGACATAAAAGACATGGAGCTCGAAGTACTTGGTCGAGTTGA 1603
a TTGCGACCTGGCCGTCGCTTTCAGCCTGGAATTCTTGAGACGATTTTCTCGAGTGGCCGA 1618
b TTGCGACCTGGCCGTCGCCTTCAGCCTGGAATTCTTGAGACGATTTTCTAGAGTGGCCGA 1663

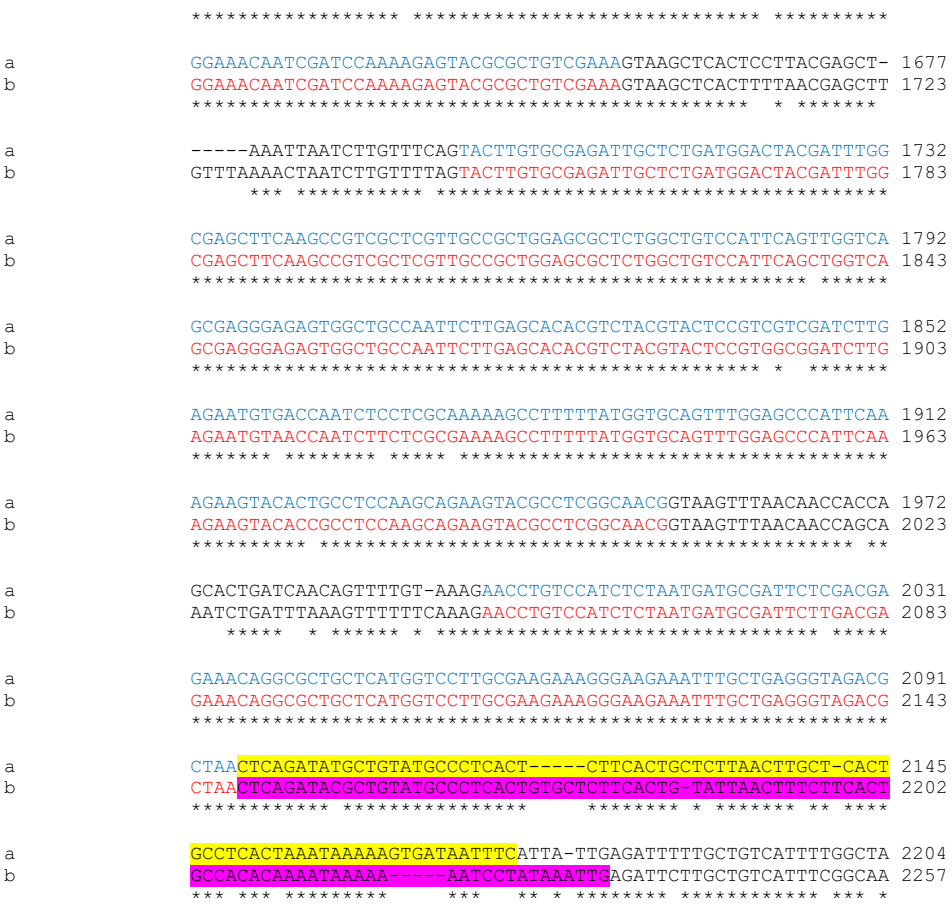

Figure A4-A. Sequence alignment of *Cyclin Ba* and *Bb* genes. Exons of *Cyclin Ba* and *Bb* are color-coded in blue and red respectively. UTRs of *Cyclin Ba* and *Bb* are shaded in yellow and purple, respectively. Identical nucleotides are marked by asters below. qPCR forward primers used to distinguish their transcripts are marked by rectangles. The reverse primers are marked by green wavy lines.

```
a               MNTEREQLQALNRDVNIQESGPVKAVVNAENVEEMTWEADDSGADALEAQLKRIESSDEK 60
b               MNSEREQLQALNRDLNIQESGPVKAVVNAENVEEMTWEADDSGADALAAQLKKIESSDEK 60
                **:***********:******************************** ****:*******

a               DERWSKDHVEQIYGYLRFLEHAKEVRPDFLAHHGQNATPKMRMILVNWMVQVARRFRLLN 120
b               DERWSKDHVEQVYGYLRFLEHAKEVRPNFLAHHGQNATPKMRMILVNWMVQVARRFRLLN 120
                ***********:***************:********************************

a               ETLFLTVAYMDRYLQKTEKIDKAQMQLIGMASMMLASKNEEIYSPSLSDYVYVCDKAYTA 180
b               ETLFLTVAYMDRYLQKTETIDKAQMQLIGIASMMLASKNEEIYSPSLSDYVYVCDKAYTA 180
                ******************.**********:******************************

a               EDIKDMELEVLGRVDCDLAVAFSLEFLRRFSRVAEETIDPKEYALSKYLCEIALMDYDLA 240
b               EDIKDMELEVLGRVDCDLAVAFSLEFLRRFSRVAEETIDPKEYALSKYLCEIALMDYDLA 240
                ************************************************************

a               SFKPSLVAAGALWLSIQLVSEGEWLPILEHTSTYSVVDLENVTNLLAKSLFMVQFGAHSK 300
b               SFKPSLVDAGALWLSIQLVSEGEWLPILEHTSTYSVADLENVTNLLAKSLFMVQFGAHSK 300
                ******* ****************************.**********************

a               KYTASKQKYASATNLSISNDAILDEKQALLMVLAKKGKKFAEGRR 345
b               KYTASKQKYASATNLSISNDAILDEKQALLMVLAKKGKKFAEGRR 345
                *********************************************
```

Figure A4-B. Protein sequence alignment of Cyclins Ba and Bb. Identical residues are indicated by asters and similar residues by dots.

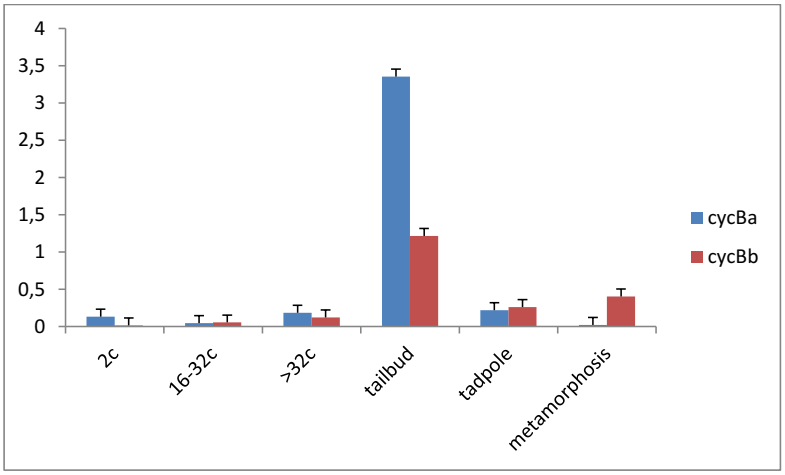

Figure A4-C. mRNA expression profiles of *Cyclin Ba* and *Bb* during embryogenesis. qPCR analysis showed that *Cyclin Ba* was expressed at higher levels until the tailbud stage, and *Cyclin Bb* was expressed at relatively higher levels at tadpole and metamorphosis stages. Expression values with SE (n=3) were normalized to EF1β.

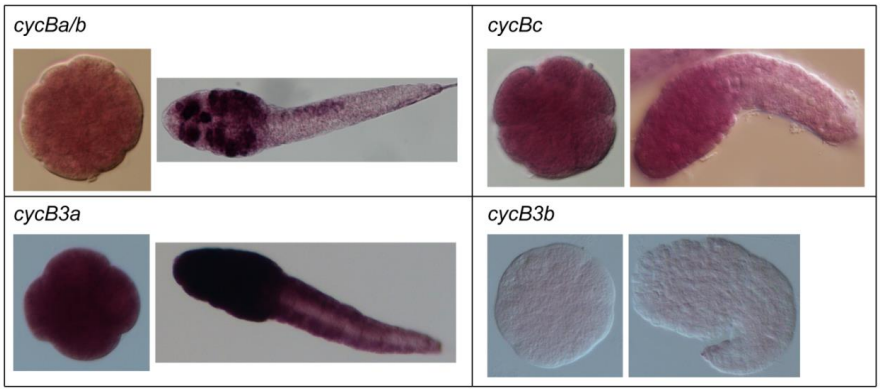

Figure A5. The distribution of B-type *Cyclin* transcripts (*in situ* hybridization) in *O. dioica* embryos. Signals labeled by anti-sense probes are shown. Negative controls with sense probes showed no signal.

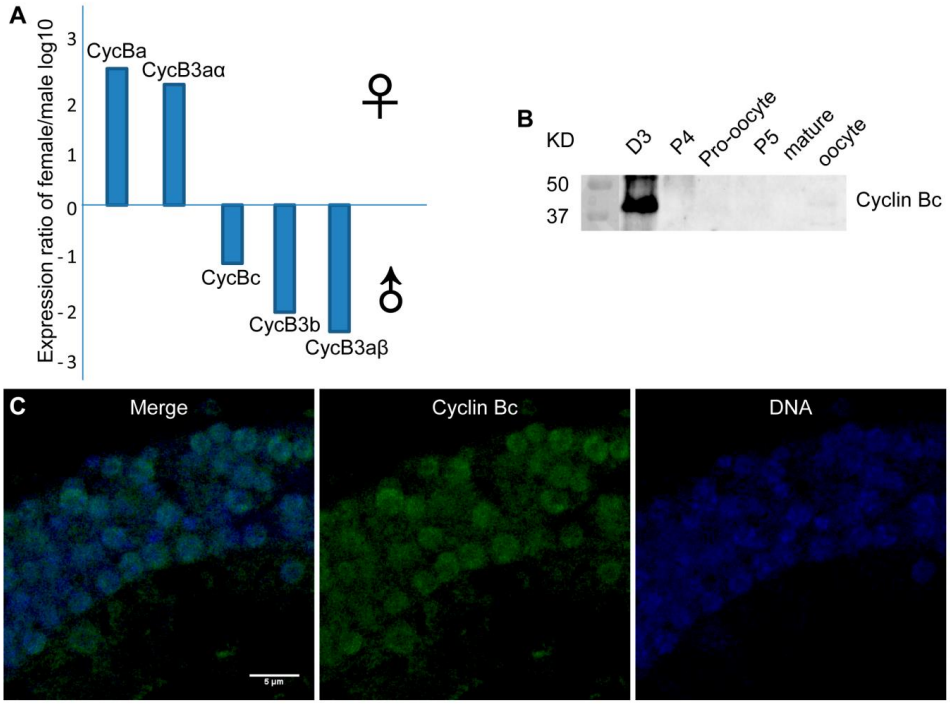

Figure A6. (A) Relative expression levels of B-type Cyclins in the ovaries and testes. Modified from Campsteijn et al (2012). (B) Western blot using custom made Cyclin Bc antibody showed Cyclin Bc protein was highly expressed in D3 gonads, but not expressed during oogenesis. Equal amounts of total animal lysate were loaded. (C) Immunostaining using a Cyclin Bc antibody showed Cyclin Bc protein (green) is present in germline nuclei of D3 animals. TO-PRO-3 staining (blue) marks DNA. Scale bar: 5 µm.

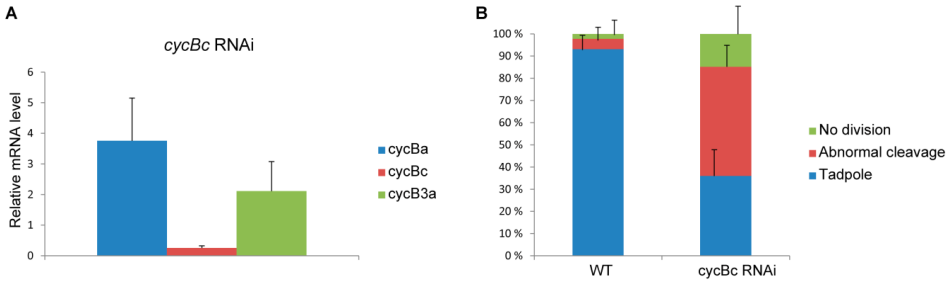

Figure A7. Knockdown of Cyclin Bc caused partial mitotic arrest. (A) Knockdown efficiency of cyclin Bc mRNA levels was assayed by RT-PCR. No significant off-target effects on other cyclin B paralogs were detected. (B) Knockdown of Cyclin Bc resulted in an elevated degree of embryonic arrest. Compared to wild-type, about 50% of *cycBc* RNAi embryos divided abnormally and arrested before the tadpole stage. Standard errors from three biological replicates are shown in each category.

```
HsCycB1      MALRVTRNSKINAENKAKINMAGAKRVPTAPAATSKPGLRPRTALGDIGN
OdCycBa      --------------------------------------------------
OdCycBc      MEARRLNPRNRLEGDGLVSKGIGGI----------AKQRTALGAVHG

HsCycB1      KVSEQ-LQAKMPMKKE-AKPSATGKVIDKKLPKPLEKVPMLVPVPVSEPV
OdCycBa      -------------------------MNTE--------------------
OdCycBc      SNRQIKDEASKPHVRTTRAQMLRSKMVDNQRTKPAVK-------------

HsCycB1      PEPEPEPEPEPVKEEKLSPEPILVDTASPSPMETSGCAPAEEDLCQAF-S
OdCycBa      ----------------------------REQL-QALNR
OdCycBc      ----------------------------SQN-QPIKR

HsCycB1      DVIL----------------------------------------AVN
OdCycBa      DVNIQESGPVKAVVNAENVEEMTW----------EADDSGADALEAQLK
OdCycBc      KAEA-KKAKIEIIEEKPQVQEMSFDCPMDVSMSSLKSEDEVDEKLQEAIK

HsCycB1      DVDAEDGADPNLCSEYVKDIYAYLRQLEEEQAVRPKYLLG--REVTGNMR
OdCycBa      RIESSDEKDERWSKDHVEQIYGYLRFLEHAKEVRPDFLAHHGQNATPKMR
```

```
OdCycBc      KVEELDNKDDGNGGPYVNEIYDYTKYLEHAYAVKPRFLDEHKE-VSHKMR

HsCycB1      AILIDWLVQVQMKFRLLQETMYMTVSIIDRFMQN-NCVPKKMLQLVGVTA
OdCycBa      MILVNWMVQVARRFRLLNETLFLTVAYMDRYLQKTEKIDKAQMQLIGMAS
OdCycBc      TILVDWIVQVHQRFKLQNETLHLTVAIMDRYLSKVQDLPRKEMQMIGLTS

HsCycB1      MFIASKYEEMYPPEIGDFAFVTDNTYTKHQIRQMEMKILRALNFGLGRPL
OdCycBa      MMLASKNEEIYSPSLSDYVYVCDKAYTAEDIKDMELEVLGRVDCDLAVAF
OdCycBc      MLLASKYEEIYMPDLGDFEFICDNAYTRDDFKATELEILDVLQCNLAFGL

HsCycB1      PLHFLRRASKIGE--VDVEQHTLAKYLMELTMLDYDMVHFPPSQIAAGAF
OdCycBa      SLEFLRRFSRVAEETIDPKEYALSKYLCEIALMDYDLASFKPSLVAAGAL
OdCycBc      SIEHLRRFSTVLTDEIDGMHHSLGKYFLELALMDYDLCTFKPSIIAAGSM

HsCycB1      CLALKILDNGEWTPTLQHYLSYTEESLLPVMQHLAKNVVMVNQGLTKH--
OdCycBa      WLSIQLVSEGEWLPILEHTSTYSVVDLENVTNLLAKSLFMVQFGAHSKKY
OdCycBc      KLALEMHGDKEWDCRLTHFSGYKSDDLEFFINLLCKTIYMVHFTKS--KY

HsCycB1      --MVSQYSGIVRC--------------------------------
OdCycBa      TASKQKYASATNLSISNDAILDEKQALLMVLAKKGKKFAEGRR
OdCycBc      QAIKKKYSSDKLCAAAKYDKFDELKEEIYRRAKLAKEQTDKR-
```

Figure A8. Amino acid sequence alignment of human (Hs) Cyclin B1, *O. dioica* (Od) Cyclin Ba and Bc. Functional domains are shaded: Cyclin box, grey; D-box, purple; cytoplasmic retention regions (CRS) with nuclear export sequence (NES) underlined, yellow; nuclear localization signal (NLS), cyan. Putative CDK1 phosphorylation sites are marked in red, and Plk1 phosphorylation sites in blue shading.

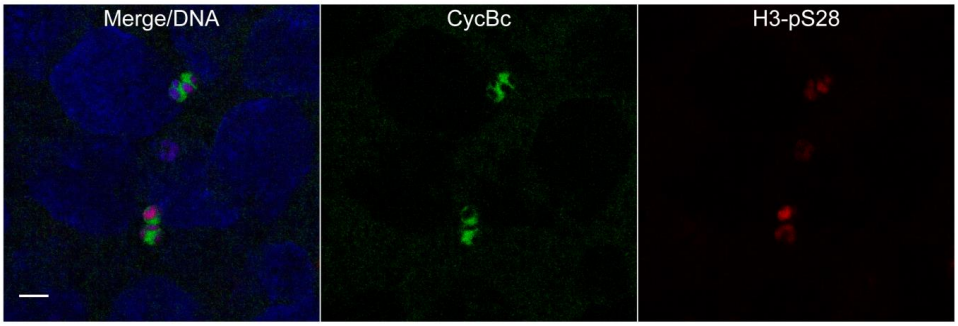

Figure A9. Cyclin Bc retains the potential for localization in meiotic nuclei. GFP-fused *Cyclin Bc* cmRNA was injected to P3 ovaries, and Cyclin Bc fusion protein (green) was detect by GFP antibodies in selected meiotic nuclei labeled by H3pS28 (red). TO-PRO-3 staining (blue) marks DNA. Scale bar: 5 μm.

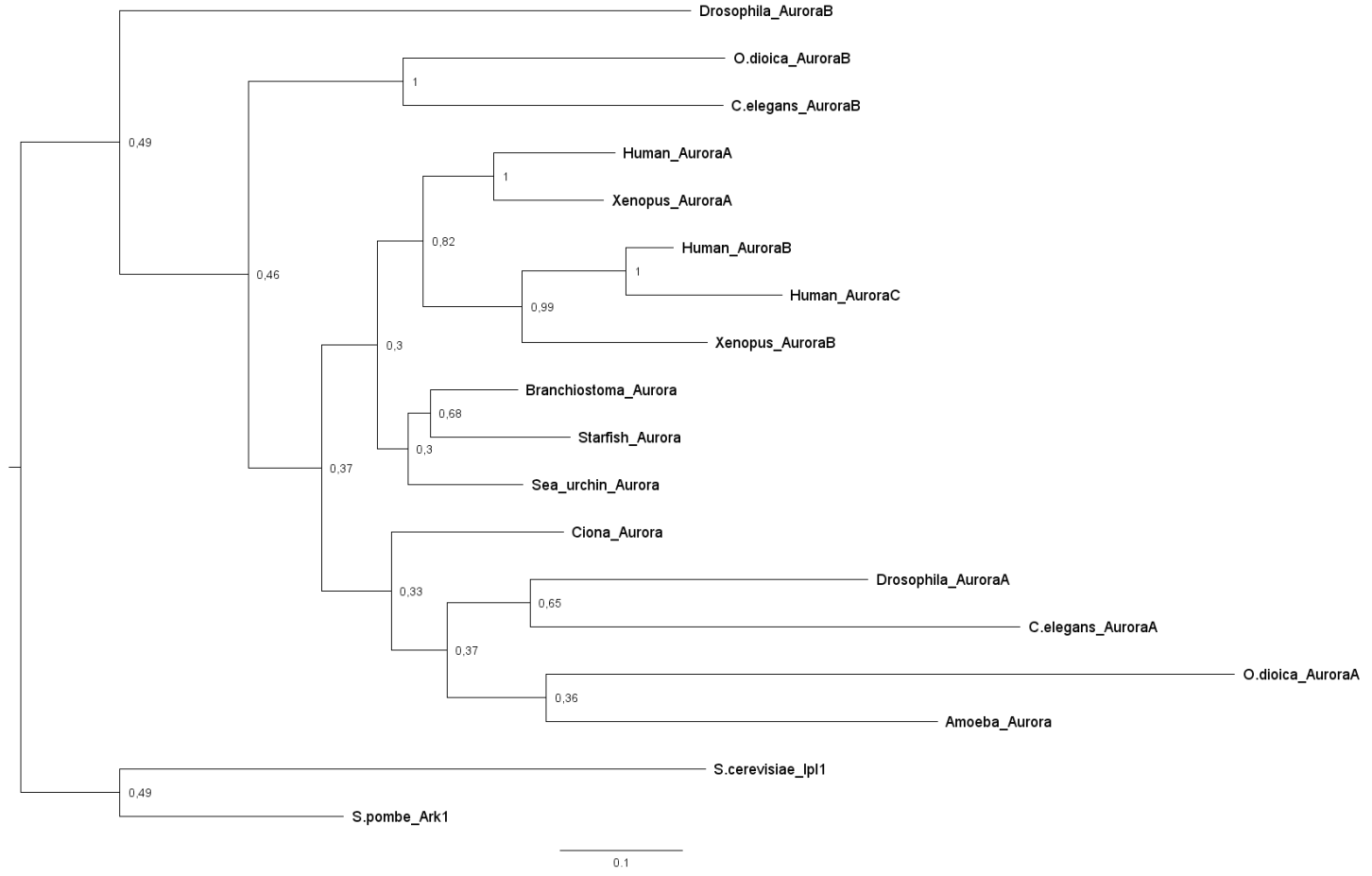

Figure A10. Phylogenetic tree of Aurora kinases was constructed with Bayesian methods based on the alignment of the catalytic domain. A mixed amino acid model was used with 2,000,000 generations sampled every 100 generations. Posterior probabilities were indicated at the nodes.

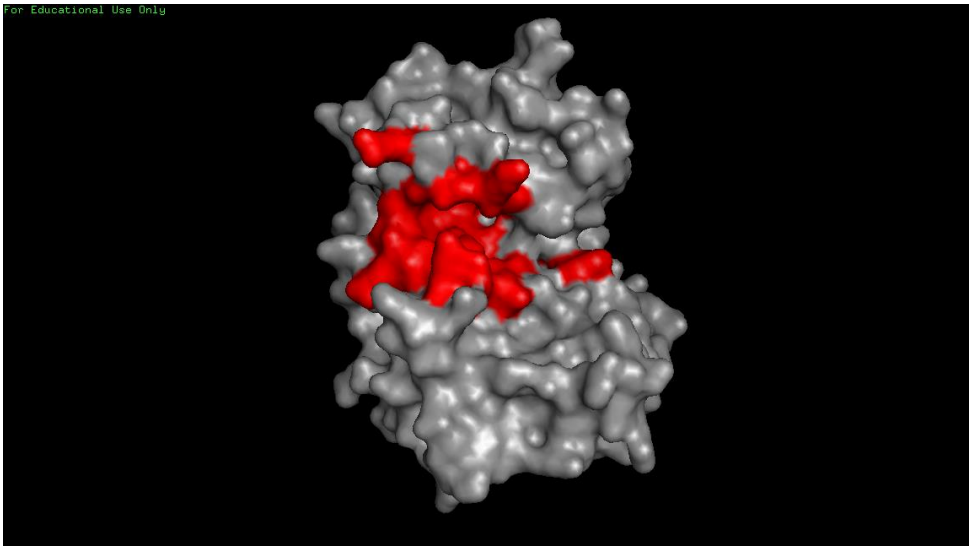

Figure A11-A. Crystal structure of the catalytic domain of *Xenopus* Aurora B (PDB ID 2BFY). Residues lining the catalytic pocket are colored in red.

```
                ....|....| ....|....| ....|....| ....|....| ....|....|
                    5          15         25         35         45
OdAuroraA       FDMGKALGKG RFGHVYCARE TKSGYVVALK IMFKNQIKDA NLQHQVRREV
OdAuroraB       FDIGKPLGKG KFGSVYLART KKEKYIVAVK ILFKSQLVTG GVEAQLRREI
HsAuroraA       FEIGRPLGKG KFGNVYLARE KQSKFILALK VLFKAQLEKA GVEHQLRREV
HsAuroraB       FEIGRPLGKG KFGNVYLARE KKSHFIVALK VLFKSQIEKE GVEHQLRREI
HsAuroraC       FEIGRPLGKG KFGNVYLARL KESHFIVALK VLFKSQIEKE GLEHQLRREI
XlAuroraA       FEIGRPLGKG KFGNVYLARE RESKFILALK VLFKSQLEKA GVEHQLRREV
XlAuroraB       FDIGRPLGKG KFGNVYLARE KQNKFIMALK VLFKSQLEKE GVEHQLRREI
CiAurora        FDIGKPLGRG KFGSVYLARE KKSKFIVALK VLFKSQLMKS NVEHQLRREI
BfAurora        FDIGRPLGKG KFGNVYLARE KNSKFIVALK VLFKSQLMKA GVEHQLRREI
ApAurora        FDIGRPLGKG KFGNVYLARE KKSKFIVALK VLFKSQLQKA KVEHQLRREI
SpAurora        FDIGRPLGKG KFGSVYLARE KQTKYIVALK VLFKSQLQKA QVEHQLRREI
DmAuroraA       FDIGRLLGRG KFGNVYLARE KESQFVVALK VLFKRQIGES NVEHQVRREI
DmAuroraB       FEMGAHLGRG KFGRVYLARE RHSHYLVAMK VMFKEELRKG CVQRQVLREI
CeAuroraA       FDVGRPLGKG KFGNVFISRE KKTKRIIALK VLFKTQLLQL GVSHQLKREI
CeAuroraB       FEIGRPLGKG KFGSVYLART KTGHFHVAIK VLFKSQLISG GVEHQLEREI
DdAurora        FDIGKLLGMG RFGHVYLARE KKSQFIVALK VLFKNQLQTH NIEHQLRREI
ScIpl1          FELGKKLGKG KFGKVYCVRH RSTGYICALK VMEKEEIIKY NLQKQFRREV
SpArk1          FEIGKPLGKG KFGRVYLAKE KKTGFIVALK TLHKSELVQS KIEKQVRREI

                ....|....| ....|....| ....|....| ....|....| ....|....|
                    55         65         75         85         95
OdAuroraA       EIQSHIKHKN ICRLYGYFHD DRRVYIILEF CKNGNLFTKL KEVKK--FES
OdAuroraB       EIQSHLRHPH ILRLFGWFHD VKKIYLVLEY AAQGELYKEL MKK--GRLSE
HsAuroraA       EIQSHLRHPN ILRLYGYFHD ATRVYLILEY APLGTVYREL QKLSK--FDE
HsAuroraB       EIQAHLHHPN ILRLYNYFYD RRRIYLILEY APRGELYKEL QKSCT--FDE
HsAuroraC       EIQAHLQHPN ILRLYNYFHD ARRVYLILEY APRGELYKEL QKSEK--LDE
```

```
XlAuroraA    EIQSHLRHPN ILRLYGYFHD ASRVYLILDY APGGELFREL QKCTR--FDD
XlAuroraB    EIQSHLRHPN ILRMYNYFHD RKRIYLMLEF APRGELYKEL QKHGR--FDE
CiAurora     EIQSHLRHPH ILRLYGYFHD ETRVYLILEY ASRGEMYKEL QKQGK--FTE
BfAurora     EIQSHLRHPH ILRLYGYFYD DTRVYLILEY APRGELYKEL QKQVR--FDE
ApAurora     EIQSHLRHDH ILRLYGYFYD DTRVYLILEY AARGELYKEM QAQKAGHFDE
SpAurora     EIQSHLRHPN ILRLFGYFYD ESRVYLILEY APRGELYKQL QRAGR--FDE
DmAuroraA    EIQSHLRHPH ILRLYAYFHD DVRIYLILEY APQGTLFNAL QAQPMKRFDE
DmAuroraB    EIQSRLKHPH ILRLLTWFHD ESRIYLALEI ASEGELFKHL RGAPNHRFDE
CeAuroraA    EIQYHLRHPN ILTLYGYFHD DKRVFVILDY ASRGELFNVL QSQPGHKVNE
CeAuroraB    EIQSHLNHPN IIKLYTYFWD AKKIYLVLEY APGGEMYKQL TVS--KRFSE
DdAurora     EIQSHLRHPN ILRLFGYFYD DKRVFLIIEF AKGGECFKEL QKVGS--FNE
ScIpl1       EIQTSLNHPN LTKSYGYFHD EKRVYLLMEY LVNGEMYKLL RLHGP--FND
SpArk1       EIQSNLRHKN ILRLYGHFHD EKRIYLILEF AGRGELYQHL RRA--KRFSE

                ....|....| ....|....| ....|....| ....|....| ....|....|
                   105        115        125        135        145
OdAuroraA    IEAARYVREI AEGLDYIHKL NVIHRDLKPE NVLLGRNNEV KLADFGWCVF
OdAuroraB    FRTATIIHEV SDAMKYCHAN KIIHRDLKPE NVLIGLQGEA KLADFGWSVR
HsAuroraA    QRTATYITEL ANALSYCHSK RVIHRDIKPE NLLLGSAGEL KIADFGWSVH
HsAuroraB    QRTATIMEEL ADALMYCHGK KVIHRDIKPE NLLLGLKGEL KIADFGWSVH
HsAuroraC    QRTATIIEEL ADALTYCHDK KVIHRDIKPE NLLLGFRGEV KIADFGWSVH
XlAuroraA    QRSAMYIKQL AEALLYCHSK KVIHRDIKPE NLLLGSNGEL KIADFGWSVH
XlAuroraB    QRSATFMEEL ADALHYCHER KVIHRDIKPE NLLMGYKGEL KIADFGWSVH
CiAurora     EMSATYIAEL ADALNYCHSK QVIHRDIKPE NLLMGLRGEL KIADFGWSVH
BfAurora     RRSATYIAQL ADALKYCHSK KVIHRDIKPE NLLLGLKGDL KIADFGWSVH
ApAurora     DRSAVYIYQL AKALLYCHEK KVIHRDIKPE NLLLDLKGDL KIADFGWSVH
SpAurora     QRTASYISQL ADALKYCHSK KVIHRDIKPE NLLLGLLGDL KIADFGWSVH
DmAuroraA    RQSATYIQAL CSALLYLHER DIIHRDIKPE NLLLGHKGVL KIADFGWSVH
DmAuroraB    PRSAKYTYQV ANALNYCHLN NVIHRDLKPE NILLTSTDDL KLADFGWSAH
CeAuroraA    VIAGRFVRQL ANALHYCHSK GVIHRDIKPE NLLLDSKLNL KLADFGWSVV
CeAuroraB    PTAAKYMYEI ADALSYCHRK NVIHRDIKPE NLLIGSQGEL KIGDFGWSVH
DdAurora     QTAATYTLQI ADALRYCHSK HVIHRDIKPE NLLIGVGGEI KIADFGWSVH
ScIpl1       ILASDYIYQI ANALDYMHKK NIIHRDIKPE NILIGFNNVI KLTDFGWSII
SpArk1       EVASKYIFQM ANALSYLHKK HVIHRDIKPE NILLGIDGEI KLSDFGWSVH

                ....|....| ....|....| ....|....| ....|....| ....|....|
                   155        165        175        185        195
OdAuroraA    TP-QSRRQTF CGTMDYLSPE MLNGVSHDKK IDHWALGCIA FELLTGYPPF
OdAuroraB    TP-SRRRETM CGTLDYLPPE MVEQVDYTFT VDNWTIGVLC YELLTGKPPF
HsAuroraA    AP-SSRRTTL CGTLDYLPPE MIEGRMHDEK VDLWSLGVLC YEFLVGKPPF
HsAuroraB    AP-SLRRKTM CGTLDYLPPE MIEGRMHNEK VDLWCIGVLC YELLVGNPPF
HsAuroraC    TP-SLRRKTM CGTLDYLPPE MIEGRTYDEK VDLWCIGVLC YELLVGYPPF
XlAuroraA    AP-SSRRTTL CGTLDYLPPE MIEGRMHDET VDLWSLGVLC YEFLVGKPPF
XlAuroraB    AP-SLRRRTM CGTLDYLPPE MIEGKTHDEK VDLWCAGVLC YEFLVGMPPF
CiAurora     AP-SSKRQTL CGTLDYLPPE MIEAKDHDAN VDLWTLGILC YEFLVGKPPF
BfAurora     AP-SSRRATL CGTLDYLPPE MIEGKMHDEK VDLWSLGVLC YEFLVGKPPF
ApAurora     AP-SSRRATL CGTLDYLPPE MIEGKTHDEK VDLWSLGVLC YEFLVGKPPF
SpAurora     AP-SSRRNTL CGTMDYLPPE MIEGRMHDDK VDLWSLGVLC YEFLVGKPPF
DmAuroraA    EP-NSMRMTL CGTVDYLPPE MVQGKPHTKN VDLWSLGVLC FELLVGHAPF
DmAuroraB    TP-NNKRRTL CGTLDYLPPE MVDGNSYDDS VDQWCLGILC YEFVVGCPPF
CeAuroraA    AD-HSKRHTL CGTMDYLAPE MVSNQPHDFN VDIWAIGILL FEMLVGYAPF
CeAuroraB    AP-SNKRQTM CGTMDYLPPE MVNGADHSDA VDLWAIGVLC YEFLVGKPPF
DdAurora     AP-NTKRSTF CGTLEYLPPE VIEKKGYDQT ADVWSLGILI FEFLVGRSPF
ScIpl1       NPPENRRKTV CGTIDYLSPE MVESREYDHT IDAWALGVLA FELLTGAPPF
SpArk1       AP-SNRRTTL CGTLDYLPPE MVEGKEHTEK VDLWSLGVLT YEFLVGAPPF

                ....|....| ....|....| ....|....| ....|....| ....|....|
                   205        215        225        235        245
OdAuroraA    VGDK-KNPTV EVTRSLIVSG TIDFEKAKEV NEQEQEVVDA LVQLEPNDRI
OdAuroraB    EHDD-KNVTY QR------IV NTQFTYPNHV KEGARDLITR LLQYKGANRI
HsAuroraA    EANT-YQETY KR------IS RVEFTFPDFV TEGARDLISR LLKHNPSQRP
```

```
HsAuroraB    ESAS-HNETY RR------IV KVDLKFPASV PMGAQDLISK LLRHNPSERL
HsAuroraC    ESAS-HSETY RR------IL KVDVRFPLSM PLGARDLISR LLRYQPLERL
XlAuroraA    ETDT-HQETY RR------IS KVEFQYPPYV SEEARDLVSK LLKHNPNHRL
XlAuroraB    DSPS-HTETH RR------IV NVDLKFPPFL SDGSKDLISK LLRYHPPQRL
CiAurora     ETKS-TQETY LR------IT SLKYSFPPHV SEGARDLIRR LLKLEPRHRL
BfAurora     EAEG-HSETY RR------IS KVDLRFPPHV TSGARDLISK LLRHNPMLRL
ApAurora     ESQG-NTETY RK------IT KVEFTFPKHV SEGARDLICK LLKHNPSHRL
SpAurora     EAEG-STETY RR------IT KVHYQFPSYV SAGARDVIKR LLQHNPANRL
DmAuroraA    YSKN-YDETY KK------IL KVDYKLPEHI SKAASHLISK LLVLNPQHRL
DmAuroraB    ESNS-TESTY SK------IR RMEISYPSHL SKGCKELIGG LLRKESKGRI
CeAuroraA    ANQT-GDKLI AR------IK ECKIYIPSVV TDGAASLINA IIKKEPQERL
CeAuroraB    EHED-QSKTY AA------IK AARFTYPDSV KKGARDLIGR LLVVDPKARC
DdAurora     TSDE-EKNIF HN------IQ ENDVYYPSSI SPEAKDLISR LLVSDPHQRI
ScIpl1       EEEM-KDTTY KR------IA ALDIKMPSNI SQDAQDLILK LLKYDPKDRM
SpArk1       EDMSGHSATY KR------IA KVDLKIPSFV PPDARDLISR LLQHNPEKRM

             ....|....|
                255
OdAuroraA    ELVELLKMRW
OdAuroraB    PLDQLQRHAW
HsAuroraA    MLREVLEHPW
HsAuroraB    PLAQVSAHPW
HsAuroraC    PLAQILKHPW
XlAuroraA    PLKGVLEHPW
XlAuroraB    PLKGVMEHPW
CiAurora     PLESVMAHPW
BfAurora     PLDSVLSHPW
ApAurora     SLEGVIAHAW
SpAurora     PLEQVLAHPW
DmAuroraA    PLDQVMVHPW
DmAuroraB    TLVDVMTHYW
CeAuroraA    PLVDIMAHPW
CeAuroraB    TLEQVKEHYW
DdAurora     TLKDVINHPW
ScIpl1       RLGDVKMHPW
SpArk1       SLEQVMRHPW
```

Figure A11-B. Sequence alignments of Aurora kinases. Residues lining the catalytic pocket are colored in red. Gly198 in human Aurora A and Asn142 in human Aurora B and C are shaded in grey.

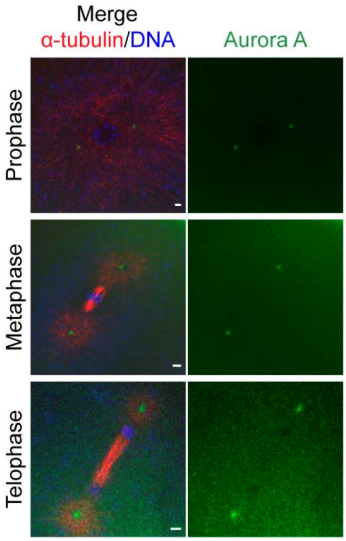

Figure A12. Aurora A (green) is localized on centrosomes during early embryonic cell cycles. α-Tubulin staining (red) marks the mitotic spindle. TO-PRO-3 staining (blue) marks DNA. Scale: 5 µm.

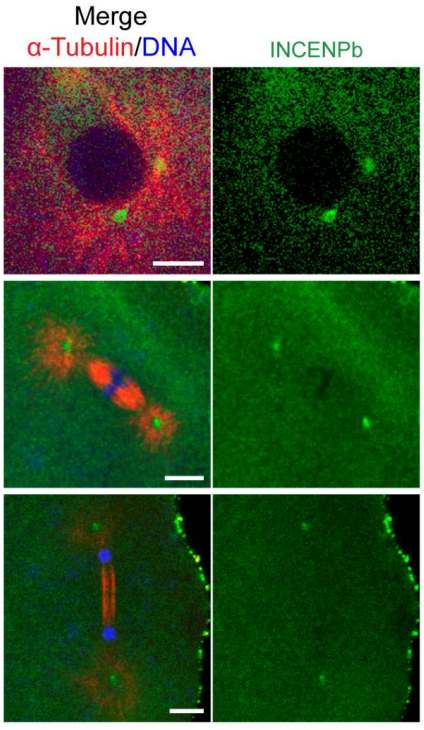

Figure A13. INCENPb (green) is localized on centrosomes during early embryonic cell cycles. α-Tubulin staining (red) marks the mitotic spindle. TO-PRO-3 staining (blue) marks DNA. Scale: 5 µm.

7 References

Abe, S., Nagasaka, K., Hirayama, Y., Kozuka-Hata, H., Oyama, M., Aoyagi, Y., Obuse, C., and Hirota, T. (2011). The initial phase of chromosome condensation requires Cdk1-mediated phosphorylation of the CAP-D3 subunit of condensin II. Genes Dev. *25*, 863–874.

Abe, Y., Okumura, E., Hosoya, T., Hirota, T., and Kishimoto, T. (2010). A single starfish Aurora kinase performs the combined functions of Aurora-A and Aurora-B in human cells. J. Cell Sci. *123*, 3978–3988.

Adams, R.R., Maiato, H., Earnshaw, W.C., and Carmena, M. (2001). Essential roles of *Drosophila* Inner Centromere Protein (Incenp) and Aurora B in histone H3 phosphorylation, metaphase chromosome alignment, kinetochore disjunction, and chromosome segregation. J. Cell Biol. *153*, 865–880.

Altieri, D.C. (2003). Validating survivin as a cancer therapeutic target. Nat. Rev. Cancer *3*, 46–54.

Andrews, P.D., Ovechkina, Y., Morrice, N., Wagenbach, M., Duncan, K., Wordeman, L., and Swedlow, J.R. (2004). Aurora B regulates MCAK at the mitotic centromere. Dev. Cell *6*, 253–268.

Aprelikova, O., Xiong, Y., and Liu, E.T. (1995). Both p16 and p21 families of Cyclin-dependent kinase (CDK) inhibitors block the phosphorylation of Cyclin-dependent kinases by the CDK-activating kinase. J. Biol. Chem. *270*, 18195–18197.

Araujo, A.R., Gelens, L., Sheriff, R.S.M., and Santos, S.D.M. (2016). Positive feedback keeps duration of mitosis temporally insulated from upstream cell-cycle events. Mol. Cell *64*, 362–375.

Asaoka-Taguchi, M., Yamada, M., Nakamura, A., Hanyu, K., and Kobayashi, S. (1999). Maternal Pumilio acts together with Nanos in germline development in *Drosophila* embryos. Nat. Cell Biol. *1*, 431–437.

Asteriti, I.A., De Mattia, F., and Guarguaglini, G. (2015). Cross-talk between AURKA and Plk1 in mitotic entry and spindle assembly. Front. Oncol. *5*, 283.

Bastock, R., and St Johnston, D. (2008). *Drosophila* oogenesis. Curr. Biol. *18*, R1082–R1087.

Baumbach, J., Novak, Z.A., Raff, J.W., and Wainman, A. (2015). Dissecting the function and assembly of acentriolar microtubule organizing centers in *Drosophila* cells in vivo. PLoS Genet. *11*, e1005261.

Bayliss, R., Sardon, T., Vernos, I., and Conti, E. (2003). Structural basis of Aurora-A activation by TPX2 at the mitotic spindle. Mol. Cell *12*, 851–862.

Bayliss, R., Fry, A., Haq, T., and Yeoh, S. (2012). On the molecular mechanisms of mitotic kinase activation. Open Biol. *2*, 120136.

Beck, H., Nähse, V., Larsen, M.S.Y., Groth, P., Clancy, T., Lees, M., Jørgensen, M., Helleday, T., Syljuåsen, R.G., and Sørensen, C.S. (2010). Regulators of cyclin-dependent kinases are crucial for maintaining genome integrity in S phase. J. Cell Biol. *188*, 629–638.

Bekier, M.E., Mazur, T., Rashid, M.S., and Taylor, W.R. (2015). Borealin dimerization mediates optimal CPC checkpoint function by enhancing localization to centromeres and kinetochores. Nat. Commun. *6*, 6775.

Bennabi, I., Terret, M.E., and Verlhac, M.H. (2016). Meiotic spindle assembly and chromosome segregation in oocytes. J. Cell Biol. *215*, 611–619.

Bentley, A., and King, R. (2006). Distinct sequence elements of Cyclin B1 promote localization to chromatin, centrosomes, and kinetochores during mitosis. Mol. Biol. Cell *17*, 4847–4858.

Bird, A.W., and Hyman, A.A. (2008). Building a spindle of the correct length in human cells requires the interaction between TPX2 and Aurora A. J. Cell Biol. *182*, 289–300.

Bloom, J., and Cross, F.R. (2007). Multiple levels of cyclin specificity in cell-cycle control. Nat Rev Mol Cell Biol *8*, 149–160.

Bohnert, K.A., Chen, J.S., Clifford, D.M., Vander Kooi, C.W., Gould, K.L., and Lew, D.J. (2009). A link between Aurora kinase and Clp1/Cdc14 regulation uncovered by the identification of a fission yeast Borealin-like protein. Mol. Biol. Cell *20*, 3646–3659.

Boldrin, F., Martinucci, G., Holland, L.Z., Miller, R.L., and Burighel, P. (2009). Internal fertilization in the salp *Thalia democratica*. Can. J. Zool. *87*, 928–940.

Bourhis, E., Hymowitz, S.G., and Cochran, A.G. (2007). The mitotic regulator Survivin binds as a monomer to its functional interactor Borealin. J. Biol. Chem. *282*, 35018–35023.

Bourouh, M., Dhaliwal, R., Rana, K., Sinha, S., Guo, Z., and Swan, A. (2016). Distinct and overlapping requirements for Cyclins A, B, and B3 in *Drosophila* female meiosis. G3 Genes|Genomes|Genetics *6*, 3711–3724.

Boutros, R., Lobjois, V., and Ducommun, B. (2007). CDC25 phosphatases in cancer cells: key players? good targets? Nat Rev Cancer *7*, 495–507.

Brandeis, M., and Hunt, T. (1996). The proteolysis of mitotic cyclins in mammalian cells persists from the end of mitosis until the onset of S phase. EMBO J. *15*, 5280–5289.

Brandeis, M., Rosewell, I., Carrington, M., Crompton, T., Jacobs, M.A., Kirk, J., Gannon, J., and Hunt, T. (1998). Cyclin B2-null mice develop normally and are fertile whereas cyclin B1-null mice die in utero. Proc. Natl. Acad. Sci. U. S. A. *95*, 4344–4349.

Brito, D.A., and Rieder, C.L. (2006). Mitotic checkpoint slippage in humans occurs via Cyclin B destruction in the presence of an active checkpoint. Curr. Biol. *16*, 1194–1200.

Brown, J.R., Koretke, K.K., Birkeland, M.L., Sanseau, P., and Patrick, D.R. (2004). Evolutionary relationships of Aurora kinases: Implications for model organism studies and the development of anti-cancer drugs. BMC Evol. Biol. *4*, 39.

Brown, N.R., Korolchuk, S., Martin, M.P., Stanley, W.A., Moukhametzianov, R., Noble, M.E.M., and Endicott, J.A. (2015). CDK1 structures reveal conserved and unique features of the essential cell cycle CDK. Nat. Commun. *6*, 6769.

Bulavin, D.V., Higashimoto, Y., Demidenko, Z.N., Meek, S., Graves, P., Phillips, C., Zhao, H., Moody, S.A., Appella, E., Piwnica-Worms, H., et al. (2003). Dual phosphorylation

controls Cdc25 phosphatases and mitotic entry. Nat. Cell Biol. *5*, 545–551.

Burton, J.L., and Solomon, M.J. (2007). Mad3p, a pseudosubstrate inhibitor of APC^{Cdc20} in the spindle assembly checkpoint. Genes Dev. *21*, 655–667.

Cabral, G., Sanegre Sans, S., Cowan, C.R., and Dammermann, A. (2017). Multiple mechanisms contribute to centriole separation in *C. elegans*. Curr. Biol. *23*, 1380–1387.

Campsteijn, C., Øvrebø, J.I., Karlsen, B.O., and Thompson, E.M. (2012). Expansion of cyclin D and CDK1 paralogs in *Oikopleura dioica*, a chordate employing diverse cell cycle variants. Mol. Biol. Evol. *29*, 487–502.

Canman, J.C., Lewellyn, L., Laband, K., Smerdon, S.J., Desai, A., Bowerman, B., and Oegema, K. (2008). Inhibition of Rac by the GAP activity of centralspindlin is essential for cytokinesis. Science *322*, 1543–1546.

Capalbo, L., Mela, I., Abad, M.A., Jeyaprakash, A.A., Edwardson, J.M., and D'Avino, P.P. (2016). Coordinated regulation of the ESCRT-III component CHMP4C by the chromosomal passenger complex and centralspindlin during cytokinesis. Open Biol. *6*, 160248.

Cardoso, M.C., Leonhardt, H., and Nadal-Ginard, B. (1993). Reversal of terminal differentiation and control of DNA replication: Cyclin A and Cdk2 specifically localize at subnuclear sites of DNA replication. Cell *74*, 979–992.

Carlton, J.G., Caballe, A., Agromayor, M., Kloc, M., and Martin-Serrano, J. (2012). ESCRT-III Governs the Aurora B–mediated abscission checkpoint through CHMP4C. Science *336*, 220–225.

Carmena, M., Wheelock, M., Funabiki, H., and Earnshaw, W.C. (2012). The chromosomal passenger complex (CPC): from easy rider to the godfather of mitosis. Nat. Rev. Mol. Cell Biol. *13*, 789–803.

Chase, D., Serafinas, C., Ashcroft, N., Kosinski, M., Longo, D., Ferris, D.K., and Golden, A. (2000). The Polo-like kinase Plk-1 is required for nuclear envelope breakdown and the completion of meiosis in *Caenorhabditis elegans*. Genesis *26*, 26–41.

Chen, Q., Zhang, X., Jiang, Q., Clarke, P.R., and Zhang, C. (2008). Cyclin B1 is localized to unattached kinetochores and contributes to efficient microtubule attachment and proper chromosome alignment during mitosis. Cell Res. *18*, 268–280.

Chu, Y., Yao, P.Y., Wang, W., Wang, D., Wang, Z., Zhang, L., Huang, Y., Ke, Y., Ding, X., and Yao, X. (2011). Aurora B kinase activation requires survivin priming phosphorylation by Plk1. J. Mol. Cell Biol. *3*, 260–267.

Clarke, P.R., and Zhang, C. (2008). Spatial and temporal coordination of mitosis by Ran GTPase. Nat. Rev. Mol. Cell Biol. *9*, 464–477.

Clift, D., and Schuh, M. (2015). A three-step MTOC fragmentation mechanism facilitates bipolar spindle assembly in mouse oocytes. Nat. Commun. *6*, 1–12.

Collin, P., Nashchekina, O., Walker, R., and Pines, J. (2013). The spindle assembly checkpoint works like a rheostat rather than a toggle switch. Nat. Cell Biol. *15*, 1378–1385.

Colombié, N., Cullen, C.F., Brittle, A.L., Jang, J.K., Earnshaw, W.C., Carmena, M., McKim,

K., and Ohkura, H. (2008). Dual roles of Incenp crucial to the assembly of the acentrosomal metaphase spindle in female meiosis. Development *135*, 3239–3246.

Connell, C.M., Colnaghi, R., and Wheatley, S.P. (2008). Nuclear Survivin has reduced stability and is not cytoprotective. J. Biol. Chem. *283*, 3289–3296.

Connolly, T., and Beach, D. (1994). Interaction between the Cig1 and Cig2 B-type cyclins in the fission yeast cell cycle. Mol. Cell. Biol. *14*, 768–776.

Cooke, C.A., Heck, M.M., and Earnshaw, W.C. (1987). The inner centromere protein (INCENP) antigens: movement from inner centromere to midbody during mitosis. J. Cell Biol. *105*, 2053–2067.

Delsuc, F., Tsagkogeorga, G., Lartillot, N., and Philippe, H. (2008). Additional molecular support for the new chordate phylogeny. Genesis *46*, 592–604.

DeLuca, K.F., Lens, S.M.A., and DeLuca, J.G. (2011). Temporal changes in Hec1 phosphorylation control kinetochore–microtubule attachment stability during mitosis. J. Cell Sci. *124*, 622–634.

DeLuca, K.F., Meppelink, A., Broad, A.J., Mick, J.E., Peersen, O.B., Pektas, S., Lens, S.M.A., and DeLuca, J.G. (2018). Aurora A kinase phosphorylates Hec1 to regulate metaphase kinetochore–microtubule dynamics. J. Cell Biol. *217*, 163–177.

Denoeud, F., Henriet, S., Mungpakdee, S., Aury, J.M., Da Silva, C., Brinkmann, H., Mikhaleva, J., Olsen, L.C., Jubin, C., Canestro, C., et al. (2010). Plasticity of animal genome architecture unmasked by rapid evolution of a pelagic tunicate. Science *330*, 1381–1385.

Deyter, G.M., Furuta, T., Kurasawa, Y., and Schumacher, J.M. (2010). *Caenorhabditis elegans* Cyclin B3 is required for multiple mitotic processes including alleviation of a spindle checkpoint-dependent block in anaphase chromosome segregation. PLoS Genet *6*, e1001218.

Dieterich, K., Rifo, R.S., Faure, A.K., Hennebicq, S., Amar, B.B., Zahi, M., Perrin, J., Martinez, D., Sèle, B., Jouk, P.S., et al. (2007). Homozygous mutation of AURKC yields large-headed polyploid spermatozoa and causes male infertility. Nat. Genet. *39*, 661–665.

Dobrynin, G., Popp, O., Romer, T., Bremer, S., Schmitz, M.H.A., Gerlich, D.W., and Meyer, H. (2011). Cdc48/p97–Ufd1–Npl4 antagonizes Aurora B during chromosome segregation in HeLa cells. J. Cell Sci. *124*, 1571–1580.

Douglas, M.E., Davies, T., Joseph, N., and Mishima, M. (2010). Aurora B and 14-3-3 coordinately regulate clustering of centralspindlin during cytokinesis. Curr. Biol. *20*, 927–933.

Draviam, V.M., Orrechia, S., Lowe, M., Pardi, R., and Pines, J. (2001). The localization of human Cyclins B1 and B2 determines Cdk1 substrate specificity and neither enzyme requires mek to disassemble the Golgi apparatus. J. Cell Biol. *152*, 945–958.

Du, J., Cao, Y., Wang, Q., Zhang, N., Liu, X., Chen, D., Liu, X., Xu, Q., and Ma, W. (2015). Unique subcellular distribution of phosphorylated Plk1 (Ser137 and Thr210) in mouse oocytes during meiotic division and pPlk1Ser137 involvement in spindle formation and REC8 cleavage. Cell Cycle *14*, 3566–3579.

Dumollard, R., Levasseur, M., Hebras, C., Huitorel, P., Carroll, M., Chambon, J.P., and McDougall, A. (2011). Mos limits the number of meiotic divisions in urochordate eggs. Development *138*, 885–895.

Dumont, J., and Desai, A. (2012). Acentrosomal spindle assembly and chromosome segregation during oocyte meiosis. Trends Cell Biol. *22*, 241–249.

Dumont, J., Petri, S., Pellegrin, F., Terret, M.E., Bohnsack, M.T., Rassinier, P., Georget, V., Kalab, P., Gruss, O.J., and Verlhac, M.H. (2007). A centriole- and RanGTP-independent spindle assembly pathway in meiosis I of vertebrate oocytes. J. Cell Biol. *176*, 295–305.

Dupre, A., Daldello, E.M., Nairn, A.C., Jessus, C., and Haccard, O. (2014). Phosphorylation of ARPP19 by protein kinase A prevents meiosis resumption in *Xenopus* oocytes. Nat. Commun. *5*, 3318.

Dutertre, S., Cazales, M., Quaranta, M., Froment, C., Trabut, V., Dozier, C., Mirey, G., Bouché, J.P., Theis-Febvre, N., Schmitt, E., et al. (2004). Phosphorylation of CDC25B by Aurora-A at the centrosome contributes to the G2–M transition. J. Cell Sci. *117*, 2523–2531.

Edgar, B.A., Zielke, N., and Gutierrez, C. (2014). Endocycles: a recurrent evolutionary innovation for post-mitotic cell growth. Nat. Rev. Mol. Cell Biol. *15*, 197–210.

Elia, A.E.H., Cantley, L.C., and Yaffe, M.B. (2003). Proteomic screen finds pSer/pThr-binding domain localizing Plk1 to mitotic substrates. Science *299*, 1228–1231.

Encalada, S.E., Willis, J., Lyczak, R., and Bowerman, B. (2005). A spindle checkpoint functions during mitosis in the early *Caenorhabditis elegans* embryo. Mol. Biol. Cell *16*, 1056–1070.

Errico, A., Deshmukh, K., Tanaka, Y., Pozniakovsky, A., and Hunt, T. (2010). Identification of substrates for cyclin dependent kinases. Adv. Enzyme Regul. *50*, 375–399.

Evans, T., Rosenthal, E.T., Youngblom, J., Distel, D., and Hunt, T. (1983). Cyclin: a protein specified by maternal mRNA in sea urchin eggs that is destroyed at each cleavage division. Cell *33*, 389–396.

Fang, G., Yu, H., and Kirschner, M.W. (1998). The checkpoint protein MAD2 and the mitotic regulator CDC20 form a ternary complex with the anaphase-promoting complex to control anaphase initiation. Genes Dev. *12*, 1871–1883.

Ferguson, R.L., Pascreau, G., and Maller, J.L. (2010). The Cyclin A centrosomal localization sequence recruits MCM5 and Orc1 to regulate centrosome reduplication. J. Cell Sci. *123*, 2743–2749.

Fernández-Miranda, G., de Castro, I.P., Carmena, M., Aguirre-Portolés, C., Ruchaud, S., Fant, X., Montoya, G., Earnshaw, W.C., and Malumbres, M. (2010). SUMOylation modulates the function of Aurora-B kinase. J. Cell Sci. *123*, 2823–2833.

Fernández-Miranda, G., Trakala, M., Martín, J., Escobar, B., González, A., Ghyselinck, N.B., Ortega, S., Cañamero, M., de Castro, I.P., and Malumbres, M. (2011). Genetic disruption of aurora B uncovers an essential role for aurora C during early mammalian development. Development *138*, 2661–2672.

Foster, D.A., Yellen, P., Xu, L., and Saqcena, M. (2010). Regulation of G1 cell cycle

progression: Distinguishing the restriction point from a nutrient-sensing cell growth checkpoint(s). Genes Cancer *1*, 1124–1131.

Fourest-Lieuvin, A., Peris, L., Gache, V., Garcia-Saez, I., Juillan-Binard, C., Lantez, V., and Job, D. (2006). Microtubule regulation in mitosis: tubulin phosphorylation by the Cyclin-dependent kinase Cdk1. Mol. Biol. Cell *17*, 1041–1050.

Frick, J.E., Ruppert, E.E., Bush, R.M., Smouse, P.E., Ledig, F.T., Conklin, E.G., Eckelbarger, K.J., Larson, R.L., Eddy, E.M., Frick, J.E., et al. (1997). Primordial germ cells and oocytes of *Branchiostoma virginiae* (Cephalochordata, Acrania) are flagellated epithelial cells: relationship between epithelial and primary egg polarity. Zygote *5*, 139–151.

Fu, J., Bian, M., Liu, J., Jiang, Q., and Zhang, C. (2009). A single amino acid change converts Aurora-A into Aurora-B-like kinase in terms of partner specificity and cellular function. Proc. Natl. Acad. Sci. *106*, 6939–6944.

Fu, Z., Malureanu, L., Huang, J., Wang, W., Li, H., van Deursen, J.M., Tindall, D.J., and Chen, J. (2008). Plk1-dependent phosphorylation of FoxM1 regulates a transcriptional programme required for mitotic progression. Nat. Cell Biol. *10*, 1076–1082.

Fung, S.Y.S., Kitagawa, M., Liao, P.J., Wong, J., and Lee, S.H. (2017). Opposing activities of Aurora B kinase and B56-PP2A phosphatase on MKlp2 determine abscission timing. Curr. Biol. *27*, 78–86.

Gabrielli, B.G., Clark, J.M., McCormack, A.K., and Ellem, K.A.O. (1997). Hyperphosphorylation of the N-terminal domain of Cdc25 regulates activity toward Cyclin B1/Cdc2 but not Cyclin A/Cdk2. J. Biol. Chem. *272*, 28607–28614.

Gaffré, M., Martoriati, A., Belhachemi, N., Chambon, J.P., Houliston, E., Jessus, C., and Karaiskou, A. (2011). A critical balance between Cyclin B synthesis and Myt1 activity controls meiosis entry in *Xenopus* oocytes. Development *138*, 3735–3744.

Gallant, P., and Nigg, E.A. (1994). Identification of a novel vertebrate cyclin: cyclin B3 shares properties with both A- and B-type cyclins. EMBO J *13*, 595–605.

Galli, M., and Morgan, D.O. (2016). Cell size determines the strength of the spindle assembly checkpoint during embryonic development. Dev. Cell *36*, 344–352.

Ganot, P., and Thompson, E.M. (2002). Patterning through differential endoreduplication in epithelial organogenesis of the chordate, *Oikopleura dioica*. Dev Biol *252*, 59–71.

Ganot, P., Bouquet, J.M., and Thompson, E.M. (2006). Comparative organization of follicle, accessory cells and spawning anlagen in dynamic semelparous clutch manipulators, the urochordate *Oikopleuridae*. Biol Cell *98*, 389–401.

Ganot, P., Kallesøe, T., and Thompson, E.M. (2007). The cytoskeleton organizes germ nuclei with divergent fates and asynchronous cycles in a common cytoplasm during oogenesis in the chordate *Oikopleura*. Dev Biol *302*, 577–590.

Ganot, P., Moosmann-Schulmeister, A., and Thompson, E.M. (2008). Oocyte selection is concurrent with meiosis resumption in the coenocystic oogenesis of *Oikopleura*. Dev Biol *324*, 266–276.

Gao, S., Giansanti, M.G., Buttrick, G.J., Ramasubramanyan, S., Auton, A., Gatti, M., and

Wakefield, J.G. (2008). Australin: a chromosomal passenger protein required specifically for *Drosophila melanogaster* male meiosis. J. Cell Biol. *180*, 521–535.

Garrett, S., Barton, W.A., Knights, R., Jin, P., Morgan, D.O., and Fisher, R.P. (2001). Reciprocal activation by Cyclin-dependent kinases 2 and 7 is directed by substrate specificity determinants outside the T loop. Mol. Cell. Biol. *21*, 88–99.

Gassmann, R., Carvalho, A., Henzing, A.J., Ruchaud, S., Hudson, D.F., Honda, R., Nigg, E.A., Gerloff, D.L., and Earnshaw, W.C. (2004). Borealin: a novel chromosomal passenger required for stability of the bipolar mitotic spindle. J. Cell Biol. *166*, 179–191.

Gautier, J., and Maller, J.L. (1991). Cyclin B in *Xenopus* oocytes: implications for the mechanism of pre-MPF activation. EMBO J. *10*, 177–182.

Gavet, O., and Pines, J. (2010). Activation of cyclin B1-Cdk1 synchronizes events in the nucleus and the cytoplasm at mitosis. J. Cell Biol. *189*, 247–259.

Glover, D.M., Leibowitz, M.H., McLean, D.A., and Parry, H. (1995). Mutations in aurora prevent centrosome separation leading to the formation of monopolar spindles. Cell *81*, 95–105.

Gong, D., and Ferrell Jr, J.E. (2010). The roles of cyclin A2, B1, and B2 in early and late mitotic events. Mol. Biol. Cell *21*, 3149–3161.

Goshima, G. (2011). Identification of a TPX2-like microtubule-associated protein in *Drosophila*. PLoS One *6*, e28120.

Greenstein, D. (2005). Control of oocyte meiotic maturation and fertilization. Wormbook. doi/10.1895/wormbook.1.53.1

Grive, K.J., and Freiman, R.N. (2015). The developmental origins of the mammalian ovarian reserve. Development *142*, 2554–2563.

Gui, L., and Homer, H. (2013). Hec1-dependent Cyclin B2 stabilization regulates the G2-M transition and early prometaphase in mouse oocytes. Dev. Cell *25*, 43–54.

Hagting, A., Karlsson, C., Clute, P., Jackman, M., and Pines, J. (1998). MPF localization is controlled by nuclear export. EMBO J. *17*, 4127–4138.

Hajnal, A., and Berset, T. (2002). The *C.elegans* MAPK phosphatase LIP-1 is required for the G_2/M meiotic arrest of developing oocytes. EMBO J. *21*, 4317–4326.

Hammond, M.P., and Laird, C.D. (1985). Chromosome structure and DNA replication in nurse and follicle cells of *Drosophila melanogaster*. Chromosoma *91*, 267–278.

Hara, M., Abe, Y., Tanaka, T., Yamamoto, T., Okumura, E., and Kishimoto, T. (2012). Greatwall kinase and cyclin B-Cdk1 are both critical constituents of M-phase-promoting factor. Nat. Commun. *3*, 1059.

Hara, T., Abe, M., Inoue, H., Yu, L.R., Veenstra, T.D., Kang, Y.H., Lee, K.S., and Miki, T. (2006). Cytokinesis regulator ECT2 changes its conformation through phosphorylation at Thr-341 in G2/M phase. Oncogene *25*, 566–578.

Harashima, H., Dissmeyer, N., and Schnittger, A. (2013). Cell cycle control across the eukaryotic kingdom. Trends Cell Biol. *23*, 345–356.

Hebras, C., and McDougall, A. (2012). Urochordate ascidians possess a single isoform of Aurora kinase that localizes to the midbody via TPX2 in eggs and cleavage stage embryos. PLoS One *7*, e45431.

Herzog, F., Primorac, I., Dube, P., Lenart, P., Sander, B., Mechtler, K., Stark, H., and Peters, J.M. (2009). Structure of the Anaphase-Promoting Complex/Cyclosome interacting with a mitotic checkpoint complex. Science *323*, 1477–1481.

Hochegger, H., Klotzbücher, A., Kirk, J., Howell, M., le Guellec, K., Fletcher, K., Duncan, T., Sohail, M., and Hunt, T. (2001). New B-type cyclin synthesis is required between meiosis I and II during *Xenopus* oocyte maturation. Development *128*, 3795–3807.

Hochegger, H., Takeda, S., and Hunt, T. (2008). Cyclin-dependent kinases and cell cycle transitions: does one fit all? Nat. Rev. Mol. Cell Biol. *9*, 1–6.

Hochegger, H., Hegarat, N., and Pereira-Leal, J.B. (2013). Aurora at the pole and equator: overlapping functions of Aurora kinases in the mitotic spindle. Open Biol *3*, 120185.

Honda, R., Körner, R., and Nigg, E.A. (2003). Exploring the functional interactions between Aurora B, INCENP, and Survivin in mitosis. Mol. Biol. Cell *14*, 3325–3341.

Houghtaling, B., Yang, G., Matov, A., Danuser, G., and Kapoor, T. (2009). Op18 reveals the contribution of nonkinetochore microtubules to the dynamic organization of the vertebrate meiotic spindle. Proc. Natl. Acad. Sci. U. S. A. *106*, 15338–15343.

Howell, B.J., McEwen, B.F., Canman, J.C., Hoffman, D.B., Farrar, E.M., Rieder, C.L., and Salmon, E.D. (2001). Cytoplasmic dynein/dynactin drives kinetochore protein transport to the spindle poles and has a role in mitotic spindle checkpoint inactivation. J. Cell Biol. *155*, 1159–1172.

Huang, Y., Sramkoski, R.M., and Jacobberger, J.W. (2013). The kinetics of G2 and M transitions regulated by B cyclins. PLoS One *8*, e80861.

Hümmer, S., and Mayer, T.U. (2009). Cdk1 negatively regulates midzone localization of the mitotic kinesin Mklp2 and the chromosomal passenger complex. Curr. Biol. *19*, 607–612.

Inoue, D., and Sagata, N. (2005). The Polo-like kinase Plx1 interacts with and inhibits Myt1 after fertilization of *Xenopus* eggs. EMBO J. *24*, 1057–1067.

Ivanovska, I., Lee, E., Kwan, K.M., Fenger, D.D., and Orr-Weaver, T.L. (2004). The *Drosophila* MOS ortholog is not essential for meiosis. Curr. Biol. *14*, 75–80.

Jackman, M., Firth, M., and Pines, J. (1995). Human cyclins B1 and B2 are localized to strikingly different structures: B1 to microtubules, B2 primarily to the Golgi apparatus. EMBO J *14*, 1646–1654.

Jackman, M., Kubota, Y., den Elzen, N., Hagting, A., and Pines, J. (2002). Cyclin A- and Cyclin E-Cdk complexes shuttle between the nucleus and the cytoplasm. Mol. Biol. Cell *13*, 1030–1045.

Jackman, M., Lindon, C., Nigg, E.A., and Pines, J. (2003). Active cyclin B1-Cdk1 first appears on centrosomes in prophase. Nat. Cell Biol. *5*, 143–148.

Jacobs, H.W., Knoblich, J.A., and Lehner, C.F. (1998). *Drosophila* Cyclin B3 is required for

female fertility and is dispensable for mitosis like Cyclin B. Genes Dev *12*, 3741–3751.

Jaspersen, S.L., Huneycutt, B.J., Giddings Jr., T.H., Resing, K.A., Ahn, N.G., and Winey, M. (2004). Cdc28/Cdk1 regulates spindle pole body duplication through phosphorylation of Spc42 and Mps1. Dev. Cell *7*, 263–274.

Jelluma, N., Brenkman, A.B., van den Broek, N.J.F., Cruijsen, C.W.A., van Osch, M.H.J., Lens, S.M.A., Medema, R.H., and Kops, G.J.P.L. (2008). Mps1 phosphorylates Borealin to control Aurora B activity and chromosome alignment. Cell *132*, 233–246.

Jeyaprakash, A.A., Klein, U.R., Lindner, D., Ebert, J., Nigg, E.A., and Conti, E. (2007). Structure of a Survivin–Borealin–INCENP core complex reveals how chromosomal passengers travel together. Cell *131*, 271–285.

Jong, H.K., and Richter, J.D. (2007). RINGO/cdk1 and CPEB mediate poly(A) tail stabilization and translational regulation by ePAB. Genes Dev. *21*, 2571–2579.

Joukov, V., Walter, J.C., and De Nicolo, A. (2014). The Cep192-organized Aurora A-Plk1 cascade is essential for centrosome cycle and bipolar spindle assembly. Mol. Cell *55*, 578–591.

Kadyrova, L.Y., Habara, Y., Lee, T.H., and Wharton, R.P. (2007). Translational control of maternal Cyclin B mRNA by Nanos in the *Drosophila* germline. Development *134*, 1519–1527.

Kaitna, S., Mendoza, M., Jantsch-Plunger, V., and Glotzer, M. (2000). Incenp and an Aurora-like kinase form a complex essential for chromosome segregation and efficient completion of cytokinesis. Curr. Biol. *10*, 1172–1181.

Kalab, P., and Heald, R. (2008). The RanGTP gradient - a GPS for the mitotic spindle. J. Cell Sci. *121*, 1577–1586.

Kang, J., Chaudhary, J., Dong, H., Kim, S., Brautigam, C.A., and Yu, H. (2011). Mitotic centromeric targeting of HP1 and its binding to Sgo1 are dispensable for sister-chromatid cohesion in human cells. Mol. Biol. Cell *22*, 1181–1190.

Kim, S., Spike, C., and Greenstein, D. (2013). Control of oocyte growth and meiotic maturation in *C. elegans*. Adv. Exp. Med. Biol. *757*, 277–320.

Kishimoto, T. (2003). Cell-cycle control during meiotic maturation. Curr Opin Cell Biol *15*, 654–663.

Kishimoto, T. (2011). A primer on meiotic resumption in starfish oocytes: The proposed signaling pathway triggered by maturation-inducing hormone. Mol. Reprod. Dev. *78*, 704–707.

Kitagawa, M., and Lee, S.H. (2015). The chromosomal passenger complex (CPC) as a key orchestrator of orderly mitotic exit and cytokinesis. Front. Cell Dev. Biol. *3*, 14.

Kitagawa, M., Fung, S.Y.S., Onishi, N., Saya, H., and Lee, S.H. (2013). Targeting Aurora B to the equatorial cortex by MKlp2 is required for cytokinesis. PLoS One *8*, e64826.

Kitagawa, M., Fung, S.Y.S., Hameed, U.F.S., Goto, H., Inagaki, M., and Lee, S.H. (2014). Cdk1 coordinates timely activation of MKlp2 kinesin with relocation of the chromosome

passenger complex for cytokinesis. Cell Rep. *7*, 166–179.

Knauer, S.K., Krämer, O.H., Knösel, T., Engels, K., Rödel, F., Kovács, A.F., Dietmaier, W., Klein-Hitpass, L., Habtemichael, N., Schweitzer, A., et al. (2006). Nuclear export is essential for the tumor-promoting activity of Survivin. FASEB J. *21*, 207–216.

Knoblich, J.A., and Lehner, C.F. (1993). Synergistic action of *Drosophila* cyclins A and B during the G2-M transition. EMBO J. *12*, 65–74.

Kõivomägi, M., Valk, E., Venta, R., Iofik, A., Lepiku, M., Morgan, D.O., and Loog, M. (2011). Dynamics of Cdk1 substrate specificity during the cell cycle. Mol. Cell *42*, 610–623.

Kotani, T., Yasuda, K., Ota, R., and Yamashita, M. (2013). Cyclin B1 mRNA translation is temporally controlled through formation and disassembly of RNA granules. J. Cell Biol. *202*, 1041–1055.

Krenn, V., and Musacchio, A. (2015). The Aurora B kinase in chromosome bi-orientation and spindle checkpoint signaling. Front. Oncol. *5*, 225.

Kubiak, J.Z., Ciemerych, M.A., Hupalowska, A., Sikora-Polaczek, M., and Polanski, Z. (2008). On the transition from the meiotic to mitotic cell cycle during early mouse development. Int. J. Dev. Biol. *52*, 201–217.

Lampson, M.A., and Cheeseman, I.M. (2011). Sensing centromere tension: Aurora B and the regulation of kinetochore function. Trends Cell Biol. *21*, 133–140.

Landino, J., Norris, S.R., Li, M., Ballister, E.R., Lampson, M.A., and Ohi, R. (2017). Two mechanisms coordinate the recruitment of the chromosomal passenger complex to the plane of cell division. Mol. Biol. Cell. *28*, 3634–3646.

Laoukili, J., Kooistra, M.R., Bras, A., Kauw, J., Kerkhoven, R.M., Morrison, A., Clevers, H., and Medema, R.H. (2005). FoxM1 is required for execution of the mitotic programme and chromosome stability. Nat. Cell Biol. *7*, 126–136.

Lara-Gonzalez, P., Westhorpe, F.G., and Taylor, S.S. (2012). The spindle assembly checkpoint. Curr. Biol. *22*, R966–R980.

Lee, M.H., Ohmachi, M., Arur, S., Nayak, S., Francis, R., Church, D., Lambie, E., and Schedl, T. (2007). Multiple functions and dynamic activation of MPK-1 extracellular signal-regulated kinase signaling in *Caenorhabditis elegans* germline development. Genetics *177*, 2039–2062.

Van Leene, J., Hollunder, J., Eeckhout, D., Persiau, G., Van De Slijke, E., Stals, H., Van Isterdael, G., Verkest, A., Neirynck, S., Buffel, Y., et al. (2010). Targeted interactomics reveals a complex core cell cycle machinery in *Arabidopsis thaliana*. Mol. Syst. Biol. *6*, 397.

Lei, L., and Spradling, A.C. (2013). Mouse primordial germ cells produce cysts that partially fragment prior to meiosis. Development *140*, 2075–2081.

Li, H., Chen, Q., Kaller, M., Nellen, W., Gräf, R., and De Lozanne, A. (2008). Dictyostelium Aurora Kinase has properties of both Aurora A and Aurora B kinases. Eukaryot. Cell *7*, 894–905.

Lindqvist, A., Källström, H., Lundgren, A., Barsoum, E., and Rosenthal, C.K. (2005).

Cdc25B cooperates with Cdc25A to induce mitosis but has a unique role in activating cyclin B1–Cdk1 at the centrosome. J. Cell Biol. *171*, 35–45.

Lindqvist, A., Rodríguez-Bravo, V., and Medema, R.H. (2009). The decision to enter mitosis: feedback and redundancy in the mitotic entry network. J. Cell Biol. *185*, 193–202.

Liu, W., Tanasa, B., Tyurina, O.V., Zhou, T.Y., Gassmann, R., Liu, W.T., Ohgi, K.A., Benner, C., Garcia-Bassets, I., Aggarwal, A.K., et al. (2010). PHF8 mediates histone H4 lysine 20 demethylation events involved in cell cycle progression. Nature *466*, 508–512.

Lolli, G., and Johnson, L.N. (2005). CAK-Cyclin-dependent activating kinase: A key kinase in cell cycle control and a target for drugs? Cell Cycle *4*, 572–577.

Lozano, J.C., Vergé, V., Schatt, P., Juengel, J.L., and Peaucellier, G. (2012). Evolution of Cyclin B3 shows an abrupt three-fold size increase, due to the extension of a single exon in placental mammals, allowing for new protein–protein interactions. Mol. Biol. Evol. *29*, 3855–3871.

Lu, L.X., Domingo-Sananes, M.R., Huzarska, M., Novak, B., and Gould, K.L. (2012). Multisite phosphoregulation of Cdc25 activity refines the mitotic entrance and exit switches. Proc. Natl. Acad. Sci. *109*, 9899–9904.

Mackay, A.M., Eckley, D.M., Chue, C., and Earnshaw, W.C. (1993). Molecular analysis of the INCENPs (inner centromere proteins): separate domains are required for association with microtubules during interphase and with the central spindle during anaphase. J. Cell Biol. *123*, 373–385.

Major, M.L., Lepe, R., and Costa, R.H. (2004). Forkhead box M1b transcriptional activity requires binding of Cdk-Cyclin complexes for phosphorylation-dependent recruitment of p300/CBP coactivators. Mol. Cell. Biol. *24*, 2649–2661.

Maldonado, M., and Kapoor, T.M. (2011). Constitutive Mad1 targeting to kinetochores uncouples checkpoint signalling from chromosome biorientation. Nat. Cell Biol. *13*, 475–482.

Malumbres, M., and Barbacid, M. (2009). Cell cycle, CDKs and cancer: a changing paradigm. Nat Rev Cancer *9*, 153–166.

Marangos, P., and Carroll, J. (2004). The dynamics of cyclin B1 distribution during meiosis I in mouse oocytes. Reproduction *128*, 153–162.

Maresca, T.J., and Salmon, E.D. (2009). Intrakinetochore stretch is associated with changes in kinetochore phosphorylation and spindle assembly checkpoint activity. J. Cell Biol. *184*, 373–381.

Matova, N., and Cooley, L. (2001). Comparative aspects of animal oogenesis. Dev. Biol. *231*, 291–320.

Matthews, H.K., Delabre, U., Rohn, J.L., Guck, J., Kunda, P., and Baum, B. (2012). Changes in Ect2 localization couple actomyosin-dependent cell shape changes to mitotic progression. Dev. Cell *23*, 371–383.

McCleland, M.L., Farrell, J.A., and O'Farrell, P.H. (2009). Influence of cyclin type and dose on mitotic entry and progression in the early *Drosophila* embryo. J. Cell Biol. *184*, 639–646.

McKee, B.D. (2004). Homologous pairing and chromosome dynamics in meiosis and mitosis. Biochim. Biophys. Acta. *1677*, 165–180.

Meraldi, P., Lukas, J., Fry, A.M., Bartek, J., and Nigg, E.A. (1999). Centrosome duplication in mammalian somatic cells requires E2F and Cdk2-Cyclin A. Nat Cell Biol *1*, 88–93.

Michael, W.M. (2016). Cyclin CYB-3 controls both S-phase and mitosis and is asymmetrically distributed in the early *C. elegans* embryo. Development *143*, 3119–3127.

Minoshima, Y., Kawashima, T., Hirose, K., Tonozuka, Y., Kawajiri, A., Bao, Y.C., Deng, X., Tatsuka, M., Narumiya, S., May, W.S., et al. (2003). Phosphorylation by Aurora B converts MgcRacGAP to a RhoGAP during cytokinesis. Dev. Cell *4*, 549–560.

Mirchenko, L., and Uhlmann, F. (2010). Sli15(INCENP) dephosphorylation prevents mitotic checkpoint reengagement due to loss of tension at anaphase onset. Curr. Biol. *20*, 1396–1401.

Molinari, M., Mercurio, C., Dominguez, J., Goubin, F., and Draetta, G.F. (2000). Human Cdc25A inactivation in response to S phase inhibition and its role in preventing premature mitosis. EMBO Rep. *1*, 71–79.

Morgan, D.O. (2007). The cell cycle: principles of control (New Science Press; Sinauer Associates).

Motta, P.M., Makabe, S., and Notttola, S.A. (1997). The ultrastructure of human reproduction. 1. The natural history of the female germ cell: origin, migration and differentiation inside the developing ovary. Hum. Reprod. Update *3*, 281–297.

Nagahama, Y., and Yamashita, M. (2008). Regulation of oocyte maturation in fish. Dev. Growth Differ. *50 Suppl 1*, S195–219.

Nakajima, Y., Tyers, R.G., Wong, C.C.L., Yates, J.R., Drubin, D.G., Barnes, G., and Bloom, K.S. (2009). Nbl1p: a Borealin/Dasra/CSC-1-like protein essential for Aurora/Ipl1 complex function and integrity in *Saccharomyces cerevisiae*. Mol. Biol. Cell *20*, 1772–1784.

Nakajima, Y., Cormier, A., Tyers, R.G., Pigula, A., Peng, Y., Drubin, D.G., and Barnes, G. (2011). Ipl1/Aurora-dependent phosphorylation of Sli15/INCENP regulates CPC–spindle interaction to ensure proper microtubule dynamics. J. Cell Biol. *194*, 137–153.

Nam, H.J., and van Deursen, J.M. (2014). Cyclin B2 and p53 control proper timing of centrosome separation. Nat Cell Biol *16*, 538–549.

Nguyen, A.L., and Schindler, K. (2017). Specialize and divide (Twice): Functions of three Aurora kinase homologs in mammalian oocyte meiotic maturation. Trends Genet. *33*, 349–363.

Nguyen, H.G., Chinnappan, D., Urano, T., and Ravid, K. (2005). Mechanism of Aurora-B degradation and its dependency on intact KEN and A-boxes: Identification of an aneuploidy-promoting property. Mol. Cell. Biol. *25*, 4977–4992.

Nguyen, T.B., Manova, K., Capodieci, P., Lindon, C., Bottega, S., Wang, X.Y., Refik-Rogers, J., Pines, J., Wolgemuth, D.J., and Koff, A. (2002). Characterization and expression of mammalian cyclin B3, a prepachytene meiotic cyclin. J. Biol. Chem. *277*, 41960–41969.

Niedzialkowska, E., Wang, F., Porebski, P.J., Minor, W., Higgins, J.M.G., and Stukenberg,

P.T. (2012). Molecular basis for phosphospecific recognition of histone H3 tails by Survivin paralogues at inner centromeres. Mol. Biol. Cell *23*, 1457–1466.

Niiya, F., Tatsumoto, T., Lee, K.S., and Miki, T. (2006). Phosphorylation of the cytokinesis regulator ECT2 at G2/M phase stimulates association of the mitotic kinase Plk1 and accumulation of GTP-bound RhoA. Oncogene *25*, 827–837.

Nishida, H. (2008). Development of the appendicularian *Oikopleura dioica*: Culture, genome, and cell lineages. Dev. Growth Differ. *50*, S239–256.

Norris, R.P., Freudzon, M., Mehlmann, L.M., Cowan, A.E., Simon, A.M., Paul, D.L., Lampe, P.D., and Jaffe, L.A. (2008). Luteinizing hormone causes MAP kinase-dependent phosphorylation and closure of connexin 43 gap junctions in mouse ovarian follicles: one of two paths to meiotic resumption. Development *135*, 3229–3238.

Norris, R.P., Ratzan, W.J., Freudzon, M., Mehlmann, L.M., Krall, J., Movsesian, M.A., Wang, H., Ke, H., Nikolaev, V.O., and Jaffe, L.A. (2009). Cyclic GMP from the surrounding somatic cells regulates cyclic AMP and meiosis in the mouse oocyte. Development *136*, 1869–1878.

Okano-Uchida, T., Sekiai, T., Lee, K., Okumura, E., Tachibana, K., and Kishimoto, T. (1998). In vivo regulation of Cyclin A/Cdc2 and Cyclin B/Cdc2 through meiotic and early cleavage cycles in starfish. Dev. Biol. *197*, 39–53.

Oliveira, R.A., and Nasmyth, K. (2013). Cohesin cleavage is insufficient for centriole disengagement in *Drosophila*. Curr. Biol. *23*, R601–R603.

Ookata, K., Hisanaga, S., Okano, T., Tachibana, K., and Kishimoto, T. (1992). Relocation and distinct subcellular localization of p34cdc2-cyclin B complex at meiosis reinitiation in starfish oocytes. EMBO J. *11*, 1763–1772.

Ozlü, N., Monigatti, F., Renard, B.Y., Field, C.M., Steen, H., Mitchison, T.J., and Steen, J.J. (2010). Binding partner switching on microtubules and Aurora-B in the mitosis to cytokinesis transition. Mol. Cell. Proteomics *9*, 336–350.

Pagliuca, F.W., Collins, M.O., Lichawska, A., Zegerman, P., Choudhary, J.S., and Pines, J. (2011). Quantitative proteomics reveals the basis for the biochemical specificity of the cell-cycle machinery. Mol. Cell *43*, 406–417.

Palancade, B., and Bensaude, O. (2003). Investigating RNA polymerase II carboxyl-terminal domain (CTD) phosphorylation. Eur. J. Biochem. *270*, 3859–3870.

Pascreau, G., Eckerdt, F., Churchill, M.E.A., and Maller, J.L. (2010). Discovery of a distinct domain in cyclin A sufficient for centrosomal localization independently of Cdk binding. Proc. Natl. Acad. Sci. *107*, 2932–2937.

Van de Peer, Y., Maere, S., and Meyer, A. (2009). The evolutionary significance of ancient genome duplications. Nat. Rev. Genet. *10*, 725–732.

Pepling, M.E., De Cuevas, M., and Sprading, A.C. (1999). Germline cysts: a conserved phase of germ cell development? Trends Cell Biol. *9*, 257–262.

Pereira, G., and Schiebel, E. (2003). Separase regulates INCENP-Aurora B anaphase spindle function through Cdc14. Science *302*, 2120–2124.

Petri, E.T., Errico, A., Escobedo, L., Hunt, T., and Basavappa, R. (2007). The crystal structure of human Cyclin B. Cell Cycle *6*, 1342–1349.

Petsalaki, E., Akoumianaki, T., Black, E.J., Gillespie, D.A.F., and Zachos, G. (2011). Phosphorylation at serine 331 is required for Aurora B activation. J. Cell Biol. *195*, 449–466.

Pike, T., Brownlow, N., Kjaer, S., Carlton, J., and Parker, P.J. (2016). PKCε switches Aurora B specificity to exit the abscission checkpoint. Nat. Commun. *7*, 13853.

Polanski, Z., Ledan, E., Brunet, S., Louvet, S., Verlhac, M.H., Kubiak, J.Z., and Maro, B. (1998). Cyclin synthesis controls the progression of meiotic maturation in mouse oocytes. Development *125*, 4989–4997.

Preisinger, C., Körner, R., Wind, M., Lehmann, W.D., Kopajtich, R., and Barr, F.A. (2005). Plk1 docking to GRASP65 phosphorylated by Cdk1 suggests a mechanism for Golgi checkpoint signalling. EMBO J. *24*, 753–765.

Qian, W., Liao, B.Y., Chang, A.Y.F., and Zhang, J. (2010). Maintenance of duplicate genes and their functional redundancy by reduced expression. Trends Genet. *26*, 425–430.

Qian, Y.W., Erikson, E., Taieb, F.E., and Maller, J.L. (2001). The Polo-like kinase Plx1 is required for activation of the phosphatase Cdc25C and Cyclin B-Cdc2 in *Xenopus* oocytes. Mol. Biol. Cell *12*, 1791–1799.

Queralt, E., and Uhlmann, F. (2008). Cdk-counteracting phosphatases unlock mitotic exit. Curr Opin Cell Biol *20*, 661–668.

Ramadan, K., Bruderer, R., Spiga, F.M., Popp, O., Baur, T., Gotta, M., and Meyer, H.H. (2007). Cdc48/p97 promotes reformation of the nucleus by extracting the kinase Aurora B from chromatin. Nature *450*, 1258–1262.

Ramanathan, S.P., Helenius, J., Stewart, M.P., Cattin, C.J., Hyman, A.A., and Muller, D.J. (2015). Cdk1-dependent mitotic enrichment of cortical myosin II promotes cell rounding against confinement. Nat Cell Biol *17*, 148–159.

Rasmussen, S.W. (1977). Meiosis in Bombyx mori Females. Philos. Trans. R. Soc. B Biol. Sci. *277*, 343–350.

Rattani, A., Vinod, P.K., Godwin, J., Tachibana-Konwalski, K., Wolna, M., Malumbres, M., Novák, B., and Nasmyth, K. (2014). Dependency of the spindle assembly checkpoint on Cdk1 renders the anaphase transition irreversible. Curr. Biol. *24*, 630–637.

Reich, A., Yanai, A., Mesilaty-Gross, S., Chen-Moses, A., Wides, R., and Motro, B. (1999). Cloning, mapping, and expression of ial, a novel *Drosophila* member of the Ipl1/aurora mitotic control kinase family. DNA Cell Biol. *18*, 593–603.

Rieder, C.L., and Maiato, H. (2004). Stuck in division or passing through. Dev. Cell *7*, 637–651.

Rogers, E., Bishop, J.D., Waddle, J.A., Schumacher, J.M., and Lin, R. (2002). The aurora kinase AIR-2 functions in the release of chromosome cohesion in *Caenorhabditis elegans* meiosis. J. Cell Biol. *157*, 219–229.

Rosasco-Nitcher, S.E., Lan, W., Khorasanizadeh, S., and Stukenberg, P.T. (2008).

Centromeric Aurora-B activation requires TD-60, microtubules, and substrate priming phosphorylation. Science *319*, 469–472.

Ruchaud, S., Carmena, M., and Earnshaw, W.C. (2007). Chromosomal passengers: conducting cell division. Nat Rev Mol Cell Biol *8*, 798–812.

Samejima, K., Platani, M., Wolny, M., Ogawa, H., Vargiu, G., Knight, P.J., Peckham, M., and Earnshaw, W.C. (2015). The Inner Centromere Protein (INCENP) coil is a single α-helix (SAH) domain that binds directly to microtubules and is important for chromosome passenger complex (CPC) localization and function in mitosis. J. Biol. Chem. *290*, 21460–21472.

Sampath, S.C., Ohi, R., Leismann, O., Salic, A., Pozniakovski, A., and Funabiki, H. (2004). The chromosomal passenger complex is required for chromatin-induced microtubule stabilization and spindle assembly. Cell *118*, 187–202.

Santaguida, S., Vernieri, C., Villa, F., Ciliberto, A., and Musacchio, A. (2011). Evidence that Aurora B is implicated in spindle checkpoint signalling independently of error correction. EMBO J. *30*, 1508–1519.

Santos, S.D.M., Wollman, R., Meyer, T., and Ferrell Jr, J.E. (2012). Spatial positive feedback at the onset of mitosis. Cell *149*, 1500–1513.

Satyanarayana, A., and Kaldis, P. (2009). Mammalian cell-cycle regulation: several Cdks, numerous cyclins and diverse compensatory mechanisms. Oncogene *28*, 2925–2939.

Schindler, K., Davydenko, O., Fram, B., Lampson, M.A., and Schultz, R.M. (2012). Maternally recruited Aurora C kinase is more stable than Aurora B to support mouse oocyte maturation and early development. Proc. Natl. Acad. Sci. *109*, E2215–E2222.

Schuh, M., and Ellenberg, J. (2007). Self-organization of MTOCs replaces centrosome function during acentrosomal spindle assembly in live mouse oocytes. Cell *130*, 484–498.

Schumacher, J.M., Golden, A., and Donovan, P.J. (1998). AIR-2: An Aurora/Ipl1-related protein kinase associated with chromosomes and midbody microtubules is required for polar body extrusion and cytokinesis in *Caenorhabditis elegans* embryos. J. Cell Biol. *143*, 1635–1646.

Sessa, F., Mapelli, M., Ciferri, C., Tarricone, C., Areces, L.B., Schneider, T.R., Stukenberg, P.T., and Musacchio, A. (2005). Mechanism of Aurora B activation by INCENP and inhibition by hesperadin. Mol. Cell *18*, 379–391.

Shaltiel, I.A., Krenning, L., Bruinsma, W., and Medema, R.H. (2015). The same, only different – DNA damage checkpoints and their reversal throughout the cell cycle. J. Cell Sci. *128*, 607–620.

Shindo, N., Kumada, K., and Hirota, T. (2012). Separase sensor reveals dual roles for Separase coordinating cohesin cleavage and Cdk1 inhibition. Dev. Cell *23*, 112–123.

Shuda, K., Schindler, K., Ma, J., Schultz, R.M., and Donovan, P.J. (2009). Aurora kinase B modulates chromosome alignment in mouse oocytes. Mol. Reprod. Dev. *76*, 1094–1105.

Sigrist, S., Jacobs, H., Stratmann, R., and Lehner, C.F. (1995). Exit from mitosis is regulated by *Drosophila* fizzy and the sequential destruction of cyclins A, B and B3. EMBO J. *14*,

4827–4838.

Silvestre, F., Gallo, A., Cuomo, A., Covino, T., and Tosti, E. (2011). Role of cyclic AMP in the maturation of *Ciona intestinalis* oocytes. Zygote *19*, 365–371.

Sivakumar, S., and Gorbsky, G.J. (2015). Spatiotemporal regulation of the Anaphase-Promoting Complex in mitosis. Nat. Rev. Mol. Cell Biol. *16*, 82–94.

Skold, H.N., Komma, D.J., and Endow, S.A. (2005). Assembly pathway of the anastral *Drosophila* oocyte meiosis I spindle. J Cell Sci *118*, 1745–1755.

Spalluto, C., Wilson, D.I., and Hearn, T. (2013). Evidence for centriolar satellite localization of CDK1 and cyclin B2. Cell Cycle *12*, 1802–1803.

Stach, T., Winter, J., Bouquet, J.M., Chourrout, D., and Schnabel, R. (2008). Embryology of a planktonic tunicate reveals traces of sessility. Proc. Natl. Acad. Sci. U. S. A. *105*, 7229–7234.

Steigemann, P., Wurzenberger, C., Schmitz, M.H.A., Held, M., Guizetti, J., Maar, S., and Gerlich, D.W. (2009). Aurora B-mediated abscission checkpoint protects against tetraploidization. Cell *136*, 473–484.

Stern, B., and Nurse, P. (1996). A quantitative model for the cdc2 control of S phase and mitosis in fission yeast. Trends Genet. *12*, 345–350.

Von Stetina, J.R., and Orr-Weaver, T.L. (2011). Developmental control of oocyte maturation and egg activation in metazoan models. Cold Spring Harb. Perspect. Biol. *3*, a005553.

Stewart, S., and Fang, G. (2005). Destruction box–dependent degradation of Aurora B is mediated by the Anaphase-Promoting Complex/Cyclosome and Cdh1. Cancer Res. *65*, 8730–8735.

Su, K.C., Takaki, T., and Petronczki, M. (2011). Targeting of the RhoGEF Ect2 to the equatorial membrane controls cleavage furrow formation during cytokinesis. Dev. Cell *21*, 1104–1115.

Subramaniam, G., Campsteijn, C., and Thompson, E.M. (2014). Lifespan extension in a semelparous chordate occurs via developmental growth arrest just prior to meiotic entry. PLoS One *9*, e93787.

Sudakin, V., Chan, G.K.T., and Yen, T.J. (2001). Checkpoint inhibition of the APC/C in HeLa cells is mediated by a complex of BUBR1, BUB3, CDC20, and MAD2. J. Cell Biol. *154*, 925–936.

Sugino, Y.M., Tominaga, A., and Takashima, Y. (1987). Differentiation of the accessory cells and structural regionalization of the oocyte in the ascidian *Ciona savignyi* during early oogenesis. J. Exp. Zool. *242*, 205–214.

Sullivan, C., Liu, Y., Shen, J., Curtis, A., Newman, C., Hock, J.M., and Li, X. (2012). Novel interactions between FOXM1 and CDC25A regulate the cell cycle. PLoS One *7*, e51277.

Sumara, I., Quadroni, M., Frei, C., Olma, M.H., Sumara, G., Ricci, R., and Peter, M. (2007). A Cul3-based E3 ligase removes Aurora B from mitotic chromosomes, regulating mitotic progression and completion of cytokinesis in human cells. Dev. Cell *12*, 887–900.

Swaffer, M.P., Jones, A.W., Flynn, H.R., Snijders, A.P., and Nurse, P. (2016). CDK substrate phosphorylation and ordering the cell cycle. Cell *167*, 1750–1761.

Tarailo-Graovac, M., Wong, T., Qin, Z., Flibotte, S., Taylor, J., Moerman, D.G., Rose, A.M., and Chen, N. (2014). Cyclin B3 and dynein heavy chain cooperate to increase fitness in the absence of mdf-1/MAD1 in *Caenorhabditis elegans*. Cell Cycle *13*, 3089–3199.

Thomas, S., and Kaplan, K.B. (2007). A Bir1p–Sli15p kinetochore passenger complex regulates septin organization during anaphase. Mol. Biol. Cell *18*, 3820–3834.

Thoresen, S.B., Campsteijn, C., Vietri, M., Schink, K.O., Liestøl, K., Andersen, J.S., Raiborg, C., and Stenmark, H. (2014). ANCHR mediates Aurora-B-dependent abscission checkpoint control through retention of VPS4. Nat. Cell Biol. *16*, 550–560.

Toyoshima-Morimoto, F., Taniguchi, E., Shinya, N., Iwamatsu, A., and Nishida, E. (2001). Polo-like kinase 1 phosphorylates cyclin B1 and targets it to the nucleus during prophase. Nature *410*, 215–220.

Troedsson, C., Bouquet, J.M., Aksnes, D.L., and Thompson, E.M. (2002). Resource allocation between somatic growth and reproductive output in the pelagic chordate *Oikopleura dioica* allows opportunistic response to nutritional variation. Mar. Ecol. Prog. Ser. *243*, 83–91.

Troedsson, C., Bouquet, J.M., Skinnes, R., Acuna, J.L., Zech, K., Frischer, M.E., and Thompson, E.M. (2009). Regulation of filter-feeding house components in response to varying food regimes in the appendicularian, *Oikopleura dioica*. J Plankt. Res *31*, 1453–1463.

Tsai, J.H., and McKee, B.D. (2011). Homologous pairing and the role of pairing centers in meiosis. J. Cell Sci. *124*, 1955–1963.

Tsai, T.Y.C., Theriot, J.A., and Ferrell Jr, J.E. (2014). Changes in oscillatory dynamics in the cell cycle of early *Xenopus laevis* embryos. PLOS Biol. *12*, e1001788.

Tseng, B.S., Tan, L., Kapoor, T.M., and Funabiki, H. (2010). Dual detection of chromosomes and microtubules by the chromosomal passenger complex drives spindle assembly. Dev. Cell *18*, 903–912.

Vázquez-Novelle, M.D., and Petronczki, M. (2010). Relocation of the chromosomal passenger complex prevents mitotic checkpoint engagement at anaphase. Curr. Biol. *20*, 1402–1407.

Vidwans, S.J., and Su, T.T. (2001). Cycling through development in *Drosophila* and other metazoa. Nat Cell Biol *3*, E35–E39.

van der Voet, M., Lorson, M.A., Srinivasan, D.G., Bennett, K.L., and van den Heuvel, S. (2009). *C. elegans* mitotic cyclins have distinct as well as overlapping functions in chromosome segregation. Cell Cycle *8*, 4091–4102.

Voronina, E., Marzluff, W.F., and Wessel, G.M. (2003). Cyclin B synthesis is required for sea urchin oocyte maturation. Dev. Biol. *256*, 258–275.

Wall, N.R., O'Connor, D.S., Plescia, J., Pommier, Y., and Altieri, D.C. (2003). Suppression of Survivin phosphorylation on Thr^{34} by flavopiridol enhances tumor cell apoptosis. Cancer

Res. *63*, 230–235.

Wang, J.D., and Levin, P.A. (2009). Metabolism, cell growth and the bacterial cell cycle. Nat Rev Micro *7*, 822–827.

Wang, F., Dai, J., Daum, J.R., Niedzialkowska, E., Banerjee, B., Stukenberg, P.T., Gorbsky, G.J., and Higgins, J.M.G. (2010). Histone H3 Thr-3 phosphorylation by Haspin positions Aurora B at centromeres in mitosis. Science *330*, 231–235.

Wang, R., He, G., Nelman-Gonzalez, M., Ashorn, C.L., Gallick, G.E., Stukenberg, P.T., Kirschner, M.W., and Kuang, J. (2007). Regulation of Cdc25C by ERK-MAP kinases during the G2/M transition. Cell *128*, 1119–1132.

Watanabe, N., Arai, H., Nishihara, Y., Taniguchi, M., Watanabe, N., Hunter, T., and Osada, H. (2004). M-phase kinases induce phospho-dependent ubiquitination of somatic Wee1 by SCFβ-TrCP. Proc. Natl. Acad. Sci. U. S. A. *101*, 4419–4424.

van de Weerdt, B.C., van Vugt, M.A., Lindon, C., Kauw, J.J., Rozendaal, M.J., Klompmaker, R., Wolthuis, R.M., and Medema, R.H. (2005). Uncoupling Anaphase-Promoting Complex/Cyclosome activity from spindle assembly checkpoint control by deregulating polo-like kinase 1. Mol. Cell. Biol. *25*, 2031–2044.

Wei, J.H., Zhang, Z.C., Wynn, R.M., and Seemann, J. (2015). GM130 regulates Golgi-derived spindle assembly by activating TPX2 and capturing microtubules. Cell *162*, 287–299.

Welburn, J.P.I., Tucker, J.A., Johnson, T., Lindert, L., Morgan, M., Willis, A., Noble, M.E.M., and Endicott, J.A. (2007). How Tyrosine 15 phosphorylation inhibits the activity of Cyclin-dependent Kinase 2-Cyclin A. J. Biol. Chem. *282*, 3173–3181.

Wheelock, M.S., Wynne, D.J., Tseng, B.S., and Funabiki, H. (2017). Dual recognition of chromatin and microtubules by INCENP is important for mitotic progression. J. Cell Biol. *216*, 925–941.

Wiebusch, L., and Hagemeier, C. (2010). p53- and p21-dependent premature APC/C–Cdh1 activation in G2 is part of the long-term response to genotoxic stress. Oncogene *29*, 3477–3489.

Wong, O.K., and Fang, G. (2007). Cdk1 phosphorylation of BubR1 controls spindle checkpoint arrest and Plk1-mediated formation of the 3F3/2 epitope. J. Cell Biol. *179*, 611–617.

Wu, C.F., Liu, S., Lee, Y.C., Wang, R., Sun, S., Yin, F., Bornmann, W.G., Yu-Lee, L.Y., Gallick, G.E., Zhang, W., et al. (2014). RSK promotes G2/M transition through activating phosphorylation of Cdc25A and Cdc25B. Oncogene *33*, 2385–2394.

Xiang, Y., Takeo, S., Florens, L., Hughes, S.E., Huo, L.J., Gilliland, W.D., Swanson, S.K., Teeter, K., Schwartz, J.W., Washburn, M.P., et al. (2007). The inhibition of Polo kinase by matrimony maintains G2 arrest in the meiotic cell cycle. PLOS Biol. *5*, e323.

Xu, X., Huang, S., Zhang, B., Huang, F., Chi, W., Fu, J., Wang, G., Li, S., Jiang, Q., and Zhang, C. (2017). DNA replication licensing factor Cdc6 and Plk4 kinase antagonistically regulate centrosome duplication via Sas-6. Nat. Commun. *8*, 15164.

Xu, Z., Ogawa, H., Vagnarelli, P., Bergmann, J.H., Hudson, D.F., Ruchaud, S., Fukagawa,

T., Earnshaw, W.C., and Samejima, K. (2009). INCENP-aurora B interactions modulate kinase activity and chromosome passenger complex localization. J. Cell Biol. *187*, 637–653.

Yamashita, M. (1998). Molecular mechanisms of meiotic maturation and arrest in fish and amphibian oocytes. Semin. Cell Dev. Biol. *9*, 569–579.

Yamashita, M., Kajiura, H., Tanaka, T., Onoe, S., and Nagahama, Y. (1995). Molecular mechanisms of the activation of maturation-promoting factor during goldfish oocyte maturation. Dev. Biol. *168*, 62–75.

Yang, J., Bardes, E.S.G., Moore, J.D., Brennan, J., Powers, M.A., and Kornbluth, S. (1998). Control of cyclin B1 localization through regulated binding of the nuclear export factor CRM1. Genes Dev *12*, 2131–2143.

Yasui, Y., Urano, T., Kawajiri, A., Nagata, K., Tatsuka, M., Saya, H., Furukawa, K., Takahashi, T., Izawa, I., and Inagaki, M. (2004). Autophosphorylation of a newly identified site of Aurora-B is indispensable for cytokinesis. J. Biol. Chem. *279*, 12997–13003.

Yoshitome, S., Furuno, N., Prigent, C., and Hashimoto, E. (2012). The subcellular localization of cyclin B2 is required for bipolar spindle formation during *Xenopus* oocyte maturation. Biochem. Biophys. Res. Commun. *422*, 770–775.

Yuan, K., and O'Farrell, P.H. (2015). Cyclin B3 is a mitotic cyclin that promotes the metaphase-anaphase transition. Curr. Biol. *25*, 811–816.

Yüce, Ö., Piekny, A., and Glotzer, M. (2005). An ECT2–centralspindlin complex regulates the localization and function of RhoA. J. Cell Biol. *170*, 571–582.

Yue, Z., Carvalho, A., Xu, Z., Yuan, X., Cardinale, S., Ribeiro, S., Lai, F., Ogawa, H., Gudmundsdottir, E., Gassmann, R., et al. (2008). Deconstructing Survivin: comprehensive genetic analysis of Survivin function by conditional knockout in a vertebrate cell line. J. Cell Biol. *183*, 279–296.

Zhang, J. (2003). Evolution by gene duplication: an update. Trends Ecol. Evol. *18*, 292–298.

Zhang, M., Kothari, P., and Lampson, M.A. (2015a). Spindle assembly checkpoint acquisition at the mid-blastula transition. PLoS One *10*, e0119285.

Zhang, T., Qi, S.T., Huang, L., Ma, X.S., Ouyang, Y.C., Hou, Y., Shen, W., Schatten, H., and Sun, Q.Y. (2015b). Cyclin B3 controls anaphase onset independent of spindle assembly checkpoint in meiotic oocytes. Cell Cycle *14*, 2648–2654.

Zickler, D., and Kleckner, N. (2015). Recombination, pairing, and synapsis of homologs during meiosis. Cold Spring Harb. Perspect. Biol. *7*, 1–28.

Paper I

Specialization of CDK1 and Cyclin B paralog functions in a coenocystic mode of oogenic meiosis

CELL CYCLE
https://doi.org/10.1080/15384101.2018.1486167

Taylor & Francis
Taylor & Francis Group

RESEARCH PAPER

OPEN ACCESS Check for updates

Specialization of CDK1 and cyclin B paralog functions in a coenocystic mode of oogenic meiosis

Haiyang Feng[a,b] and Eric M. Thompson [a,b]

[a]Department of Biological Sciences, University of Bergen, Bergen, Norway; [b]Sars International Centre for Marine Molecular Biology, University of Bergen, Bergen, Norway

ABSTRACT

Oogenesis in the urochordate, *Oikopleura dioica*, occurs in a large coenocyst in which vitellogenesis precedes oocyte selection in order to adapt oocyte production to nutrient conditions. The animal has expanded Cyclin-Dependant Kinase 1 (CDK1) and Cyclin B paralog complements, with several expressed during oogenesis. Here, we addressed functional redundancy and specialization of CDK1 and cyclin B paralogs during oogenesis and early embryogenesis through spatiotemporal analyses and knockdown assays. CDK1a translocated from organizing centres (OCs) to selected meiotic nuclei at the beginning of the P4 phase of oogenesis, and its knockdown impaired vitellogenesis, nurse nuclear dumping, and entry of nurse nuclei into apoptosis. CDK1d-Cyclin Ba translocated from OCs to selected meiotic nuclei in P4, drove meiosis resumption and promoted nuclear envelope breakdown (NEBD). CDK1d-Cyclin Ba was also involved in histone H3S28 phosphorylation on centromeres and meiotic spindle assembly through regulating Aurora B localization to centromeres during prometaphase I. In other studied species, Cyclin B3 commonly promotes anaphase entry, but we found *O. dioica* Cyclin B3a to be non-essential for anaphase entry during oogenic meiosis. Instead, Cyclin B3a contributed to meiotic spindle assembly though its loss could be compensated by Cyclin Ba.

ARTICLE HISTORY
Received 13 March 2018
Accepted 29 May 2018

KEYWORDS
Urochordate; chromosomal passenger complex; vitellogenesis; cyclin B3; oogenesis; meiosis resumption

Introduction

Oogenesis in many animal species arrests at a prolonged diplotene stage of prophase I (called dictyate in mammals), permitting oocyte differentiation, growth and stockpiling of maternal mRNA and proteins for early embryonic development [1]. The duration of prophase I arrest varies among species: ~ 23 minutes in the hermaphroditic nematode, *C. elegans*, when sperm is present, ~ 2 days in *Drosophila*, several months in mice, or up to decades in humans. Release from prophase I arrest in response to appropriate stimuli relies on activation of maturation promoting factor (MPF), consisting of Cyclin-Dependant Kinase 1 (CDK1) kinase and its regulatory subunit Cyclin B. After primary arrest, most species, except nematodes, will experience a secondary arrest at metaphase I (most invertebrates), metaphase II (most vertebrates) or the pronuclear stage (sea urchins and sea stars). Secondary arrest is maintained by high activity of MPF and cytostatic factor (CSF) including early mitotic inhibitor 2 (Emi2), responsible for APC/C inhibition [2]. The roles of CDK1-Cyclin B complexes during oocyte maturation have been studied in a variety of species including mice, *Xenopus*, clams, starfish, and several fish species [3]. CDK1 collaborates with multiple kinases to complete meiosis, and the interrelations are focused on where these mitotic kinases lie in signaling pathways. For instance, the mitogen-activated protein kinase (MAPK) is activated ahead of CDK1 activation by progesterone stimulation in *Xenopus* or sperm-derived major sperm protein (MSP) in *C. elegans*, whereas in starfish, Mos synthesis and MAPK activation depend on CDK1 activation [4]. Polo-like kinases (Plk) are also involved in CDK1 activation, either as a trigger kinase initiating CDK1 activation during mitotic entry [5], or in a CDK1 positive feedback loop during meiosis [6].

In the urochordate, appendicularian, *Oikopleura dioica*, among the closest extant relatives to vertebrates [7], oogenesis occurs over a period of 2–3 days in a single-cell coenocyst, where thousands of meiotic and nurse nuclei share a common cytoplasm, surrounded

CONTACT Eric M. Thompson Eric.Thompson@uib.no
Supplemental data for this article can be accessed here.

by a monolayer of follicle cells [8]. Cellularization of oocytes occurs at the end of oogenesis shortly before spawning [9]. This is different from other chordate species and most deuterostomes, where germline, cystoblast, cyst breakdown occurs during early stages of oogenesis, around the period of oocyte determination and before vitellogenesis [10]. There are similarities to *Drosophila*, where nurse cells synthesize RNAs and proteins, followed by transport through ring canals to the growing pro-oocyte by cytoplasmic streaming to support vitellogenesis [11]. The cytoplasmic transport process is slow until stage 10, but from stage 11, the entire cytoplasmic content of nurse cells is transferred within 30 minutes to the oocyte by contraction of the actin network at the end of vitellogenesis [12]. An important distinction is that in *Drosophila*, oocyte determination occurs prior to vitellogenesis, whereas in *O. dioica*, oocyte selection occurs after vitellogenesis has begun, and final oocyte number is determined very late in the life cycle as a function of accumulated energetic resources [13]. In all studied deuterostomes, except *O. dioica*, maturing oocytes contain a transcriptionally active meiotic nucleus termed the germinal vesicle (GV). *O. dioica* meiotic nuclei harbor three bivalents, and with the exception of two small foci [13], they are transcriptionally quiescent, a probable adaptation to coenocystic oogenesis. Regardless of the transcriptional status of the meiotic nucleus, meiosis resumption is shortly followed by kinase-induced nuclear envelope breakdown (NEBD) and termination of transcription.

During female meiosis, substrate specificities of CDK1 are largely determined by their Cyclin partner [14], principally the B-type Cyclins. Three B-type Cyclins, B1, B2, and B3, (amphibians also possess Cyclins B4 and B5 [15]), have been studied in metazoans, with different degrees of functional redundancy being reported. From an evolutionary standpoint, it remains unclear to what extent diversification of Cyclin B functions and/or redundancies, might in part, reflect different structural organizations of oogenesis. In *Drosophila*, where the cyst phase (15 nurse nuclei to 1 meiotic nucleus) persists late in oogenesis, Cyclin B restrains APC/C activity and is required for metaphase maintenance and meiotic spindle organization, whereas Cyclin B3, which is destroyed after Cyclin B, promotes the metaphase-anaphase transition by activating APC/C [16,17]. In *C. elegans*, where the cyst phase is resolved near the spatial midpoint of oogenesis (ratio of the cytoplasm of 1 nucleus in the rachis sacrificed for 1 nucleus continuing to complete meiosis) at the bend in the gonad arm, CYB-1, CYB-2.1, CYB-2.2 and CYB-3, show somewhat greater functional overlap in meiosis than in mitosis. In both meiosis and mitosis CYB-1 is required for chromosome congression, and CYB-3 is required for chromosome segregation [18]. CYB-3 also supports S-phase progression and is a major contributor to promote NEBD in mitotic entry [19]. In higher vertebrates, where the cyst phase is resolved very early in oogenesis, Cyclin B1 is essential, while Cyclin B2 is dispensable [20,21]. The division of functions between Cyclins B1 and B2 lies in nuclear mitotic functions for Cyclin B1, such as driving NEBD, spindle assembly, spindle checkpoint induction and M-phase maintenance, whereas Cyclin B2 is involved in earlier interphase events such as Golgi fragmentation [22] and centrosome separation [23,24]. Vertebrate Cyclin B3 shares properties of both Cyclin As and Bs, localizes in nucleus throughout the cell cycle [25] and drives the metaphase to anaphase transition by activating APC/C^{cdc} [20] independently of the spindle assembly checkpoint (SAC) during meiosis I in mouse oocytes [26].

CDK-type kinases have experienced functional differentiation during eukaryote evolution. In yeast, a single CDK1 homolog (Cdc28 in budding yeast and Cdc2 in fission yeast) and its associated cyclins drive the entire cell cycle [27]. In metazoans, CDK1 interacts with mitotic Cyclins A and B to drive M-phase, though knockouts of interphase CDKs has revealed that, as in yeast, CDK1 alone retains the ability to regulate the entire embryonic cell cycle [28]. Although the specific requirements for CDK1 in meiosis are not completely resolved due to early embryonic lethality of CDK1 knockout mice, the consensus is that CDK1 relieves prophase I arrest after vitellogenesis in *Xenopus*, starfish [29], *Drosophila* [30] and *C. elegans* [31]. Surprisingly, *O. dioica* is unique among metazoans in possessing five CDK1 paralogs (CDK1a-CDK1e) [32], none of which retains the invariant, canonical Cyclin B-interacting PSTAIRE motif of the single CDK1 homolog found in other metazoans. Its complement of B-type Cyclins has also expanded to five paralogs (Cyclins Ba, Bb, Bc, B3a and B3b) that show distinct expression patterns

during somatic and germline development [32]. Briefly, all five CDK1 paralogs exhibit expression during mitotic divisions in early embryonic development, though CDK1d and e expression is most prevalent in the ovary and declines rapidly in early development, indicative of maternal transcripts. Surprisingly, CDK1a,b and c paralogs are expressed throughout the life cycle, including stages dominated by rapid growth through endocycling, a cell cycle variant where CDK1 activity is suppressed in other model organisms that have been studied. In comparison, all cyclin B paralogs are expressed in mitotic stages but, as would be expected, are suppressed during portions of the life cycle dominated by endocycling, when they are restricted to tissues, such as the mitotically proliferating germline nuclei in the gonad. In *O. dioica*, active MAPK and Plk1 emerge on Organizing Centres (OCs) where CDK1s reside before meiosis resumption. At this point, Plk1 translocates into selected meiotic nuclei after oocyte selection, whereas MAPK is retained on OCs in maturing oocytes [33]. The consequences of differential translocation of these meiotic kinases and their interplays with different CDK1 paralogs are unknown.

In *O. dioica*, oogenesis is subdivided into 5 phases P1 to P5 (summarized in Table 1 of Ganot et al. [9]). Briefly, during P1, ovarian germline nuclei undergo an asymmetric division, generating a 1:1 ratio of endocycling nurse nuclei and meiotic nuclei. During P2, meiotic nuclei progress to zygotene and in P3, the coenocyst expands in size. Upon transition to P4, a subset of pro-oocytes increases in size via transfer of cytoplasm through their ring canal connections to the general coenocyst cytoplasm and meiotic chromatin condenses. In the final P5 stage, oocyte maturation is completed, nurse and excess meiotic nuclei undergo apoptosis, and spawning occurs via rupture of the ovarian wall. In this study, we found that two CDK1 paralogs, CDK1a and CDK1d, and a mitotic cyclin, cyclin Ba exhibited distinct spatial and temporal dynamics during oocyte selection and meiosis resumption. By RNAi knockdowns, we demonstrated the sub-functionalization of the two CDK1 paralogs in oogenic meiosis. CDK1a regulated coenocystic vitellogenesis by participating in nurse nuclei dumping during pro-oocyte growth, whereas CDK1d together with cyclin Ba, and to a lesser, non-essential extent, cyclin B3a, promoted meiosis resumption, NEBD and meiotic spindle assembly during prometaphase I.

Results

CDK1 and cyclin B paralog expressions and localizations during coenocystic oogenesis in oikopleura dioica

Previous work revealed that CDK1a and CDK1d resided on Organizing Centers (OCs) in P3, but their localizations were unclear after oocyte selection [33]. To clarify their localizations during meiosis, we injected a CDK1a capped mRNA with a full-length endogenous 3′UTR into P3 gonads, and observed CDK1a to locate to selected meiotic nuclei and their adjacent OCs during P4 (Figure 1(a)). CDK1d was also observed in selected meiotic nuclei during P4, but not on OCs (Figure 1(b)), further supporting its role in driving meiosis resumption.

We had previously identified 3 homologs (Cyclins Ba, Bb and Bc) of Cyclin B1, and 2 homologs (Cyclins B3a and B3b) of Cyclin B3 in the *O. dioica* genome [32]. Cyclin Ba and Bb share 97% amino acid identity, and their exon/intron arrangements are very similar, supporting a recent duplication. First, we quantified mRNA levels of B-type cyclins during oogenesis by RT-qPCR. *Cyclin Ba* mRNA levels were high during early stages of oogenesis, reaching a peak when pro-oocytes were growing, and then gradually declined thereafter, whereas *Cyclin Bb* mRNA levels were barely detected throughout oogenesis (Figure 2(a)). *Cyclin B3a* mRNA levels were high during late stages of oogenesis, reaching and maintaining a peak from P5 to metaphase I, whereas *Cyclin B3b* mRNA levels were barely detected throughout oogenesis. *Cyclin Bc* mRNA levels were low, with a slight increase late in oogenesis (P5) and in oocytes. We therefore focused on the Cyclin Ba, and B3a paralogs in further analyzes.

Cyclin Ba was mainly transcribed in nurse nuclei during P3 and P4 (Figure 2(c)). In P5, *cyclin Ba* mRNA was exported to the coenocyst cytoplasm, and then transferred and evenly distributed

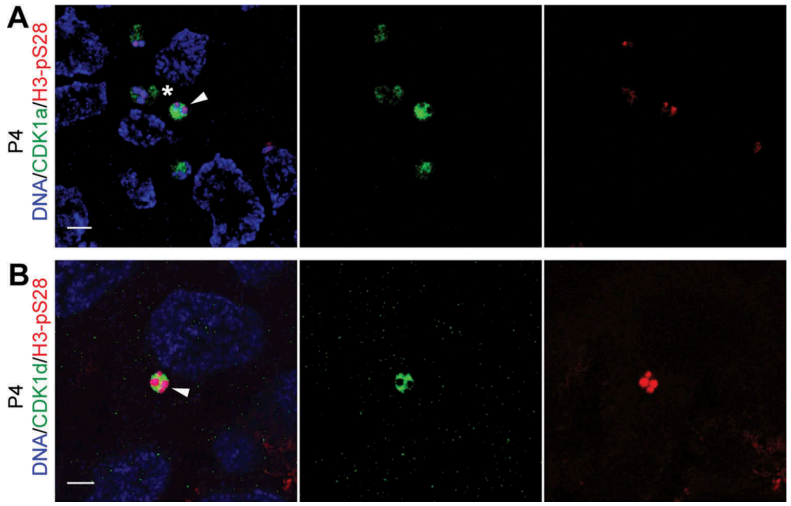

Figure 1. CDK1a and d paralogs locate to selected meiotic nuclei after oocyte selection. (A) CDK1a-GFP localized to H3-pS28 positive selected meiotic nuclei (arrowhead) and their adjacent OCs (*) in P4 ovaries. (B) CDK1d-GFP localized to H3-pS28 positive selected meiotic nuclei (arrowhead) in P4 ovaries. Scale bars: 5 μm.

in mature oocytes just prior to spawning. These distribution patterns are similar to those of *cyclin B* mRNA in syncytial *Drosophila* ovarioles [34]. Western blots showed that Cyclin Ba was detectable in P4, before increasing dramatically in P5, to achieve its highest levels in metaphase I arrested spawned oocytes (Figure 2(b)). The significant increase of Cyclin Ba during late prophase I and prometaphase I might indicate potential roles during the final stages of oocyte maturation. It is noteworthy that Cyclin Ba exhibited two bands (~ 37 KD and 39 KD), and the proportion of upper band significantly increased during prometaphase I. The upper band decreased upon phosphatase treatment, indicating a phosphorylated form of Cyclin Ba. To explore the spatial localization of Cyclin Ba during oogenesis, capped mRNA encoding Cyclin Ba fused to eGFP at its C-terminal, was injected into P3 ovaries at Day 4. Injected animals were cultured to Day 5 and harvested in late P3 and P4 for immunostaining with anti-GFP antibodies (Figure 2(d)). Cyclin Ba was found on OCs in late P3, co-staining with M-phase specific, MPM2 phospho-epitopes. At the beginning of P4, we used histone H3-pS28 staining to determine the meiotic nuclei selected to populate growing pro-oocytes. At this stage, Cyclin Ba was found on OCs adjacent to both selected (histone H3-pS28 positive) and non-selected (H3-pS28 negative) meiotic nuclei. At late P4, Cyclin Ba translocated into selected meiotic nuclei. Thus, translocation of Cyclin Ba from OCs to selected meiotic nuclei occurs after oocyte selection in late P4, consistent with a possible role of Cyclin Ba as the regulatory subunit of MPF.

CDK1a, CDK1d, cylinBa and cyclinB3a knockdown oocytes differ significantly in kinase activity

The dynamics of CDK1a and d localizations and Cyclin Ba and B3a paralog expressions and localizations during oogenesis led us to examine the effects of their respective knockdowns on meiosis and oocyte maturation. CDK1 kinase assays of oocytes (Figure 3) revealed that all individual knockdowns reduced kinase activity. The impact of *cycB3a* knockdown was relatively minor, reducing kinase activity to about 80% of that in wild type oocytes. All other knockdowns reduced kinase activity to less than 20% of wild type activity. There was no significant difference in the kinase activity of *cycBa* RNAi versus *cycBa;B3a* double RNAi knockdowns. Loss of kinase activity was more severe in *Cdk1d* knockdowns (9% of wild type) and almost eliminated in *CDK1a* knockdowns (1% of wild type).

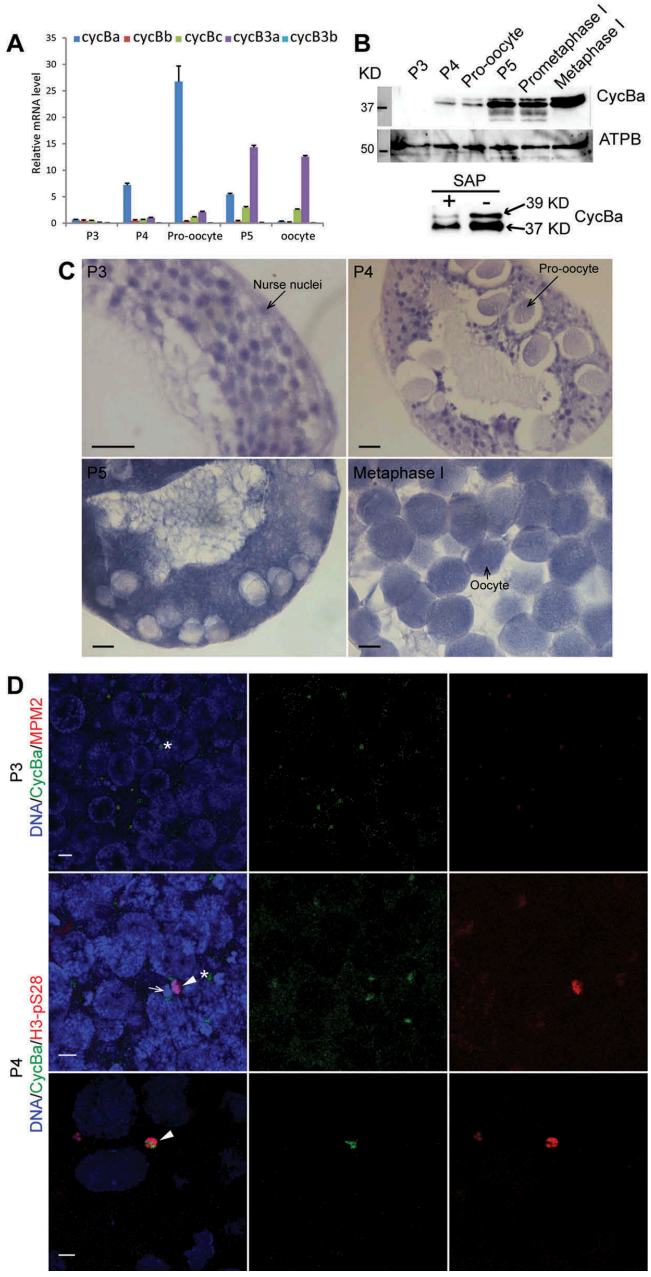

Figure 2. Expression profiles and distribution of *Oikopleura dioica* B-type cyclin transcripts and Cyclin Ba protein during oogenesis. (A) Expression levels of *O. dioica* homologs of Cyclins B1 and B3 during oogenesis. Mean values normalized to EF1β transcripts (n = 3) are shown with standard error bars. (B) Top panels: Cyclin Ba increased during maturation from P3 to metaphase I. Whole animal lysates were immunoblotted and detected with Cyclin Ba antibody (top) or ATP synthase β antibody as a loading control (bottom). Bottom panel: Shrimp alkaline phosphatase (SAP) treatment reduced the Cyclin Ba upper band, indicating this is phosphorylated form of Cyclin Ba. (C) *In situ* hybridization showed that cyclin Ba was transcribed in nurse nuclei in P3 and P4 ovaries, transported into the coenocyst cytoplasm in P5, and subsequently concentrated in mature oocytes. Scale bars: 50 µm. (D) Cyclin Ba-GFP localized at MPM2-stained OCs (*) in P3 (top panels) and early P4 ovary (mid panels), where it was adjacent to both H3-pS28 stained selected meiotic nuclei (arrowhead) and non-selected meiotic nuclei (arrow). Cyclin Ba-GFP translocated into selected meiotic nuclei in late P4 ovaries (bottom panel). Scale bars: 5 µm.

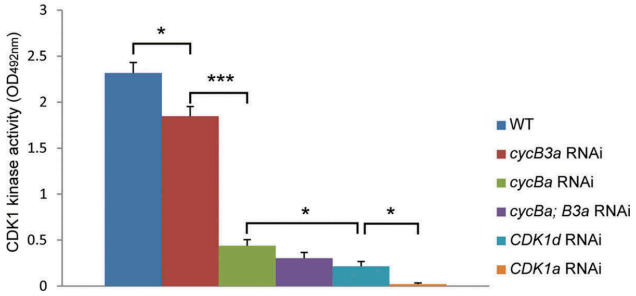

Figure 3. CDK1 kinase activity assays of *CDK1* and *cycB* paralog RNAi oocytes (n = 30 per category). The values were calculated as means from three independent assays with standard errors shown. Significant pairwise step differences in kinase activities (student's t-test) are indicated (*, $p < 0.05$; ***, $P < 0.001$).

CDK1a knockdown results in small infertile oocytes and disrupts cyclin B paralog dynamics

After observing that CDK1a knockdown severely impaired the kinase activity levels in the ovarian coenocyst, we then characterized the phenotypic effects resulting from this loss of activity. *CDK1a* knockdown females produced small infertile oocytes, which were often surrounded by excess coenocyst cytoplasm (Figure 4(a) and [33]). Lamin1 staining revealed that the nuclear envelope was intact, with OC closely associated (Figure 4(b)), whereas OC disassembled during prometaphase I in wild type oogenesis (Figure S1). In wild type selected meiotic nuclei at the P4 stage, MPM2 foci were present on chromosomes (Figure S1) whereas in *CDK1a* knockdown ovaries, MPM2 foci were absent in meiotic nuclei, but remained present on OC (Figure 4(b)). In knockdown ovaries, active Polo-like kinase 1 (Plk1) was not observed on meiotic chromatin, being retained in the nucleoplasm and on OC (Figure 4(c)). In contrast, active Plk1 translocated from OC to selected meiotic nuclei and distributed evenly on both chromosomes and in the nucleoplasm at P4 in wild type ovaries (see Figure 10(c) below). In spawned *CDK1a* RNAi oocytes, *cyclin Ba* mRNA levels were high and *cyclin B3a* mRNA levels very low (Figure S2A), similar to their expression profiles during pro-oocyte growth (Figure 2(a)). However, Cyclin Ba protein was very low, similar to Cyclin Ba protein levels at the beginning of P4 (Figure S2B). This was not the case for *CDK1d* knockdowns, where Cyclin Ba protein levels were similar to those found in wild type (Figure S2B). These data indicate that *CDK1a* RNAi oocytes were arrested at diplotene during pro-oocyte growth.

In situ hybridizations on *CDK1a* RNAi ovaries prior to spawning showed that most *cyclin Ba* mRNA was retained in nurse nuclei (Figure 4(d)), instead of being transported to the coenocystic cytoplasm during pro-oocyte growth. This likely contributes to the lower levels of Cyclin Ba protein found in *CDK1a* knockdown oocytes. During late stages of wild type oogenesis, all nurse nuclei become histone H3-pS10 positive and undergo apoptosis [13]. In *CDK1a* RNAi ovaries just before spawning, a small proportion of nurse nuclei became deformed, and were positively stained with H3-pS10, indicating they were undergoing apoptosis, whereas most nurse nuclei remained oval and did not stain for the H3-pS10 marker indicative of apoptosis (Figure 4(e)). Apoptosis and rapid cytoplasmic transport are interconnected processes, and the failure of nurse nuclei dumping blocks apoptosis [35]. Thus, *CDK1a* knockdown females produce small oocytes, similar to the "dumpless" class of oogenesis mutants described in *Drosophila* [36]. We have shown previously [33] that ring canal diameters of growing oocytes in *CDK1a* RNAi ovaries were not affected, excluding the possibility of premature constriction of ring canals and nurse nuclei did not clog the ring canals. We tried to identify the regulatory subunit of CDK1a by knocking down other mitotic cyclins including Cyclin Bc and Cyclin A, but neither knockdown showed similar defects to knockdown of *CDK1a*. Taken together, our data suggest that CDK1a is involved

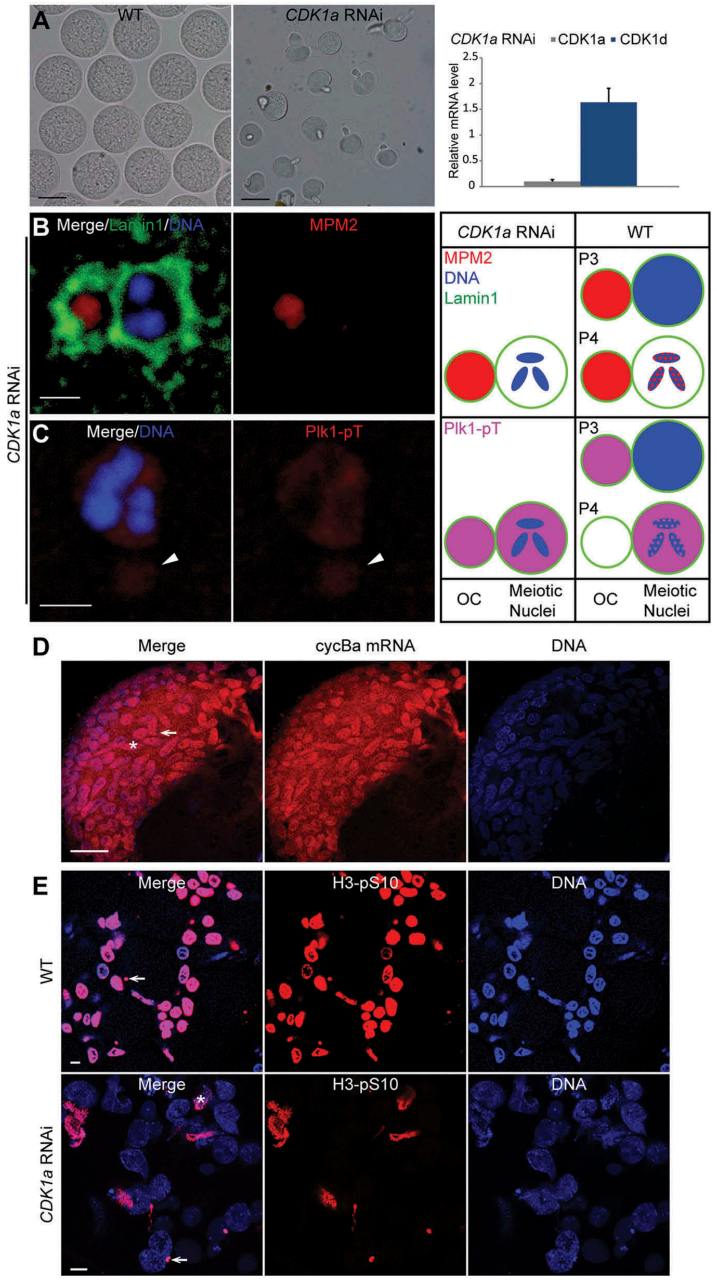

Figure 4. Meiotic defects resulting from *CDK1a* RNAi. (A) *CDK1a* RNAi oocytes (mid panel) were smaller than wild-type oocytes (left panel). Scale bars: 50 µm. In the right panel, CDK1a knockdown efficiency was confirmed by RT-qPCR. No significant off-target effects on other CDK1 paralogs were detected. (B) Lamin1 staining showed that *CDK1a* RNAi oocytes retained OC around meiotic nuclei. MPM2 epitopes were present on OC but absent in meiotic nuclei. Scale bar: 2 µm. (C) Plk1 was absent on chromosomes, but present in nucleoplasm and on OC (arrowhead). Scale bar: 2 µm. Schemas on the right compare the localizations of MPM2 epitopes (red) and Plk1 (pink) in meiotic nuclei and on OC between *CDK1a* RNAi oocytes and wild type in P3 and P4. (D) *in situ* hybridization showed that *cyclin Ba* mRNA (red) was retained in nurse nuclei of *CDK1a* RNAi ovaries in late P5 prior to spawning. Arrow indicates a meiotic nucleus, aster indicates a nurse nucleus. Scale bar: 50 µm. (E) In WT, all nurse nuclei underwent apoptosis and became H3-pS10 positive just prior to spawning. In *CDK1a* RNAi ovaries, only a small proportion of nurse nuclei underwent apoptosis and became H3-pS10 positive just before spawning. Arrow indicates a meiotic nucleus, aster indicates a nurse nucleus. Scale bars: 10 µm.

in the regulation of nurse nuclear dumping and cytoplasmic flow during later stages of coenocystic oogenesis in *O. dioica*.

Cyclin Ba is required for meiosis completion whereas cyclin B3a is dispensable

To address meiotic roles of Cyclin Ba, we injected *cyclin Ba* dsRNA into P3 ovaries, corresponding to the diplotene stage of prophase I. Efficient knockdown of *cyclin Ba* transcripts was observed with no off-target effects on paralogous genes, and western blots showed that Cyclin Ba protein could not be detected in *cyclin Ba* RNAi oocytes (Figure 5(a)). Upon exposure to wild type sperm, *cyclin Ba* RNAi oocytes were infertile, indicating that Cyclin Ba is an important regulator of oocyte maturation (Figure 5 (b)). To further analyze the infertile phenotype, progress of meiosis I in *cyclin Ba* RNAi oocytes was examined by immunostaining the nuclear lamina. Anti-odLamin1 immunostaining showed that the nuclear envelope was retained when cyclin Ba was depleted, in contrast to its disassembly in wild type oocytes arrested at metaphase I, indicating NEBD did not occur (Figure 5(c)).

Cyclin B3a is also actively transcribed during late stages of oogenesis and early stages of embryogenesis. Knockdown of Cyclin B3a lowered the kinase activity in oocytes to 80% of wild type levels (Figure 3) but did not affect the fertility of spawned oocytes nor impact early embryonic development (Figure S3). This suggests that Cyclin Ba is capable of compensating the loss of Cyclin B3a during oogenic meiosis.

Effects of CDK1*a*, CDK1d, cyclinBa and cyclinB3a knockdowns on meiotic bivalents and acentrosomal spindle formation

It has been demonstrated that the chromosomal passenger complex (CPC) is directly involved in meiotic spindle assembly during coenocystic oogenic meiosis I of *Drosophila* [37], and we wished to characterize its role in this process during the coenocystic meiosis of *O. dioica*. We observed that Aurora B, the kinase module in CPC, moved to centromeres, concurrent with the progress of meiotic acentrosomal spindle assembly during prometaphase I (Figure 6). This coincided with a change in uniform H3-pS28 staining along chromosomes to a concentration of this mark at the centromeres at prometaphase I (Figure S4). In wild type metaphase I arrested oocytes, bivalents exhibited high levels of H3-pS10 along entire chromosomes, and concentrated H3-pS28 at centromeres (Figure 7(a)). Cyclin Ba depletion resulted in a lack of concentrated H3-pS28 staining at the centromeres of bivalents (Figure 7(b)), indicating arrest of *cyclin Ba* RNAi oocytes at prometaphase I. This same effect was observed in *cycBa;B3a* double knockdowns and in knockdowns of *CDK1d* or *CDK1a* (Figure 7(c-e))

We observed that bivalents in *cyclin Ba* RNAi oocytes were not well aligned on the metaphase I plate as compared to wild type (Figure 8(a,b)). Aurora B was delocalized from centromeres and the spindle was severely compromized. Complete loss of the spindle, indicated by an absence of any tubulin staining in the region surrounding the chromosomes was observed in 39% of oocytes. In 57% of oocytes there was weak tubulin staining around chromosomes, but it was not organized into any recognizable fibre-like structures. Finally, in a very minor proportion of oocytes (4%) we observed enhanced tubulin staining around chromosomes but an absence of any assembly into fibres. In *cycBa;B3a* double knockdowns, more severe defects on meiotic spindle assembly were observed, with 84% of double RNAi oocytes showing complete loss of tubulin staining, and 16% retaining weak, diffuse tubulin staining around chromosomes (Figure 8(c)) with an absence of any detectable microtubule fibres. This suggests that Cyclin B3a may assist Cyclin Ba in promoting meiotic spindle assembly during prometaphase I, though it is not strictly required for this purpose. CDK1d is required for meiosis resumption in *O. dioica*, and its knockdown blocked NEBD [33]. The defects of *CDK1d* RNAi oocytes were similar to *cyclin Ba* RNAi oocytes regarding the distribution of H3-pS10 and H3-pS28 on chromosomes, but meiotic spindle assembly defects were more severe (Figure 8(d)) with no tubulin staining observed in any of the *CDK1d* RNAi oocytes.

The above results led us to investigate the centromeric region of bivalents in more detail. These were

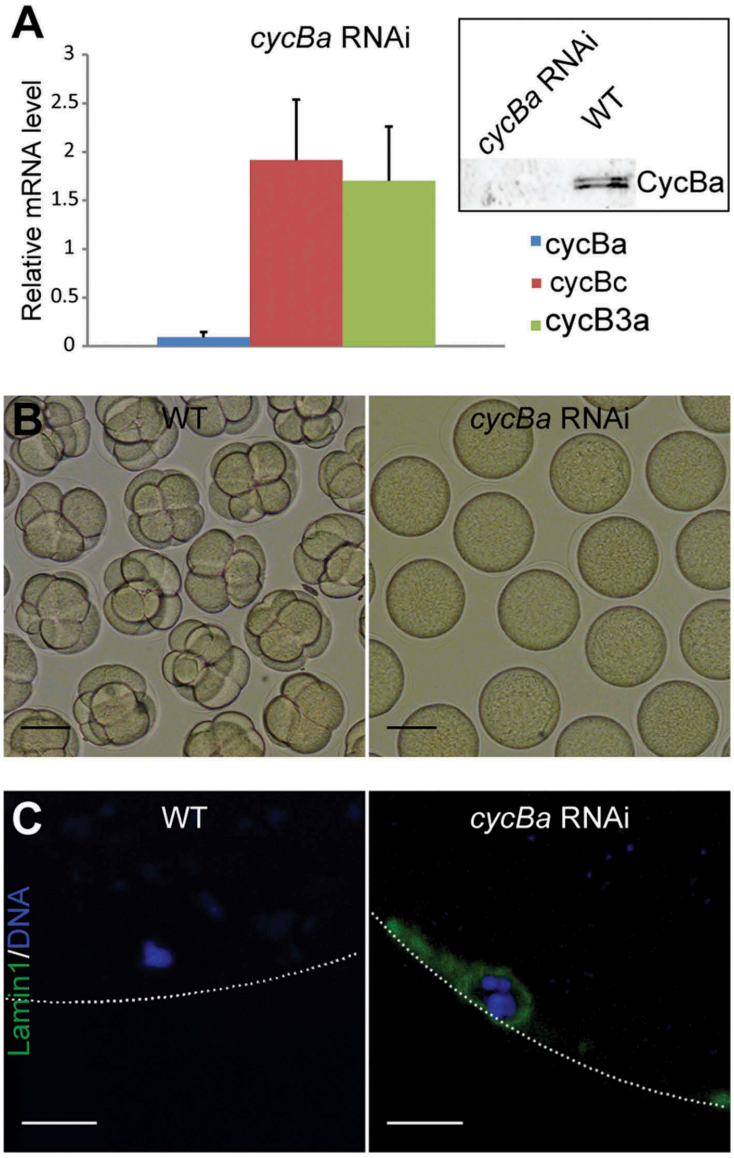

Figure 5. Depletion of Cyclin Ba blocks NEBD and generates non-fertile oocytes. (A) *Cyclin Ba* transcripts were efficiently knocked down by RNAi with no significant off-target effects on other *cyclin B* paralogs. Upper right corner: Western-blotting of *cycBa* RNAi oocytes (left lane) showed that Cyclin Ba was absent, compared to equal loading of wild-type control oocytes (right lane). (B) At 1 h post exposure to wild-type sperm, *cycBa* RNAi oocytes were infertile, whereas wild-type oocytes had developed normally to the 8-cell stage. Scale bars: 50 µm. (C) Lamin1 immunostaining revealed retention of the nuclear envelope in *cycBa* RNAi oocytes, compared to successful NEBD in wild-type oocytes at metaphase I. Dotted lines indicate the position of the oocyte plasma membrane. Scale bars: 5 µm.

decorated by strong MPM2 epitopes during prometaphase I (Figure 9(a)). Since the MPM2 antibody mostly recognizes CDK1 substrates, it is possible that CDK1 phosphorylates substrates at the centromeric region during prometaphase I. In *cyclin Ba* RNAi oocytes, MPM2 foci were absent on chromosomes,

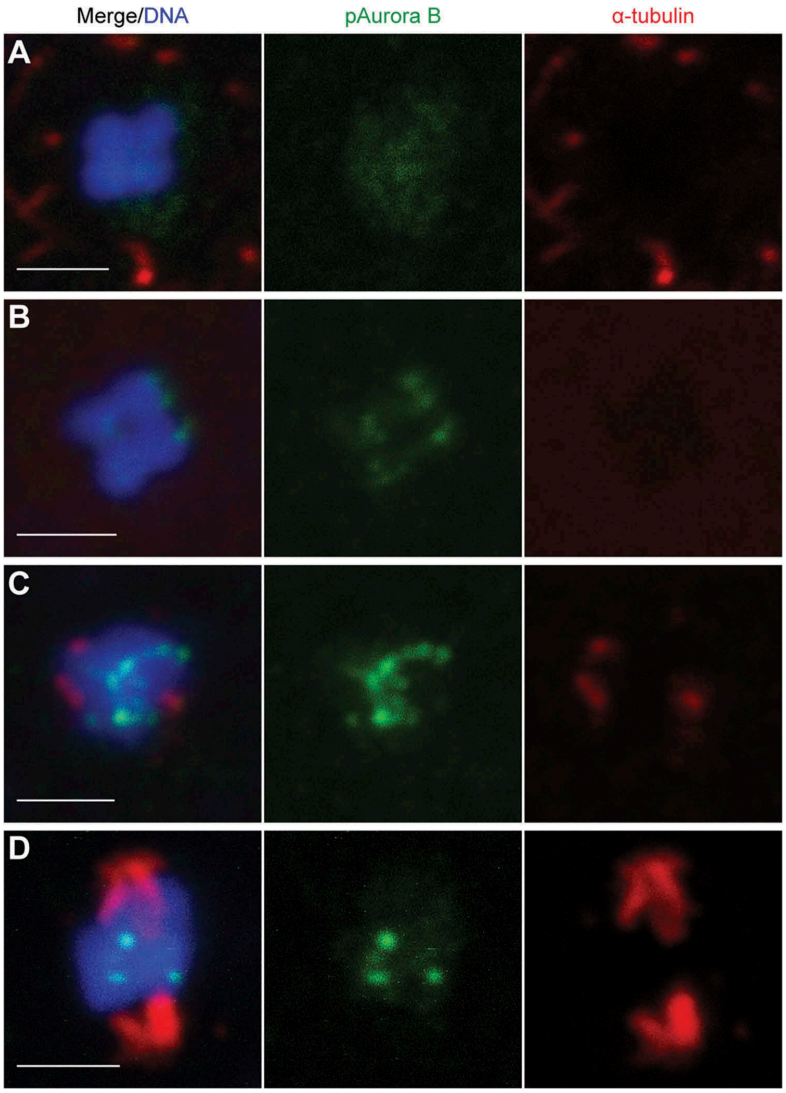

Figure 6. Acentrosomal spindle assembly during prometaphase I of *Oikopleura* oocytes is concurrent with Aurora B moving to centromeres. (A) Before NEBD, Aurora B distributed evenly through the nucleus, and a microtubule network surrounded the nuclear membrane. (B) After NEBD, Aurora B moved towards centromeres, and the microtubule network disappeared. (C) When the Aurora B signal became strong on centromeres, short microtubule fibers started to form from opposite poles. (D) When Aurora B was established on the centromeres of bivalents, the spindle elongated. Scale bars: 2 μm.

but remained in the nucleoplasm (Figure 9(b)). The same result was observed in *cycBa;B3a* double knockdowns (Figure 9(c)). When CDK1d was knocked down, MPM2 foci disappeared from centromeric regions and nucleoplasmic MPM2 staining became weak (Figure 9(d)). These results indicate that Cyclin Ba is important for CDK1 activity at centromeres and may contribute to the delocalization of Aurora B from centromeres in *cyclin Ba* or *CDK1d* knockdowns (Figure 8). We then examined upstream regulators that recruit Aurora B to centromeres. One of them is phosphorylation of histone H3 on Thr3 (H3-pT3) in the inner centromere region by Haspin [38], and this modification recruits

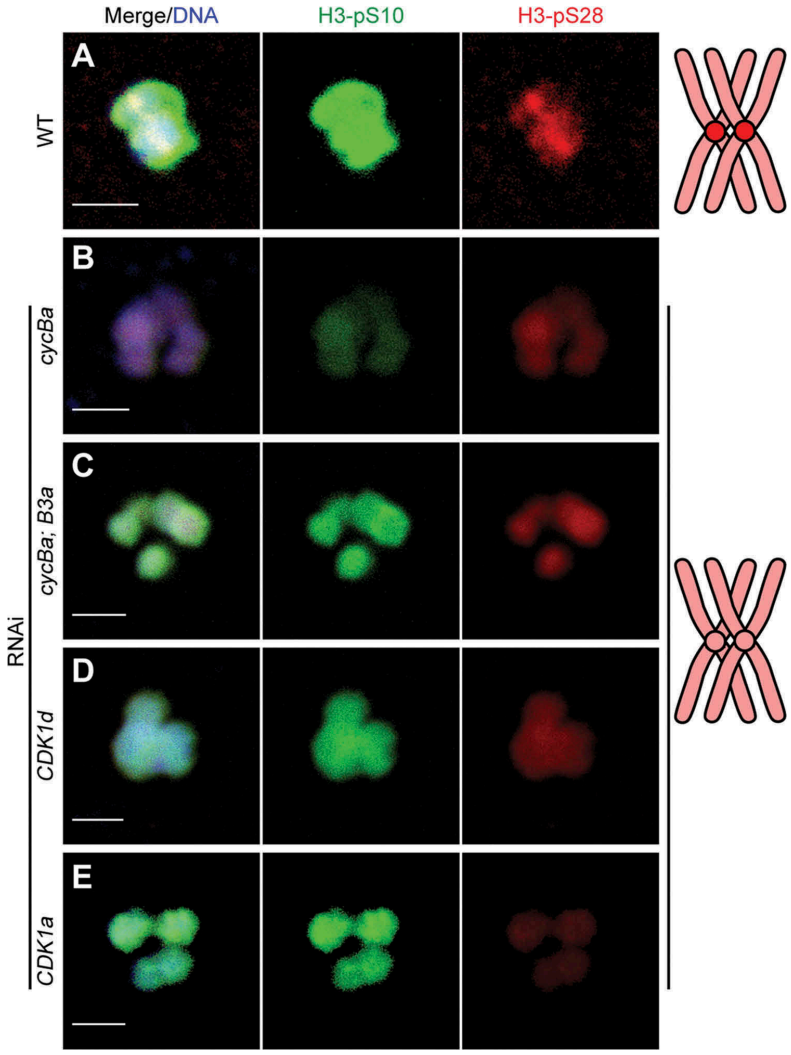

Figure 7. Histone H3-S10 and H3-S28 phosphorylations on bivalents in wild type and knockdown oocytes. (A) Wild type oocytes showed strong H3-pS10 staining on chromosome arms and H3-pS28 staining on centromeres of bivalents at metaphase I. H3-pS28 staining on centromeres was abolished after single knockdowns of *cyclin Ba* (B), *CDK1d* (D) or *CDK1a* (E), or double knockdown of *cyclin Ba* and *cyclin B3a* (C). Schemas on the right summarize H3-pS28 localization (red) on bivalents of wild type and knockdown oocytes. Scale bars: 2 μm.

CPC to centromeres (Figure 10(a)). We found that H3-pT3 was absent at centromeres in *cyclin Ba* RNAi oocytes (Figure 10(b)). Another key regulator, Plk1, localized in the nucleoplasm and along chromosomes during wild type prometaphase I (Figure 10(c)), but was either completely absent from meiotic nuclei (80%) or present in the nucleoplasm but absent from chromosomes (20%) in *cyclin Ba* RNAi oocytes (Figure 10(d)). These results indicate that in *O. dioica* ovaries, Cyclin Ba is a critical partner of CDK1 in regulating the localization and activity of Aurora B, for H3-S28 phosphorylation on centromeres, chromosome congression and meiotic spindle assembly during prometaphase I, and that CDK1d-Cyclin Ba activity is upstream of Plk1 localization to chromosomes.

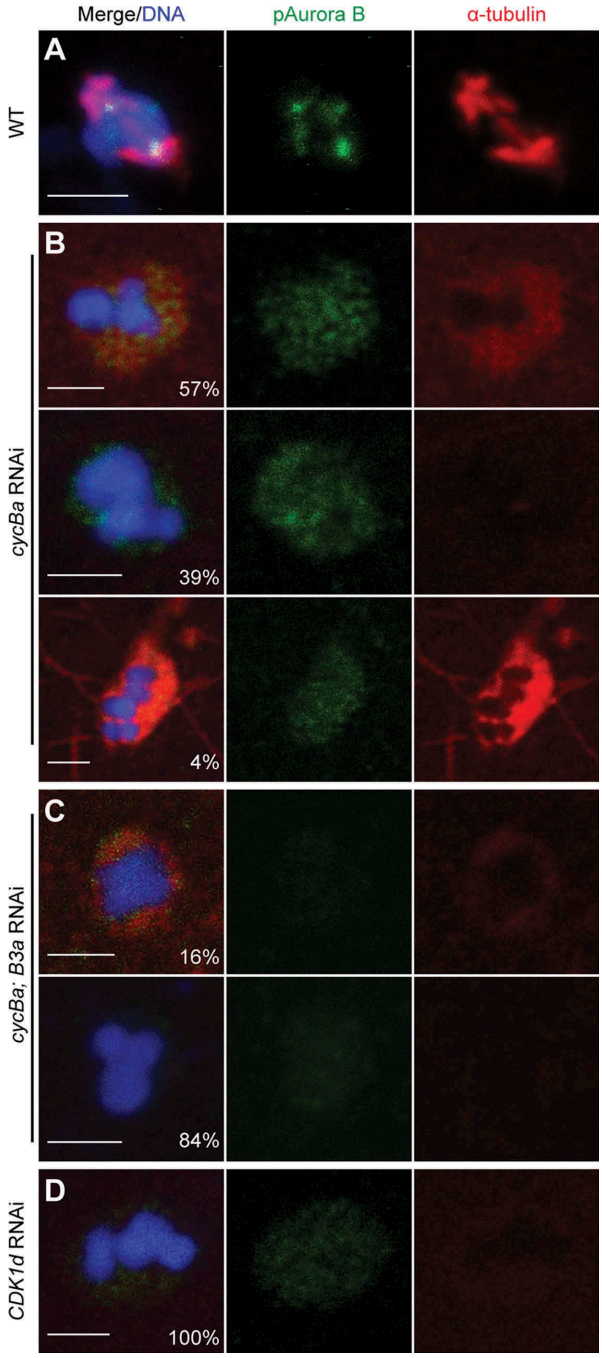

Figure 8. Aurora B is delocalized from centromeres and acentrosomal spindle assembly is blocked after RNAi of *cycBa, cycBa* and *cycB3a*, or *CDK1d*. (A) In wild-type oocytes, Aurora B localized on centromeres and a bipolar spindle formed, with microtubule fibers attaching to bivalents at metaphase I. (B) Representative defects in *cycBa* RNAi oocytes (n = 123) are shown. Proportions of each category are indicated in the merge panels. Aurora B remained dispersed in the nucleus and diffuse α-tubulin staining surrounding chromosomes was generally weak or absent. In rare cases, α-tubulin staining around chromosomes was strong and proximal microtubule fibers were observed. (C) In *cycBa; cycB3a* double RNAi oocytes (n = 104), Aurora B staining was even weaker, and the proportion of oocytes without any α-tubulin staining around chromosomes increased. (D) In *CDK1d* RNAi oocytes (n = 50), α-tubulin staining around chromosomes was absent. Scale bars: 2 μm.

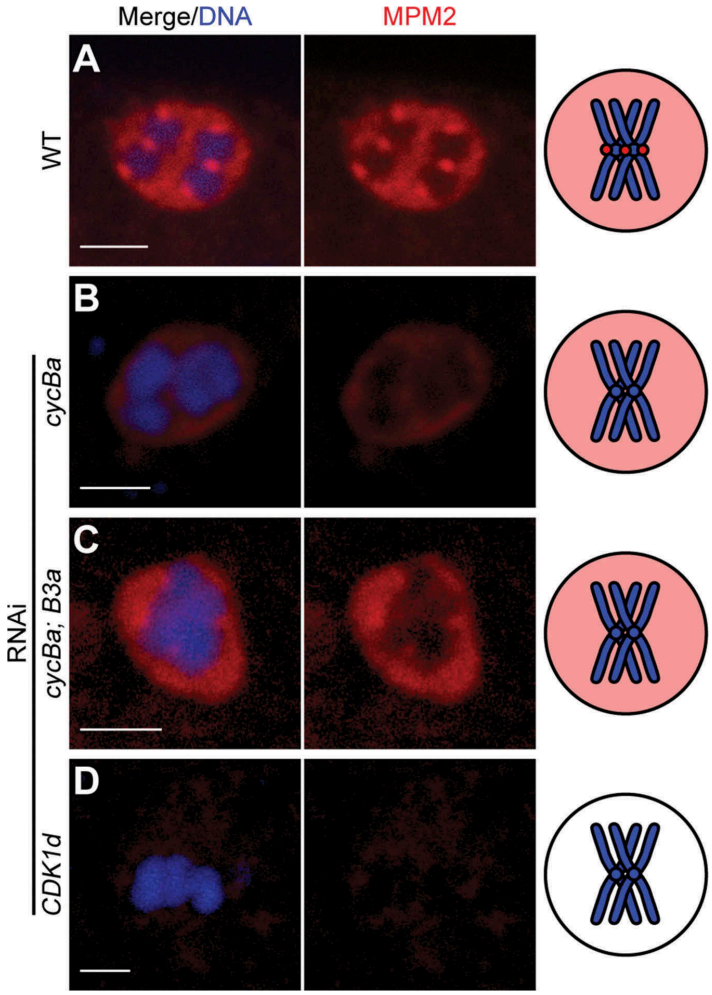

Figure 9. Knockdown of Cyclin Ba results in loss of MPM2 foci from centromeres. (A) MPM2 was present in the nucleoplasm and on the centromeres of bivalents during prometaphase I of wild-type meiotic nuclei. MPM2 foci were present in the nucleoplasm, but absent from chromosomes in *cycBa* RNAi oocytes (B) and *cycBa; cycB3a* double RNAi oocytes (C). (D) MPM2 was absent in meiotic nuclei in *CDK1d* RNAi oocytes. Schemas on the right summarize MPM2 signals (red) with only one bivalent (blue) shown for simplification. Scale bars: 2 µm.

Discussion

In this study we have shown a specialization of CDK1 paralog function during coenocystic oogenesis in *O. dioica*, in which CDK1a acts upstream of CDK1d to regulate vitellogenesis and Cyclin Ba dynamics. CDK1d, together with Cyclin Ba drives resumption of meiosis from prophase I arrest and final oocyte maturation. Cyclin B3a has a non-essential role in meiosis completion, though it may participate in regulating acentrosomal spindle assembly.

Knockdown of CDK1a disrupted vitellogenesis by interfering with nurse nuclear dumping to support pro-oocyte growth. Since the failure of rapid cytoplasmic transport inhibits the initiation of apoptosis in most nurse nuclei of *CDK1a* RNAi ovaries, we suggest that the last step of nurse

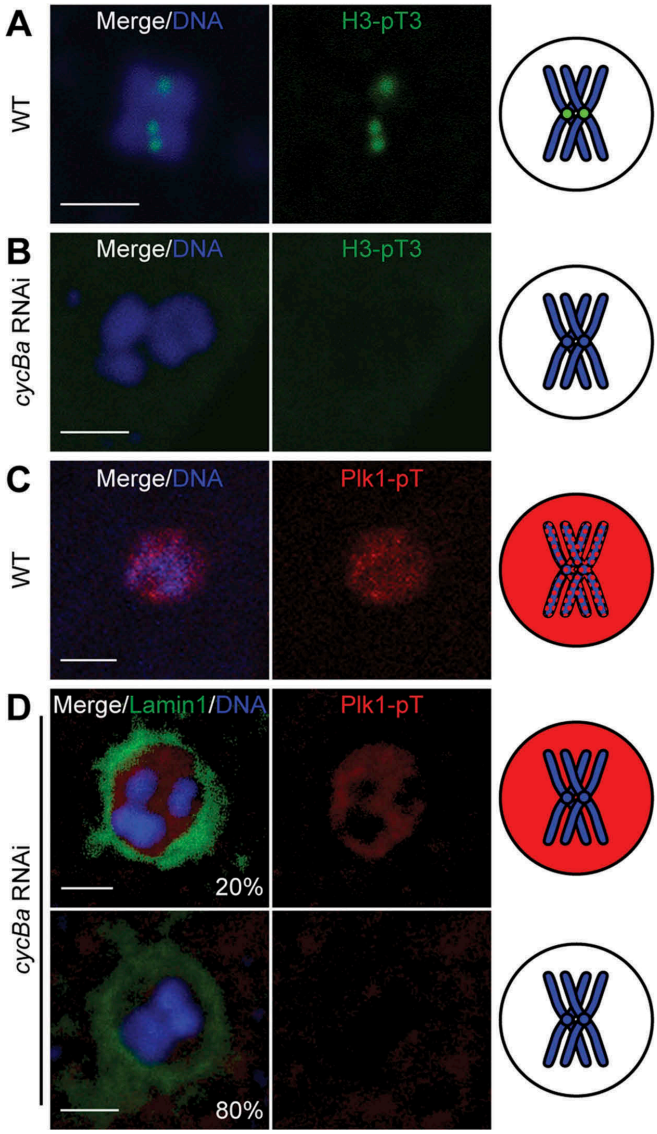

Figure 10. Knockdown of Cyclin Ba results in loss of H3T3 phosphorylation and phospho-Plk1 from centromeric regions. (A) In wild-type oocytes, H3-pT3 (green) was present on centromeric regions at metaphase I. (B) In *cycBa* RNAi oocytes, H3-pT3 was absent from chromosomes. (C) In wild-type oocytes, Plk1 located in meiotic nucleus at prometaphase I. (D) In *cycBa* RNAi oocytes (n = 30), two phenotypes were observed: Plk1 was absent from chromosomes (20%, top panel) or from the entire meiotic nucleus (80%, bottom panel). Lamin1 staining (green) indicated retention of the nuclear envelope in all cases. Schemas on the right summarize H3-pT3 (green) and Plk1-pT (red) signals in meiotic nuclei with only one bivalent (blue) shown for simplification. Scale bars: 2 μm.

nuclei contraction driven by subcortical actin-myosin network is defective. Indeed, disruption of the F-actin scaffold in the *O. dioica* ovary led to inhibition of oocyte growth [9]. Given that the fundamental molecular machinery of force-production by the actin-myosin network is conserved in a variety of cellular contexts and similarities in the coenocystic organization between *Drosophila*

and *Oikopleura*, we speculate that CDK1a works upstream of actin-myosin contraction to promote nurse nuclei dumping and/or rapid cytoplasmic flow during pro-oocyte growth. The losses of MPM2 foci and active Plk1 on chromosomes following knockdown of *CDK1a* could be indirectly caused by the subsequent, reduced expression of Cyclin Ba in selected meiotic nuclei, since both phenotypes were more severe in *cyclin Ba* RNAi oocytes. Plk1 relies on its polo-box domain (PBD) to dock on phosphorylated targets, and CDK1 is a major kinase to generate the docking site for the recruitment of Plk1 to specific substrates or cellular structures [39]. Plk1 activation did not depend on CDK1 during meiosis I of *O. dioica*, since active Plk1-pT210 was present on OCs and in the nucleoplasm of meiotic nuclei in the absence of CDK1 activity. This contrasts with starfish [40] and *Xenopus* [6], where Plk1 is a component of an MPF amplification loop during meiosis resumption and its activation depends on the prior activation of CDK1.

Several cell cycle regulators appeared first on OCs during diplotene arrest of prophase I, including CDK1a, CDK1d, Cyclin Ba, Aurora and Plk1. This is consistent with evidence that active CDK1-Cyclin B first appears on centrosomes of mammalian cells in prophase [41] and meiotic asters close to nuclear membranes before GVBD in immature oocytes of mouse [42] and starfish [43]. OCs might integrate early meiotic pathways and coordinate the temporal order of kinase translocations into meiotic nuclei. Although CDK1a, CDK1d and Cyclin Ba locate on OCs during P3 phase, their knockdowns did not have any obvious effects on OCs, since MPM2 foci and active Plk1 remained present, OCs associated with meiotic nuclei after oocyte selection, and they disassembled during prometaphase I with normal kinetics. This suggests that neither CDK1 paralog is essential for the structure or function of OCs.

All the characteristics of CDK1d-Cyclin Ba are consistent with it being MPF: 1) translocation was observed into meiotic nuclei during diplotene arrest; 2) NEBD was promoted; and 3) it drove meiotic spindle assembly and chromosome congression during prometaphase I. Levels of phosphorylated Cyclin Ba increased dramatically during late stages of oogenesis. In mitosis of mammalian cells, phosphorylated Cyclin B1 prefers to bind active CDK1, Cyclin B1 phosphorylation promotes nuclear translocation and nuclear translocation promotes Cyclin B1 phosphorylation [44]. It is possible that CDK1d-Cyclin Ba also form a spatial positive feedback loop to ensure its nuclear translocation and activation is robust and irreversible. The observed Cyclin Ba kinetics are consistent with models where rapid synthesis of Cyclin B forms excess active CDK1-Cyclin B required for meiosis resumption [45].

As in many metazoans, *O. dioica* oocytes lack centrosomes during the asymmetric partitioning of cytoplasm over the two meiotic divisions [46]. In the absence of centrosomes, chromatin-based signals play a major role in recruiting microtubules to organize a bipolar spindle. While the RanGTP pathway is not essential for meiosis I [47,48], the CPC, including Aurora B kinase, and three regulatory and targeting components INCENP, Survivin and Borealin, has been shown to be critical for acentrosomal meiotic spindle assembly during meiosis I. INCENP regulates the assembly of spindle microtubules and establishment of spindle bipolarity and chromosome biorientation in *Drosophila* [49]. Aurora B phosphorylates and suppresses the microtubule destabilizing factors mitotic centromere-associated kinesin (MCAK) at centromere to stabilize microtubule-kinetochore attachment [50]. In *O.dioica* meiotic spindles, we observed that microtubules focused at the two poles formed a broad shape and did not anchor to an acentriolar MTOC since the OC was disassembled during prometaphase I (Figure S1). Following NEBD in *O. dioica*, we found that prometaphase I spindle assembly was accompanied by the movement of Aurora B from an even distribution in meiotic nuclei to concentration on centromeres. CDK1d-Cyclin Ba was upstream of the recruitment of the CPC to centromeres during prometaphase I. In *cyclin Ba* RNAi oocytes, H3-pT3 was absent on centromeres and active Plk1 failed to localize to chromosomes. Histone H3-pT3 is the centromeric target of Haspin kinase and H3-pT3 binds Survivin to recruit Aurora B to centromeres [38]. Thus Haspin was not activated in the absence of CDK1d-Cyclin Ba. It has been shown in *Xenopus* egg extracts and human cells that during mitotic

entry, Haspin is activated by sequential phosphorylation by CDK1 and Plk1 on its N terminal [51]. Analogously, CDK1d-Cyclin Ba probably initiates activation of the H3T3 kinase Haspin, recruiting the CPC to centromeres to promote meiotic spindle assembly during prometaphase I.

Information on the roles of Cyclin B paralogs across taxonomic groups is rather patchy and is derived from mitotically proliferating cells (often embryonic) and meiotic cells (usually oogenic), though, within a given model organism, not always both. The generally emerging picture is that Cyclin B paralogs display functional redundancy but also exhibit distinct roles. In single cell budding yeast, none of Clbs 1–4 are essential and Clb2 alone is sufficient to drive meiosis [52], whereas in fission yeast a single cyclin, Cdc13, is sufficient for the entire cell cycle [53]. Cyclin B3 arose at the origin of metazoans [54], and to date, is found as a single gene in all species, except, *O. dioica*, where there are Cyclin B3a and B3b paralogs. Cyclin B3a is expressed during oogenesis and embryogenesis whereas Cyclin B3b is specifically expressed in the testis, reminiscent of the expression pattern of mammalian Cyclin B3 at leptotene and zygotene stages in spermatocytes [55]. As in other species, the Cyclin B3 genes of *O. dioica* show higher phylogenetic affinity to Cyclin B3 of other species than to other Cyclin B paralogs within *O. dioica* [32]. Selective pressures for a distinct Cyclin B3 throughout metazoan evolution might be expected to imply specific essential functions, but our results support studies in other species to suggest that this is not always the case.

A growing consensus from loss-of-function analyzes indicates an anaphase promoting role of Cyclin B3 [16–18,26,56]. Some recent evidence that Cyclin B3 regulates timely progression of S-phase and NEBD, might imply that anaphase defects observed in Cyclin B3 mutants may be indirectly caused by under-replicated chromosomes in the preceding S-phase [19]. In mitotic *C. elegans* embryonic cells, this anaphase-promoting activity appears to be SAC-dependent [56], whereas in meiotic mouse oocytes, Cyclin B3 regulation of the metaphase-anaphase transition is proposed to operate through a SAC-independent pathway [26]. The expression profile of *O. dioica* Cyclin B3a is consistent with a role in later meiotic events (Figure 2(a)), but we observed that it is not required to promote the metaphase to anaphase transition in this chordate species.

Cyclin B3 also collaborates with other mitotic cyclins (Cyclins B1 and B2 in *C. elegans* [18], Cyclin A and B in *Drosophila* [17]) to drive NEBD during oocyte maturation. In *O. dioica*, Cyclin B3a shows overlapping functions with Cyclin Ba in promoting meiotic spindle assembly. There are no functional studies of B-type Cyclins in other urochordates and cephalochordates, but the Cyclin B1 homolog maintains maximum CDK1 activity at metaphase I in the ascidian *Ciona intestinalis* [57]. It is tempting to suggest that in urochordates, Cyclin B1 homologs are critical for both NEBD and spindle assembly in oogenic meiosis I. Our observations have potential implications for the evolutionary trajectory of metazoan B-type Cyclins in oogenic meiosis. In invertebrates, Cyclin B1 collaborates with other mitotic Cyclins (Cyclin B2 and B3 in *C. elegans*, Cyclin A and B3 in *Drosophila*) to promote NEBD. Cyclin B1 seems more critical for spindle organization in *Drosophila* [17], but not in *C. elegans* [18]. In clam and starfish, Cyclin A is not expressed during meiosis I, such that Cyclin B is the sole regulator of CDK1 to drive meiosis resumption [58,59]. In sea urchin, new Cyclin B synthesis is not required for GVBD, but is required for spindle formation, and Cyclin A, though present, can't compensate for the loss of Cyclin B in meiosis I [60]. In non-mammalian vertebrates such as *Xenopus*, Cyclin B2 is the dominant subtype in meiosis I, and its neosynthesis is critical to promote GVBD and spindle assembly [45,61]. In mice, Cyclin B2 is critical for GVBD and initial stage of spindle assembly during early metaphase I [62], whereas the rate of Cyclin B1 synthesis after GVBD determines the progression of spindle assembly and the length of meiosis I [63]. Thus, Cyclin B1 homologs appear to become more dominant in driving meiotic progression over the course of animal evolution. Our results suggest that the chordate common ancestor had Cyclin B1 and Cyclin B3, with Cyclin B1 playing a major role in both GVBD and spindle assembly. Two rounds of whole genome duplication in the vertebrate stem gave rise to Cyclin B2, which shares responsibilities with Cyclin B1 in meiotic events to different extents in different vertebrates.

Materials and methods

Animal culture and sample collection

Oikopleura dioica were maintained in culture at 15°C [64]. Days 4–6 animals were placed in artificial seawater, removed from their houses, anesthetized in ethyl 3-aminobenzoate methanesulfonate salt (MS-222, 0.125 mg/ml; Sigma), and then fixed in 4% paraformaldehyde (PFA) for *in situ* hybridization or immunofluorescence, or snap frozen in liquid nitrogen for western blots or RNA extraction. For dsRNA injected animals, mature females were transferred to artificial seawater in 6-well plates coated with 0.1% gelatin. Equal numbers of spawned oocytes were collected for western blot and kinase activity assays, and remaining oocytes were used for RT-qPCR, immunofluorescence or *in vitro* fertilization as described previously [33].

In situ hybridization on paraffin sections or of whole-mount fluorescence

After fixation at 4°C overnight, samples were washed 3 times in PBS, dehydrated in 70%-95%-100% gradient ethanol (1 h each), cleared in xylene for 30 minutes, and incubated in paraffin at 55°C for 2 h before solidification on ice. Sections (5 µm) were cut using a Leica microtome RM2155 and collected on Polysine™ slides (ThermoFisher). After drying at 55°C, paraffin sections were de-paraffinized in xylene, rehydrated in 100%-95%-70% gradient ethanol, and processed for *in situ* hybridization as previously [65]. Digoxygenin-labeled anti-sense RNA probes of full-length cyclin Ba were used for hybridization. For whole-mount fluorescence *in situ*, hybridization signal was detected by anti-Digoxigenin-POD and TSA Plus Cyanine 5 Evaluation Kit, and collected by excitation at 561 nm and emission from 563 nm to 620 nm.

Microinjections

Injection solutions were prepared by mixing 400 ng/µl capped mRNA or dsRNA with 100 ng/µl Alexa Fluor 568 dye (Molecular Probes) in RNase-free PBS. Microinjection was performed as described previously [33].

eGFP fusion constructs, cmRNA and dsRNA synthesis

3′ UTRs of *CDK1a, CDK1d* and *cycBa* were obtained by 3′ RACE (SMARTer RACE 5′/3′ Kit, Clontech). For eGFP fusion constructs, the coding region (with its endogenous 3′ UTR) was driven by the T7 promoter, followed by eGFP at the C-terminal. The construct was linearized and used as template to synthesize cmRNA (Ambion mMessage mMachine T7 transcription kit) according to the manufacturer's protocol. The cmRNA was purified using Ambion MEGAclear kit. About 300 bp fragments in the N terminal of the coding region of *cycBa* and *cycB3a* were amplified as template to synthesize dsRNA as described previously [33].

Antibodies

Custom rabbit polyclonal affinity–purified anti-cyclin Ba/b (acetyl-NRDLNIQESGPVKAVVNAC-amide and acetyl-CLEFLRRFSRVAEETIDPKEY-amide), and rabbit polyclonal affinity–purified anti-lamin1 (acetyl-QSPISLPPLSGSTC-amide) were produced by 21st Century Biochemicals (Marlboro, MA). Other antibodies included anti-Histone H3-pT3 (Abcam), anti-Histone H3-pS10 (Millipore), anti-Histone H3-pS28 (Abcam), anti-phospho-Ser/Thr-Pro MPM-2 (Millipore), anti-Plk1-pT210 (BioLegend), anti-Aurora A (pT288)/Aurora B (pT232)/Aurora C (pT198) (Cell Signaling Technology), anti-MAPK-pTEpY (pERK1/2) (Promega), anti-PSTAIRE (Abcam), anti-eGFP (AMS Biotechnology), anti-Tubulin (Abcam). Secondary antibodies against rabbit, rat and mouse IgG (conjugated Alexa Fluor 488, 568 or HRP) were from Molecular Probes. For immunofluorescence, primary antibodies were used at 1:100 dilution and secondary antibodies at 1:300 dilution. For western blot, primary and secondary antibodies were used at 1:1000 and 1:5000 dilutions, respectively.

CDK1 kinase assay

CDK1 kinase activity was determined using the MESACUP CDK1 Kinase Assay Kit (MBL). Briefly, equal numbers of oocytes were frozen and thawed twice. Then the samples were mixed with biotinylated MV peptide and 1 mM ATP and

incubated at 30°C for 30 min. After stopping the phosphorylation reaction, ELISA was performed using anti-phosphorylated MV peptide antibody. Finally, POD conjugated streptavidin was used to detect phosphorylated MV peptide and color development measured at OD_{492nm}. Statistical significances of CDK1 kinase activities from different knockdown oocytes were analyzed by the Student's T-test.

Acknowledgments

We thank Xiaofei Ma, Sars Centre, for helpful discussions and A. Aasjord and K. N. Nøkling for providing animals from the *Oikopleura* culture facility.

Disclosure statement

No potential conflict of interest was reported by the authors.

Funding

This work was supported by a PhD fellowship from Department of Biological Sciences, University of Bergen (H. F.) and grants 183690/S10 NFR-FUGE and 133335/V40 from the Norwegian Research Council (E.M.T.).

Notes on contributor

H.F., and E.M.T. conceived and designed the experiments. H. F. performed experiments and H.F. and E.M.T. analyzed the data. H.F. and E.M.T. wrote the manuscript. All authors approved the manuscript.

ORCID

Eric M. Thompson http://orcid.org/0000-0002-3756-9036

References

[1] Von Stetina JR, Orr-Weaver TL. Developmental control of oocyte maturation and egg activation in metazoan models. Cold Spring Harb Perspect Biol. 2011;3:a005553. PMID:21709181.

[2] Kubiak JZ, Ciemerych MA, Hupalowska A, et al. On the transition from the meiotic to mitotic cell cycle during early mouse development. Int J Dev Biol. 2008;52:201–217. PMID:18311711.

[3] Yamashita M. Molecular mechanisms of meiotic maturation and arrest in fish and amphibian oocytes. Semin Cell Dev Biol. 1998;9:569–579. PMID:9835645.

[4] Kishimoto T. Cell-cycle control during meiotic maturation. Curr Opin Cell Biol. 2003;15:654–663. PMID:14644189.

[5] Seki A, Coppinger JA, Jang C-Y, et al. Bora and the kinase Aurora a cooperatively activate the kinase Plk1 and control mitotic entry. Science. 2008;320:1655–1658. PMID:18566290.

[6] Abrieu A, Brassac T, Galas S, et al. The Polo-like kinase Plx1 is a component of the MPF amplification loop at the G2/M-phase transition of the cell cycle in *Xenopus* eggs. J Cell Sci. 1998;111:1751–1757. PMID:9601104.

[7] Delsuc F, Tsagkogeorga G, Lartillot N, et al. Additional molecular support for the new chordate phylogeny. Genesis. 2008;46:592–604. PMID:19003928.

[8] Ganot P, Bouquet J-M, Thompson EM. Comparative organization of follicle, accessory cells and spawning anlagen in dynamic semelparous clutch manipulators, the urochordate Oikopleuridae. Biol Cell. 2006;98:389–401. PMID:16478443.

[9] Ganot P, Kallesøe T, Thompson EM. The cytoskeleton organizes germ nuclei with divergent fates and asynchronous cycles in a common cytoplasm during oogenesis in the chordate *Oikopleura*. Dev Biol. 2007;302:577–590. PMID:17123503.

[10] Pepling ME, de Cuevas M, Sprading AC. Germline cysts: a conserved phase of germ cell development? Trends Cell Biol. 1999;9:257–262. PMID:10370240.

[11] Bastock R, St Johnston D. *Drosophila* oogenesis. Curr Biol. 2008;18:R1082–R1087. PMID:19081037.

[12] Matova N, Cooley L. Comparative aspects of animal oogenesis. Dev Biol. 2001;231:291–320. PMID:11237461.

[13] Ganot P, Moosmann-Schulmeister A, Thompson EM. Oocyte selection is concurrent with meiosis resumption in the coenocystic oogenesis of *Oikopleura*. Dev Biol. 2008;324:266–276. PMID:18845138.

[14] Loog M, Morgan DO. Cyclin specificity in the phosphorylation of cyclin-dependent kinase substrates. Nature. 2005;434:104–108. PMID:15744308.

[15] Hochegger H, Klotzbücher A, Kirk J, et al. New B-type cyclin synthesis is required between meiosis I and II during *Xenopus* oocyte maturation. Development. 2001;128:3795–3807. PMID:11585805.

[16] Yuan K, O'Farrell PH. Cyclin B3 is a mitotic cyclin that promotes the metaphase-anaphase transition. Curr Biol. 2015;25:811–816. PMID:25754637.

[17] Bourouh M, Dhaliwal R, Rana K, et al. Distinct and overlapping requirements for Cyclins A, B, and B3 in *Drosophila* female meiosis. G3 Genes|Genomes|Genetics. 2016;6:3711–3724. PMID:27652889.

[18] van der Voet M, Lorson MA, Srinivasan DG, et al. *C. elegans* mitotic cyclins have distinct as well as overlapping functions in chromosome segregation. Cell Cycle. 2009;8:4091–4102. PMID:19829076.

[19] Michael WM. Cyclin CYB-3 controls both S-phase and mitosis and is asymmetrically distributed in the early *C. elegans* embryo. Development. 2016;143:3119–3127. PMID:27578178.

[20] Brandeis M, Rosewell I, Carrington M, et al. Cyclin B2-null mice develop normally and are fertile whereas cyclin B1-null mice die *in utero*. Proc Natl Acad Sci U S A. 1998;95:4344–4349. PMID:9539739.
[21] Huang Y, Sramkoski RM, Jacobberger JW. The kinetics of G2 and M transitions regulated by B cyclins. PLoS One. 2013;8:e80861. PMID:24324638.
[22] Jackman M, Firth M, Pines J. Human cyclins B1 and B2 are localized to strikingly different structures: B1 to microtubules, B2 primarily to the Golgi apparatus. EMBO J. 1995;14: 1646–1654. PMID:7737117.
[23] Spalluto C, Wilson DI, Hearn T. Evidence for centriolar satellite localization of CDK1 and cyclin B2. Cell Cycle. 2013;12:1802–1803. PMID:23656781.
[24] Nam H-J, van Deursen JM. Cyclin B2 and p53 control proper timing of centrosome separation. Nat Cell Biol. 2014;16:538–549. PMID:24776885.
[25] Gallant P, Nigg EA. Identification of a novel vertebrate cyclin: cyclin B3 shares properties with both A- and B-type cyclins. EMBO J. 1994;13: 595–605. PMID:8313904.
[26] Zhang T, Qi S-T, Huang L, et al. Cyclin B3 controls anaphase onset independent of spindle assembly checkpoint in meiotic oocytes. Cell Cycle. 2015;14:2648–2654. PMID:26125114.
[27] Morgan DO. CYCLIN-DEPENDENT KINASES: engines, clocks, and microprocessors. Annu Rev Cell Dev Biol. 1997;13:261–291. PMID:9442875.
[28] Malumbres M, Barbacid M. Cell cycle, CDKs and cancer: a changing paradigm. Nat Rev Cancer. 2009;9:153–166. PMID:19238148.
[29] Kishimoto T. A primer on meiotic resumption in starfish oocytes: the proposed signaling pathway triggered by maturation-inducing hormone. Mol Reprod Dev. 2011;78:704–707. PMID:21714029.
[30] Stern B, Ried G, Clegg NJ, et al. Genetic analysis of the *Drosophila cdc2* homolog. Development. 1993;117:219–232. PMID:8223248.
[31] Boxem M, Srinivasan DG, van den Heuvel S. The *Caenorhabditis elegans* gene *ncc-1* encodes a *cdc2*-related kinase required for M phase in meiotic and mitotic cell divisions, but not for S phase. Development. 1999;126: 2227–2239. PMID:10207147.
[32] Campsteijn C, Øvrebø JI, Karlsen BO, et al. Expansion of cyclin D and CDK1 paralogs in *Oikopleura dioica*, a chordate employing diverse cell cycle variants. Mol Biol Evol. 2012;29:487–502. PMID:21734012.
[33] Øvrebø JI, Campsteijn C, Kourtesis I, et al. Functional specialization of chordate CDK1 paralogs during oogenic meiosis. Cell Cycle. 2015;14:880–893. PMID:25714331.
[34] Becalska AN, Gavis ER. Lighting up mRNA localization in *Drosophila* oogenesis. Development. 2009;136:2493–2503. PMID:19592573.
[35] Foley K, Cooley L. Apoptosis in late stage *Drosophila* nurse cells does not require genes within the *H99* deficiency. Development. 1998;125: 1075–1082. PMID:9463354.
[36] Cooley L, Verheyen E, Ayers K. *chickadee* encodes a profilin required for intercellular cytoplasm transport during *Drosophila* oogenesis. Cell. 1992;69: 173–184. PMID:1339308.
[37] Colombié N, Cullen CF, Brittle AL, et al. Dual roles of Incenp crucial to the assembly of the acentrosomal metaphase spindle in female meiosis. Development. 2008;135:3239–3246. PMID:18755775.
[38] Yamagishi Y, Honda T, Tanno Y, et al. Two histone marks establish the inner centromere and chromosome bi-orientation. Science. 2010;330:239–243. PMID:20929775.
[39] Barr FA, Silljé HHW, Nigg EA. Polo-like kinases and the orchestration of cell division. Nat Rev Mol Cell Biol. 2004;5:429–440. PMID:15173822.
[40] Okano-Uchida T, Okumura E, Iwashita M, et al. Distinct regulators for Plk1 activation in starfish meiotic and early embryonic cycles. EMBO J. 2003;22:5633–5642. PMID:14532135.
[41] Jackman M, Lindon C, Nigg EA, et al. Active cyclin B1-Cdk1 first appears on centrosomes in prophase. Nat Cell Biol. 2003;5:143–148. PMID:12524548.
[42] Marangos P, Carroll J. The dynamics of cyclin B1 distribution during meiosis I in mouse oocytes. Reproduction. 2004;128:153–162. PMID:15280554.
[43] Ookata K, Hisanaga S, Okano T, et al. Relocation and distinct subcellular localization of $p34^{cdc2}$-cyclin B complex at meiosis reinitiation in starfish oocytes. EMBO J. 1992;11:1763–1772 PMID:1316272.
[44] Santos SDM, Wollman R, Meyer T, et al. Spatial positive feedback at the onset of mitosis. Cell. 2012;149:1500–1513. PMID:22726437.
[45] Gaffré M, Martoriati A, Belhachemi N, et al. A critical balance between Cyclin B synthesis and Myt1 activity controls meiosis entry in *Xenopus* oocytes. Development. 2011;138:3735–3744. PMID:21795279.
[46] Bennabi I, Terret M-E, Verlhac M-H. Meiotic spindle assembly and chromosome segregation in oocytes. J Cell Biol. 2016;215:611–619. PMID:27879467.
[47] Dumont J, Petri S, Pellegrin F, et al. A centriole- and RanGTP-independent spindle assembly pathway in meiosis I of vertebrate oocytes. J Cell Biol. 2007;176:295–305. PMID:17261848.
[48] Cesario J, McKim KS. RanGTP is required for meiotic spindle organization and the initiation of embryonic development in *Drosophila*. J Cell Sci. 2011;124:3797–3810. PMID:22100918.
[49] Radford SJ, Jang JK, McKim KS. The chromosomal passenger complex is required for meiotic acentrosomal spindle assembly and chromosome biorientation. Genetics. 2012;192:417–429. PMID:22865736.
[50] Andrews PD, Ovechkina Y, Morrice N, et al. Aurora B regulates MCAK at the mitotic centromere. Dev Cell. 2004;6:253–268. PMID:14960279.
[51] Ghenoiu C, Wheelock MS, Funabiki H. Autoinhibition and polo-dependent multisite phosphorylation restrict activity of the histone H3 kinase haspin to mitosis. Mol Cell. 2013;52:734–745. PMID:24184212.

[52] Richardson H, Lew DJ, Henze M, et al. Cyclin-B homologs in *Saccharomyces cerevisiae* function in S phase and in G2. Genes Dev. 1992;6:2021–2034. PMID:1427070.

[53] Fisher DL, Nurse P. A single fission yeast mitotic cyclin B $p34^{cdc2}$ kinase promotes both S-phase and mitosis in the absence of G1 cyclins. EMBO J. 1996;15: 850–860. PMID:8631306.

[54] Lozano J-C, Vergé V, Schatt P, et al. Evolution of Cyclin B3 shows an abrupt three-fold size increase, due to the extension of a single exon in placental mammals, allowing for new protein–protein interactions. Mol Biol Evol. 2012;29:3855–3871. PMID:22826462.

[55] Nguyen TB, Manova K, Capodieci P, et al. Characterization and expression of mammalian cyclin B3, a prepachytene meiotic cyclin. J Biol Chem. 2002;277:41960–41969. PMID:12185076.

[56] Deyter GM, Furuta T, Kurasawa Y, et al. *Caenorhabditis elegans* cyclin B3 is required for multiple mitotic processes including alleviation of a spindle checkpoint-dependent block in anaphase chromosome segregation. PLoS Genet. 2010;6:e1001218. PMID:21124864.

[57] Russo GL, Kyozuka K, Antonazzo L, et al. Maturation promoting factor in ascidian oocytes is regulated by different intracellular signals at meiosis I and II. Development. 1996;122:1995–2003. PMID:8681780.

[58] Hunt T, Luca FC, Ruderman JV. The requirements for protein synthesis and degradation, and the control of destruction of cyclins A and B in the meiotic and mitotic cell cycles of the clam embryo. J Cell Biol. 1992;116: 707–724. PMID:1530948.

[59] Okano-Uchida T, Sekiai T, Lee K, et al. *In vivo* regulation of Cyclin A/Cdc2 and Cyclin B/Cdc2 through meiotic and early cleavage cycles in starfish. Dev Biol. 1998;197:39–53. PMID:9578617.

[60] Voronina E, Marzluff WF, Wessel GM. Cyclin B synthesis is required for sea urchin oocyte maturation. Dev Biol. 2003;256:258–275. PMID:12679101.

[61] Yoshitome S, Furuno N, Prigent C, et al. The subcellular localization of cyclin B2 is required for bipolar spindle formation during *Xenopus* oocyte maturation. Biochem Biophys Res Commun. 2012;422:770–775. PMID:22627133.

[62] Gui L, Homer H. Hec1-dependent Cyclin B2 stabilization regulates the G2-M transition and early prometaphase in mouse oocytes. Dev Cell. 2013;25:43–54. PMID:23541922.

[63] Polanski Z, Ledan E, Brunet S, et al. Cyclin synthesis controls the progression of meiotic maturation in mouse oocytes. Development. 1998;125:4989–4997. PMID:9811583.

[64] Bouquet J-M, Spriet E, Troedsson C, et al. Culture optimization for the emergent zooplanktonic model organism *Oikopleura dioica*. J Plankton Res. 2009;31:359–370. PMID:19461862.

[65] Ganot P, Bouquet J-M, Kallesøe T, et al. The *Oikopleura* coenocyst, a unique chordate germ cell permitting rapid, extensive modulation of oocyte production. Dev Biol. 2007;302:591–600. PMID:17126826.

Supplemental Information

Specialization of CDK1 and Cyclin B paralog functions in a coenocystic mode of oogenic meiosis

Haiyang Feng and Eric M. Thompson

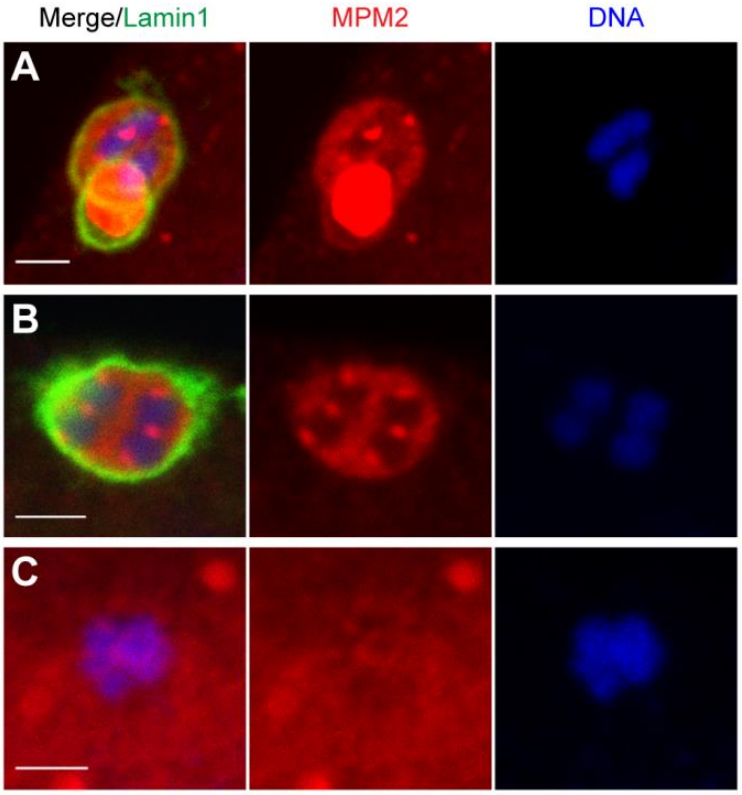

Fig. S1. The organizing centre (OC) disassembled before NEBD during the final stage of wild-type oocyte maturation. (A) In immature oocytes, MPM2 staining was found on the OC, in the nucleoplasm of meiotic nuclei, and exhibited strong foci located on chromosomes. (B) As oocyte maturation progressed, the OC disassembled, and strong MPM2 foci were observed at the centromeres of bivalents, with uniform MPM2 staining in the nucleoplasm. (C) After NEBD, MPM2 staining disappeared from chromosomes, and MPM2 foci were found in the cytoplasm. Scale bars: 2 μm.

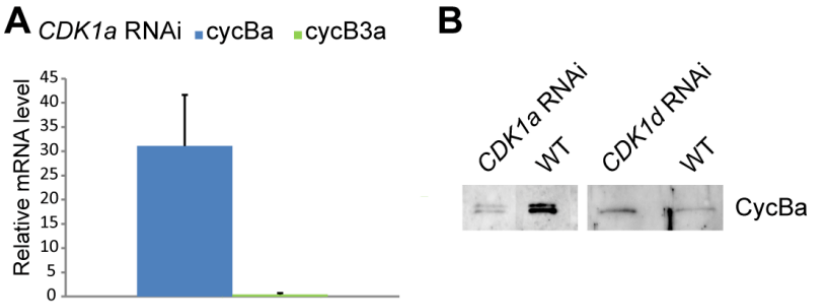

Fig. S2. Impacts of *CDK1a* and *d* knockdowns on Cyclin B paralog mRNA and protein levels. (A) RT-qPCR showed that *cyclin Ba* mRNA levels were very high, while *cyclin B3a* mRNA levels were very low in *CDK1a* RNAi ovaries. Values are presented relative to mRNA levels of EF1β and represent the mean from three biological repeats with standard errors indicated. (B) Cyclin Ba protein was low in *CDK1a* RNAi ovaries, but present as normal in *CDK1d* RNAi oocytes. Equal numbers of wild type oocytes were loaded as a positive control.

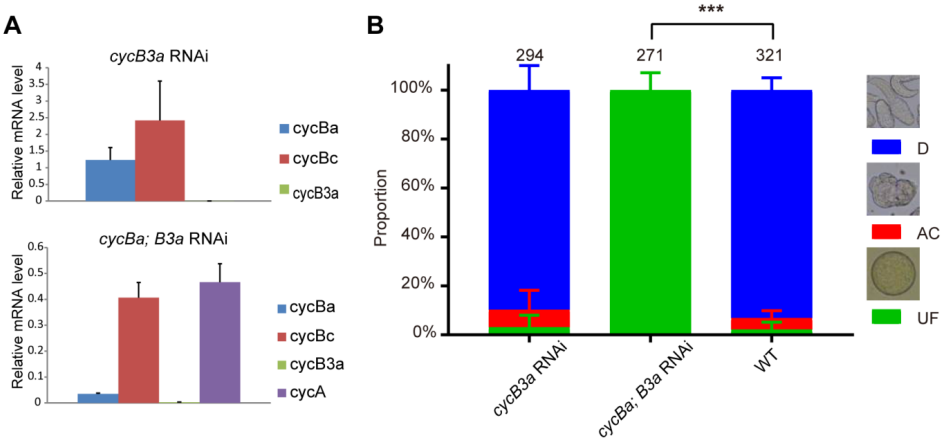

Fig. S3. Knockdown of Cyclin B3a alone did not significantly affect oogenic meiosis or early embryogenesis, whereas double knockdown of Cyclins Ba and B3a resulted in infertility. (A) Single knockdown efficiency of cyclin B3a mRNA levels and double knockdown efficiency of cyclin Ba and cyclin B3a mRNA levels. No significant off-target effects on other cyclin B paralogs or cyclin A were detected. (B) Compared to wild-type oocytes, more than 90% of *cycB3a* RNAi oocytes developed normally (no significant difference to WT), while none of *cycBa*; *cycB3a* double RNAi oocytes cleaved after fertilization using wild-type sperm (***significantly different to WT; $p<0.001$, student t-test). UF, UnFertilized; AC, Abnormal Cleavage; D, Developed normally. The number of embryos assessed at the top of each histogram bar were derived from three independent experiments with standard errors indicated.

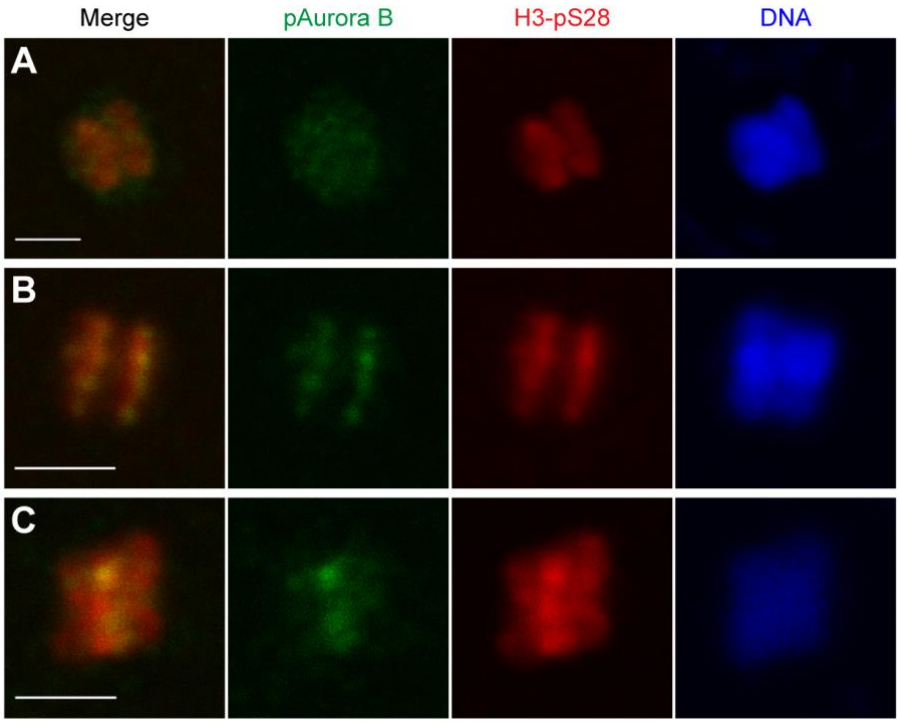

Fig. S4. In wild-type oocyte chromatin, H3-pS28 staining shifts from chromosome arms to centromeres during prometaphase I, concurrently with enrichment of Aurora B kinase on centromeres. (A) Before NEBD, Aurora B was evenly distributed in meiotic nuclei, and H3-pS28 labelled whole chromosomes. (B) After NEBD, Aurora B and H3-pS28 co-located on centromeres. C) At metaphase I, Aurora B and H3-pS28 co-localized on centromeres. Scale bars: 2 μm.

Graphic design: Communication Division, UiB / Print: Skipnes Kommunikasjon AS

uib.no

ISBN: 978-82-308-3627-9